Green Chemistry

TUTORIAL REVIEW

View Article Online
View Journal | View Issue

Cite this: *Green Chem.*, 2023, **25**, 5338

Cellulose processing in ionic liquids from a materials science perspective: turning a versatile biopolymer into the cornerstone of our sustainable future

László Szabó, *[a,b] Romain Milotskyi, [c] Gyanendra Sharma [c] and Kenji Takahashi *[c]

Shaping cellulose into functional materials entered a new era with the introduction of ionic liquids as novel, green solvents about 20 years ago. As non-volatile solvents with high thermal and chemical stability, ionic liquids can provide an environmentally more benign tunable platform for cellulose processing, compared to existing technologies. The past decades have seen fruitful efforts devoted to the development of materials based on ionic liquid/cellulose processing systems. In this review we discuss the experiences gained, and highlight the emerging applications. In particular, *coatings and thin film* applications for structural materials (*e.g.*, for packaging), *thin film filtration membranes*, *immobilisation of enzymes*, and *catalytically active nanoparticles*, *separator membranes and conductive composites for energy storage and other electronics applications*, *cellulose/biopolymer green biocomposites*, cellulose-based *ionogels, hydrogels and aerogels*, and *cellulose-based or composite fibres* will be discussed in detail. We will also take a critical look at the perspectives of this field. The use of a certain grade of technical cellulose, and the purity of the prepared materials should be more carefully justified in the future, as they have an influence not only on the properties of the fabricated material, but also on the economics of the process. Furthermore, to make ionic liquids truly green solvents, and competitive alternatives to existing technologies, more studies are needed on *recyclability* after material fabrication, and on ways to minimise the *energy consumption* of such processes, among other issues.

Received 12th December 2022,
Accepted 10th May 2023

DOI: 10.1039/d2gc04730f

rsc.li/greenchem

1. Introduction

Cellulose has been with us in various forms since ancient times, as it is the most abundant biopolymer available on Earth. Materials made from wood, cotton and cellulose fibers have shaped our way of surviving, thriving and living (to generate heat and energy, to construct buildings and tools); and determined our cultural and societal development (*e.g.*, think about the use of paper, clothing/fashion). In fact, thinking of the modern age – the first thermoplastic polymer ever made was also derived from cellulose (called celluloid, a nitrocellulose-based plastic containing camphor). Unfortunately, the momentum that cellulose once had in our life has been greatly suppressed by the emerging synthetic polymer industry utilising fossil fuels. Our society became heavily dependent on these finite resources, and our anthropogenic impact grew to its extremities. This brought about irreversible changes on Earth, such as environmental pollution by microplastics, and climate change among other unusual ecological phenomena. While many may think that humanity is already doomed to fail, we argue that it is still not too late to change our way of living: this means turning away from fossil-fuel centred life and shifting to a material-based society centred around bio-based solutions. In this regard, cellulose may come again to our rescue, as it shaped our history time and time again.

Material scientists have long been interested in shaping cellulose into functional materials. The processing and shaping of cellulose entered a new era with the introduction of ionic liquids as novel solvents, first reported in the work of Swatloski *et al.*[1] 20 years ago. Ionic liquids (IL) are a type of molten salts, defined here as those with melting point below 100 °C.[2] They are extensively recognised as green solvents mainly due to their non-volatile nature together with thermal and chemical stability.[3] These solvents gained popularity partly due to their exceptional solvating power and unpre-

[a]*Forestry and Forest Products Research Institute, 1 Matsunosato, Tsukuba, Ibaraki 305-8687, Japan. E-mail: szabo@affrc.go.jp*
[b]*International Center for Young Scientists (ICYS), National Institute for Materials Science (NIMS), 1-1 Namiki, Tsukuba 305-0044, Japan*
[c]*Institute of Science and Engineering, Kanazawa University, Kakuma-machi, Kanazawa 920-1192, Japan. E-mail: ktkenji@staff.kanazawa-u.ac.jp*

cedented tunability, as a number of cation–anion combinations exist leading to various physicochemical properties. The past two decades have seen a number of valuable works devoted to ionic liquid/cellulose processing systems to develop materials for a variety of applications. Nevertheless, there has been no systematic review published so far that would discuss material fabrication and structure in detail with a clear focus on applications. Therefore, it is time to summarise the experiences gained and highlight valuable discoveries in this field. Our aim is to discuss the emerging applications of cellulose-based advanced materials fabricated using ionic liquids from a materials science perspective, in order to give guidance in this field, and stimulate more research on these green cellulose processing systems. We really hope that this review will be helpful also for those interested in materials, but have not yet necessarily worked with ionic liquids before, to promote this topic among a wider readership and thereby facilitate industrial implementations.

2. Solid-state structure of cellulose

Cellulose is a linear-chain polymer composed of repeating β-D-glucopyranose units linked through glycosidic bonds connecting the C4 and C1 carbon atoms of neighbouring groups (Fig. 1). Due to these β-1,4 linkages, adjacent *anhydroglucose (AGU) units* are rotated 180° in plane along the chain, preferring a $^4C_1$ chair conformation. Two rings connected through β-1,4 linkages give the repeating disaccharide cellobiose units. The number of glucopyranose units is defined as the *degree of polymerisation (DP)*, which is used to describe the chain length of cellulose that can vary depending on the source and extraction/treatment method.

There are three –OH groups per glucopyranose units, which partly determines the reactivity of the polymer. These free

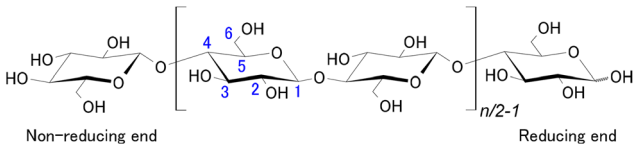

Fig. 1 Molecular structure of cellulose. *n*: degree of polymerisation.

hydroxyl groups provide exceptional tunability to the molecule, a wide variety of cellulose derivatives have been synthesised with various properties.[4] The amount of substituents on the hydroxyl groups is described with the *degree of substitution (DS)*, which takes a value of 3 for a fully substituted derivative (all hydroxyl groups are occupied). Chain degradation can take place under acidic or enzymatic hydrolysis of the glycosidic bonds, which can eventually lead to cellulose decomposition into monomeric sugars.[5] In addition, one end of the polymer chain is terminated with a monomeric unit that has the original C1–OH group. This part of the molecule is in equilibrium with the aldehyde form, a phenomenon known as *mutarotation*, and therefore, it is called the reducing end. Although reactions targeting the *reducing end* has been known for quite long,[6] *end-wise modification* has recently gained interest for nanocelluloses that can enable novel routes to their directed assembly.[7]

Cellulose is the most abundant *optically active natural macromolecule*, the *stereoregular sequences* in its structure enables chiral recognition. Several cellulose derivatives have found success in enantiomeric separation, for example as chiral separation phases for gas and liquid chromatography.[8]

The hydroxyl groups form complex *hydrogen bonding network*, determining the supramolecular arrangement of cellulose chains with various identified polymorphs and amorphous domains in the solid state. *Cellulose polymorphs* are

László Szabó

László Szabó obtained his PhD in Chemical Sciences in 2016 from the Budapest University of Technology and Economics, Hungary. He did his Postdoctoral studies in Kanazawa University (Japan) from 2017 to 2020. Between 2020 and 2022, he worked at the National Institute for Materials Science (NIMS, Japan) as an ICYS Research Fellow. He was awarded a Marie-Curie Fellowship in 2022, and stayed for a short time in KU Leuven (Belgium). From April 2023, he joined the Forestry and Forest Products Research Institute (Japan) as a tenured Senior Researcher. His broad research interest centres around environmentally more benign material concepts.

Romain Milotskyi

Romain Milotskyi obtained his Master's degree in Chemistry from Le Mans University in 2014. He moved to University of Reims Champagne-Ardenne, where he received his PhD in 2017, studying biomass chemical modification using reactive extrusion under the supervision of Dr Christophe Bliard. In 2018, he took up a position as Postdoctoral Researcher in the group of Prof. Kenji Takahashi in Kanazawa University where he worked on cellulose dissolution and chemical modification in ionic liquids. In 2022, he was appointed Assistant Professor and COI-NEXT Project Subleader in the same group, working on intensification of biomass processing using ionic liquids.

grouped into 4 types: *cellulose I* (there are two subtypes which are present concomitantly: I_α and I_β) which can be found in native cellulose, and thermodynamically more favoured *cellulose II, III and IV* crystal structures can be obtained irreversibly under certain conditions (Fig. 2A). *Cellulose II* allomorph is the most stable, and it is also the most important for materials science. It forms from cellulose I after mercerisation (treatment with aqueous NaOH), or after dissolving native cellulose followed by precipitation in an antisolvent – a process often called *regeneration*. The latter method is widely used to shape cellulose into various materials, such as regenerated films, fibres and numerous composites. As notable difference, in the cellulose I allomorph the chains are oriented parallel in the unit cell, while cellulose II has antiparallel chain polarity.[9,10] Furthermore, while for cellulose I the hydroxymethyl groups ($-CH_2OH$) adopt a *trans–gauche* (*tg*) conformation (Fig. 2B), they have a *gauche–trans* (*gt*) conformation in cellulose II.[11,12] The hydrogen bonding network also differs in these crystal structures. It was reported that the intramolecular hydrogen bonds in cellulose I_β are well defined, while the intermolecular hydrogen bonds connecting sheets are rather disorganised.[11] In cellulose II a more ordered, single hydrogen bonding system exists that forms a three-dimensional network.[12] In contrast, cellulose III is obtained by treatment of cellulose I or II with liquid ammonia. Cellulose III prepared from cellulose I is referred to as cellulose III_I in contrast to the allomorph cellulose III_{II} prepared from cellulose II. The detailed structural differences between cellulose III_I and cellulose III_{II} have not been determined.[13] It was reported that cellulose IV is formed by heat treatment of both cellulose III_I and III_{II} in glycerol,[14] although some studies debate the existence of this allomorph.[10] Fig. 3 highlights a schematic representation of the allomorphs of cellulose. It was previously reported that cellulose III exhibits enhanced hydrolysis by cellobiohydrolase I, producing cellobiose at rates more than five times higher than from cellulose I.[15] It was also shown that the surface hydrophi-

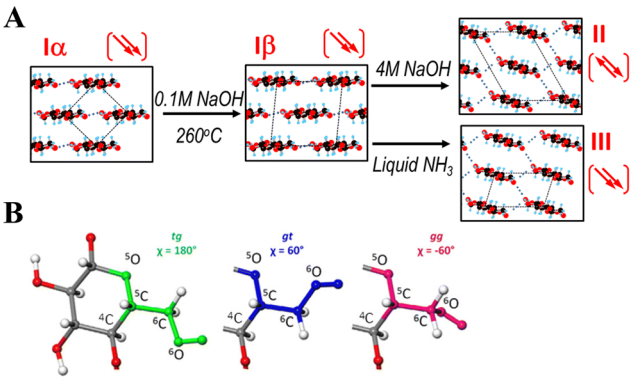

Fig. 2 (A) Formation of polymorphs under certain conditions. Arrows indicate the chain polarity, which is antiparallel for cellulose II. Chain orientation is shown on the *a*–*b* plane of the unit cell. (B) Possible conformations of the hydroxymethyl groups ($-CH_2-OH$), *tg*: *trans–gauche*, *gt*: *gauche–trans*, *gg*: *gauche–gauche*. χ indicates angles between the C5–O5 and C6–O6 bonds. Reproduced from ref. 10 with permission from Springer Nature, copyright 2019.

licity/hydrophobicity of the regenerated cellulose films can be controlled by post-treatment with liquid ammonia, or hot glycerol, due to the inherent structural anisotropy of the AGU. These results were supported by contact angle measurements as well.[16]

Cellulose can be available as *raw material* from numerous sources, with varying degree of polymerisation and crystallinity. Plant-based cellulose in its purest form can be found in *cotton fibres* (nearly 90%), this type of cellulose has high degree of polymerisation (DP) (plant fibres have DP values about 800–10 000 depending on the treatment) and crystallinity (*crystallinity index*[18] *(CI)* ≈ 50–80%).[19,20] Cellulose can be produced as an exopolysaccharide in very pure form by some bacteria. This type of cellulose is called *bacterial cellulose* or *microbial cellulose*, it can have very high degree of polymeris-

Gyanendra Sharma

Gyanendra Sharma received his PhD in Chemistry from the Indian Institute of Technology Madras. He joined Kanazawa University as Postdoctoral Fellow and now works as a specially assigned Assistant Professor in the Institute of Science and Engineering department. He has worked 10 years on ionic liquids synthesis and their applications, and co-authored 20 articles that include one Indian patent. From 2019, he started working on polysaccharides dissolution and processing. Currently he is working on modification of polysaccharides and developing biodegradable plastic materials.

Kenji Takahashi

Kenji Takahashi received his PhD in 1994 from Hokkaido University. As a researcher belonging to the Ministry of Education, Culture, Sports, Science, and Technology in Japan, he joined the Radiation Chemistry Group of Dr Charles Jonah at Argonne National Laboratory in USA, where he worked from 1995 to 1996. He was then appointed Associate Professor at Kanazawa University in 2003 and Professor in 2012. His research group is currently working on the use of ionic liquids in reaction and material engineering for biomass refineries. He is now Project Leader of COI-NEXT by JST & MEXT.

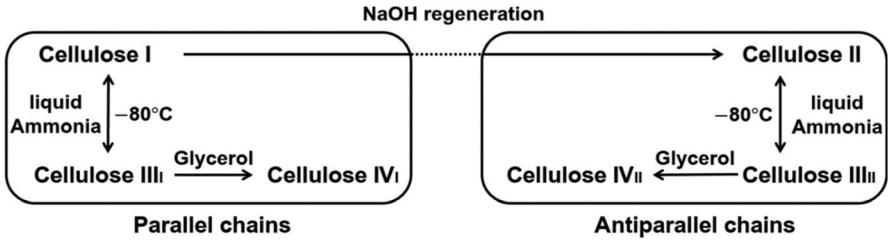

Fig. 3 Phase transition between various crystalline allomorphs of cellulose (cellulose I, II, III, and IV). Reproduced from ref. 17, copyright 2021 The Authors.

ation (DP > 10 000) and crystallinity (with CI > 80%).[21,22] Wood has about 40–50% cellulose content. After removing lignins and the hemicelluloses *via* chemical or mechanical means (pulping), *wood pulp* can be obtained. A specialty pulp called *dissolving pulp* is produced after chemical refining (*e.g.*, sulphite pulping or kraft pulping processes) and bleaching.[23] Dissolving pulp is characterised by high cellulose content (>90%) and a relatively uniform molecular weight distribution. It is an important form of technical cellulose used commercially in large quantities to prepare cellulose derivatives, regenerated cellulose and other materials. By acidic hydrolysis, *microcrystalline cellulose* can be produced from dissolving pulp, this material has relatively low molecular weight (DP 25–300), and gained interest for numerous applications (*e.g.*, pharmaceutical, food industry, *etc.*).

Another intriguing class of cellulose materials can be isolated after disintegrating the cellulose microfibrils into nanosized domains *via* chemical, mechanical or enzymatic means. The obtained *cellulose nanocrystals (CNCs)* or *nanofibers (CNFs)* have found great scientific and industrial interest. Ionic liquids can be also used for the fabrication of these materials from cellulose microfibrils. This topic has been summarised in a recent work,[24] and is excluded from this review.

This review will focus on material fabrication processes that are mostly based on the dissolution of cellulose in ionic liquids, except some special cases (ionogels based on gel-forming cellulose derivatives, bacterial cellulose and nanocellulose in combination with non-dissolving ionic liquids, see section 4.7.1).

3. Dissolution of cellulose in ionic liquids

On account of its high molecular weight, and the existence of strong intra- and intermolecular hydrogen bonding network with highly ordered crystalline domains, cellulose has low solubility in common single-component solvents, and is not melt processable. These features posed considerable obstacles for materials scientists aimed at shaping cellulose into functional structures. For long time, heterogeneous systems have been applied to chemically modify cellulose without complete solubilisation,[4] in order to prepare readily soluble and melt-processable derivatives (such as thermoplastic cellulose esters soluble in a range of organic solvents). There have been great efforts towards developing solvent systems able to directly dissolve cellulose, facilitating its direct shaping into various materials (fibres, films, composites, *etc.*), and enabling greener and controllable homogeneous chemical modification. Several aqueous (aqueous inorganic metal complexes, such as cuprammonium hydroxide; molten inorganic salt hydrates, such as $LiCl{\cdot}5H_2O$; aqueous solution of alkali hydroxides, such as NaOH/urea/H_2O; *N*-methylmorpholine *N*-oxide (NMMO) monohydrate), non-aqueous (*e.g.*, *N*,*N*-dimethylacetamide (DMA)/LiCl; dimethyl sulfoxide (DMSO)/tetrabutylammonium fluoride (TBAF)), and derivatising (*e.g.*, the viscose process through cellulose xanthate; *N*,*N*-dimethylformamide (DMF) or DMSO with N_2O_4) solvent systems have been studied. These solvent systems all have some demerits (*e.g.*, toxicity/non-recyclability/instability), which have been extensively recognised and critically evaluated in the literature.[4,25,26] The introduction of ionic liquids as direct, tunable solvents for cellulose opened new horizons in this field, leading to exciting material discoveries and properties that have not been seen before (*e.g.*, see section 4.7.1).

The first group of ionic liquids to dissolve cellulose with melting points below 100 °C were based on *dialkylimidazolium cations* (see Fig. 4) in combination with chloride, bromide and thiocyanate anions.[1] Among the studied ionic liquids, 1-butyl-3-methylimidazolium chloride ([Bmim][Cl]) was the most powerful solvent able to dissolve cellulose at 10 wt% concentration when heated to 100 °C, and up to 25 wt% with the help of microwave heating. Furthermore, 1-allyl-3-methylimidazolium chloride ([Amim][Cl]) and 1-ethyl-3-methylimidazolium acetate ([Emim][Ac]) were also reported to dissolve cellulose even at high loading around 100 °C (up to 30 wt%).[27–29] These ionic liquids have lower melting points and lower viscosities after cellulose dissolution, making them more attractive for industrial application compared to [Bmim][Cl]. Following these initial reports, the effect of the structure of the anion and cation on cellulose solubility was comprehensively studied.[30] It appeared that ionic liquids with strong dissolution power contain anions with strong hydrogen bond basicity, such as chloride,[1] carboxylate (*e.g.*, formate, acetate, lactate),[31–35] amino acid,[36] phosphate or phosphonate anions.[37] Likewise, ionic liquids containing anions with poor ability to form hydrogen bonds with the hydroxyl groups of cellulose can be classified as non-solvents, anions of hexa-

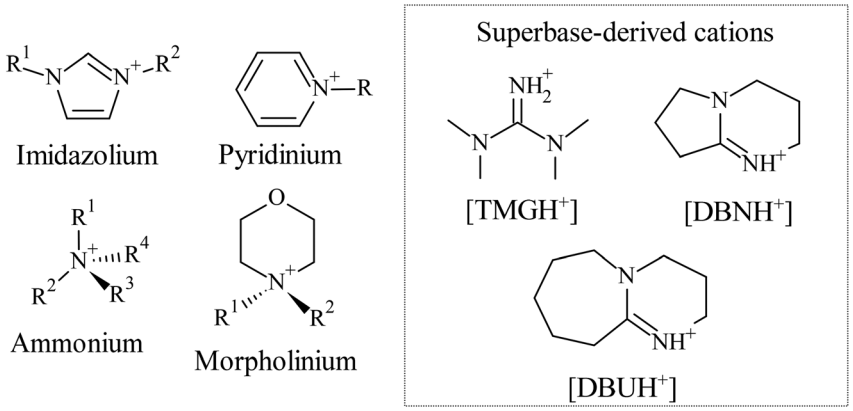

Fig. 4 Typical cations of ionic liquids with ability to dissolve cellulose.

fluorophosphate ($[PF_6]$), tetrafluoroborate ($[BF_4]$), dicyanamide ($[N(CN)_2]$) and bis(trifluoromethylsulfonyl)imide ($[NTf_2]$) are some of the examples. Some non-solvents of cellulose containing $[MeSO_4]$ and $[HSO_4]$ anions can dissolve hemicellulose and lignin, these ionic liquids gained appreciable interest for the pretreatment of lignocellulosic biomass.[38–40] Effect of the structure of imidazolium cations on the solubility of cellulose was also addressed in several works.[41,42] Long alkyl chain substituents, and moieties that increase the hydrogen bond acidity, have in general a negative effect on cellulose dissolution. It should be noted that, although dialkylimidazolium carboxylate ionic liquids, such as [Emim][Ac], may be favourable for industrial application (low melting point and viscosity compared to other cellulose dissolving ionic liquids), they are not inert media for cellulose solubilisation as reaction can take place at the reducing end of the polymer.[43] Nevertheless, such side reaction does not take place in [Bmim][Cl].

Pyridinium-based ionic liquids (Fig. 4) that are capable of dissolving cellulose, such as 1-butyl-3-methylpyridinium chloride ([BmPyr][Cl]),[44] along with other analogues,[45] were also reported. Depolymerisation of cellulose, and other side reactions were recognised in pyridinium-based ionic liquids, *e.g.*, in 1-ethylpyridinium chloride ([EtPyr][Cl]),[46] limiting their applications.

Some *quaternary ammonium-based* ionic liquids (Fig. 4) containing carboxylate anions were also reported as efficient solvents of cellulose. Ammonium ionic liquids with cyclohexyl substituent,[47] with dialkoxy functional groups,[48] with PEG side chains,[49] and derivatives with long alkyl chains[50] are some of the reported examples. Benzyl alkylammonium ionic liquids containing acetate anion were also reported to dissolve cellulose.[51] The aromatic structure in the latter work was derived from lignin monomers.

Ionic liquids based on the *morpholinium* cation (Fig. 4) proved also efficient to dissolve cellulose. It was reported that 4-benzyl-4-methylmorpholinium formate ([BMmorf][HCOO]) or acetate ([BMmorf][Ac]) can dissolve cellulose; the advantage of this type of ionic liquid is the moderate to low toxicity as evaluated by Pernak *et al.*[52] Later, *N*-allyl-*N*-methylmorpholinium acetate ([AMMorp][Ac]) was introduced as an excellent solvent able to dissolve up to 30 wt% of cellulose at 120 °C without degradation of the polymer.[53,54]

An intriguing class of ionic liquids to dissolve cellulose are *derived from superbases* (Fig. 4). First reported examples are based on cations derived from polycyclic amidine bases,[55] such as 1,5-diazabicyclo-[4.3.0]non-5-ene ([DBN]) and 1,8-diazabicyclo[5.4.0]undec-7-ene ([DBU]). When paired with carboxylic acids, such as acetate or propionate, cellulose solutions with relatively low viscosities could be obtained.[56] Another intriguing example is based on 1,1,3,3-tetramethylguanidine ([TMG]) organic superbase in combination with short-chain carboxylic acids (formic, acetic, propionic).[57] The advantage of superbase-derived ionic liquids, besides their relatively low cost and simple preparation, is that they can be readily distilled and recycled with high purity (*e.g.*, in some cases at much higher pressures than [Emim][Ac], affording more cost-effective recovery of the ionic liquid).[56]

It should be noted that cellulose solubility in ionic liquids greatly depends on the degree of polymerisation of the starting material, the temperature and method of heating (*e.g.*, microwave-assisted heating can greatly enhance solubility[1]), the amount of water and other impurities (*e.g.*, for tetrabutylammonium acetate/DMSO system some alkali metal ion impurities have negative effect on the dissolution process[58]) present in the solvent.[59] Furthermore, the addition of aprotic co-solvent to ionic liquids, such as DMSO, DMF, *etc.*, can enhance their dissolution power for cellulose.[59–61] This phenomenon might be explained by the decreasing viscosity of the system, which increases the mass transport while not affecting the forming hydrogen bonding network in the solution involving the ionic liquid and the polymer.[60] Furthermore, other additives, such as solid acids (*e.g.*, Amberlyst® 15 and $Cs_xH_{3-x}PW_{12}O_{40}$ in [Bmim][Cl])[62] and metal chlorides (*e.g.*, $ZnCl_2$, LiCl, or NaCl in [Amim][Cl])[63] were reported to enhance cellulose dissolution (*i.e.*, higher cellulose loading/shorter dissolution time/lower temperature). In a report by Yang *et al.*,[64] the addition of an amino acid, L-arginine could prevent cellulose degradation in [Bmim][Cl],

[Emim][Cl] and [Amim][Cl] ionic liquids when dissolution was performed at 130 °C for long time (24 h).

The dissolution mechanism of cellulose in ionic liquids has been the subject of intense discussions and debates over the years. Interested readers are directed to the comprehensive review of Li *et al.*[65] It may be of interest for the reader to understand some of the selection criteria to obtain suitable ionic liquid for dissolving cellulose. It has been known that the difficulties of cellulose dissolution in common organic solvents resides in the strongly concentrated hydrogen bonds present in cellulose, as we mentioned above. There are two major factors that most of the studies consider: a solvent with high hydrogen bond basicity is needed to break down the hydrogen bonding network, and it should be considered that water impurities can negatively affect the dissolution ability of such systems.[30,66] Nevertheless, this is not the case for *organic onium/inium hydroxide aqueous solutions (OHAS)*, an intriguing class of ionic liquids that needs the presence of water (upon drying they would decompose). For example, tetrabutylphosphonium hydroxide ($[P_{4444}][OH]$) and tetrabutylammonium hydroxide ($[N_{4444}][OH]$) can dissolve cellulose with presence of 40 wt% water.[67] It was reported that a weaker hydrogen bonding network around the H_2O and [OH] is preferred in these cases (*i.e.*, strong self-associating behaviour of the IL is unfavourable), as followed by the chemical shift of the protons of water molecules.[68] It is of utmost importance to develop ionic liquids that can tolerate water content, which is naturally present in biomass.

4. Cellulose-based materials using ionic liquids as processing media

4.1. Coatings and thin films

4.1.1. Conventional processing systems. Cellulose esters, such as cellulose acetate (CA), cellulose acetate propionate (CAP) and cellulose acetate butyrate (CAB) are excellent additives in *coating and ink formulations* for a wide range of substrates, including metals, plastics, wood, leather, paper, cloth, *etc.*[69] They are considered superior compared to nitrocellulose that can yellow over time, and is flammable. As an advantage, by properly selecting the degree of substitution and molecular weight of these esters, their properties can be customised for specific applications. Nevertheless, serious environmental concerns surround the application of volatile organic compounds (VOCs) as solvents for preparing the coating formulations. VOCs emissions are subject to strict regulations both in the EU (under the VOC Solvents Emissions Directive[70]), and in the US (National Volatile Organic Compound Emission Standards under the Clean Air Act[71]). In order to comply with these requirements, efforts have been made to develop water-dispersible, and radiation-curable (these formulations contain non-volatile monomers acting as both solvent and reactant) cellulose esters as greener alternatives.[72–74] Some cellulose esters with high hydroxyl content exhibit enhanced hydrophilicity, and show good properties in *waterborne coating formulations*. Furthermore, water-dispersible/soluble derivatives can be obtained by introducing carboxyl group to the cellulose ester structure *via e.g.*, grafting acrylic acid onto cellulose esters, reacting them with succinic/phthalic anhydrides, oxidising the corresponding cellulose ester (*e.g.*, using O_3 as oxidant), or by preparing cellulose acetoacetate esters.[74] In addition, esterification of carboxymethyl cellulose was shown to represent another option to obtain water-dispersible esters for coating applications (*e.g.*, carboxymethyl cellulose acetate butyrate[75]). More recently, an unconventional mixed cellulose ester with biomass-derived levulinic acid was prepared, and modified to obtain a carboxymethylamino derivative (Fig. 5(a)), and its application in waterborne coating formulations was demonstrated.[76] Based on this progress, fully biobased levulinate ester (Fig. 5(b)) was also synthesised by using alpha-angelica lactone in 1.8-diazabicyclo[5.4.0]undec-7-ene ([DBU])/dimethyl sulfoxide/carbon dioxide organocatalytic reaction system.[77] The levulinate ester with moderate DS (1.2 for the levulinate group, and 0.13 for the pseudo-levulinate moiety) showed good properties for possible applications in waterborne film preparations and coatings in limited water environments.

Thin cellulose ester films have found applications in a range of devices (*e.g.*, in liquid crystal displays (LCDs)) as protective *optical films*, based on their high transparency, unique optical characteristics, together with excellent heat resistance, and mechanical properties.[73,74,78] Advanced polariser protective films and optical retardation films can be achieved using cellulose esters by chemical modification or by specific additives.[78]

Various cellulosic films were developed for *food packaging* applications. The most notable example is cellophane, which is produced through cellulose xanthate (viscose). The viscose process, however, requires high-quality pulp and suffers from its large environmental footprint due to the use and generation of toxic chemicals and byproducts (*e.g.*, sulphur byproducts,[79] heavy metals[80]). Several alternative methods have been developed using cellulose derivatives (cellulose acetate, methyl cellulose, carboxymethyl cellulose[81]), nanocellulose films,[82] and environmentally more friendly processing systems for cellulose dissolution and regeneration (through cellulose

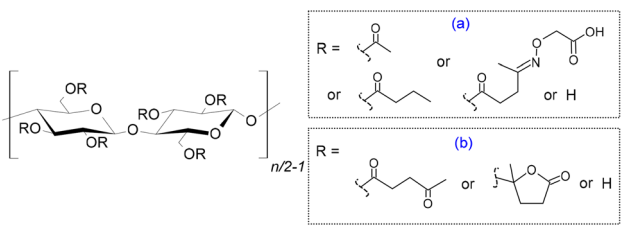

Fig. 5 Mixed cellulose ester obtained by using levulinic acid and acyl anhydrides as reactants, followed by the reaction of the corresponding mixed ester with (aminooxy)acetic acid to afford the water-dispersible derivative (a);[76] and obtained thorough alpha-angelica lactone in 1.8-diazabicyclo[5.4.0]undec-7-ene ([DBU])/dimethyl sulfoxide/carbon dioxide organocatalytic system (b).[77]

carbamate in the CarbaCell process, and using *N*-methylmorpholine *N*-oxide (NMMO)[83]).

Cellulosic coatings have gained importance in *controlled-release* applications as well. Cellulose esters,[74] cellulose ethers,[84] different forms of nanocelluloses,[85] and cellulose-based hydrogels[86] have found applications in large variety of *drug delivery systems in the biomedical field*. Cellulosic materials can be conveniently modified for targeted applications and can be readily used to create intrinsically biocompatible systems, which greatly contributed to their success in this field. Furthermore, based on their environmentally benign character, several cellulosic materials are used also for *controlled release in agrochemical formulations*.[87]

4.1.2. Use of ionic liquids for coating and thin film applications. Cellulose dissolved in an ionic liquid can be regenerated using an antisolvent (*e.g.*, water, acetone, *etc.*). Depending on this step, the *regenerated cellulose* can be shaped into various forms, such as films with various thicknesses. Please note that recycling of the ionic liquid is crucial for the sustainability and economic feasibility of the process, these aspects will be discussed later (see section 5).

Table 1 shows a list of selected works[88–100] devoted to the fabrication of regenerated cellulose films for *e.g.*, packaging application using various ionic liquids such as [Amim][Cl],[88–90,97] [Bmim][Cl],[91–95,97] [Bmim][Ac][92] and [Emim][Ac].[88,96–100] Transparent films could be obtained (Fig. 6) with optical transmittance values in some cases greater than that of commercial cellophane (optical transmittance: 85%).[92,97,98] The barrier properties (oxygen and water vapor permeability) of the regenerated cellulose films can be controlled by additives such as plasticisers, as demonstrated by Jin *et al.*[91] Furthermore, in the cellulose/ionic liquid solution active agents can be dissolved such as curcumin (using [Amim][Cl]) to prepare antibacterial regenerated cellulose films,[101] or the regenerated cellulose film can be post-modified to obtain films with antibacterial[102] or antioxidant[103] properties for state-of-the-art *active food packaging applications*.

The *degree of polymerisation (DP) and crystallinity index was strongly correlated with the mechanical properties of the regenerated cellulose films in several works*.[88,95–98] It was suggested that above a certain level of DP (given as ~450), the mechanical properties are dominated mostly by the crystallinity.[96] In addition, other secondary interactions such as intra- and intermolecular hydrogen bonding, and hydrophobic stacking interactions are also important in shaping the physical properties of the material. In general, *the structure of cellulose changes from cellulose I to cellulose II as a result of the regeneration process* (Fig. 7). The crystallinity index also decreases compared to the native cellulose, a more amorphous material is usually obtained. Cellulose II is known to be thermodynamically favoured, its stability is attributed to ring-stacking *via* hydrophobic interactions and to additional hydrogen bonding interactions between sheets (inter-molecular), forming a three-dimensional structure (see section 2).[99]

The crystallinity of the regenerated cellulose can be influenced by several factors, such as the coagulation process. Östlund *et al.*[99] dissolved pulp in [Emim][Ac], and studied the effect of the coagulation media (water, ethanol and 1-propanol) on the structure of the regenerated cellulose. When water was used as coagulation medium, mainly cellulose II structure was obtained, while other solvents yielded mostly amorphous films. This was explained by the slow diffusion of [Emim][Ac] to ethanol/1-propanol compared to water on account of their lower solubility for [Emim][Ac]. The hydroxymethyl group in cellulose dissolved in [Emim][Ac] is in *gauche–trans* (*gt*) conformation, which can be trapped in this stage during fast solvent exchange (in water). This conformation is beneficial for the formation of the cellulose II structure (hydroxymethyl group is in *gt* conformation in contrast to native cellulose I with *trans–gauche* conformation, see section 2, Fig. 2). Furthermore, *molecular mobility was suggested to be another factor that can have an effect on the crystallinity* of the regenerated films. Zheng *et al.*[97] studied the effect of ionic liquids with increasing dissolution power ([Bmim][Cl] < [Amim][Cl] < [Emim][Ac]) on the properties of the regenerated cellulose. They found that the cellulose regenerated from [Amim][Cl] solution had the highest tensile strength, which was attributed to its highest crystallinity among the samples. They argued that the higher crystallinity was due to the lower molecular weight of the sample compared to the others, resulting in enhanced molecular mobility aiding molecular arrangement during the regeneration process. The regenerated cellulose film from [Amim][Cl] showed excellent transparency (90% at 550 nm) according to their study. Pang *et al.*[96] compared the properties of regenerated films from different cellulose starting materials (microcrystalline, cotton linter, pine, bamboo celluloses) dissolved in [Emim][Ac]. They found that pine-derived cellulose sample with high DP (559) and crystallinity index (39.58%) gave the highest mechanical performance (tensile strength of 120 MPa), compared to the poorly performing microcrystalline cellulose that had although high crystallinity index (40.58%), its DP was the lowest (145) among the samples.

Several studies point out the *importance of dissolution conditions*, such as time and temperature on the structure of the regenerated cellulose, and thus on its mechanical properties.[88,95] Cao *et al.*[88] prepared regenerated cellulose films from cornhusk cellulose using [Amim][Cl] and [Emim][Ac] ionic liquids. They realised that the DP decreases with increasing dissolution time and temperature, and the latter had greater effect on cellulose degradation (Fig. 8). Chen *et al.*[95] reached a similar conclusion when dissolving wheat straw cellulose in [Bmim][Cl]. By optimising the dissolution time and temperature to avoid substantial cellulose degradation (*i.e.*, decrease in DP), a regenerated cellulose film with high tensile strength could be obtained (170 MPa).

Regenerated cellulose films can show brittle characteristics, which can be disadvantageous for packaging applications. To overcome this limitation, several studies focused on *including plasticisers* (sorbitol, glycerol and carboxymethyl cellulose (CMC)) in the ionic liquid/cellulose solution before the regeneration process using [Amim][Cl][90] and [Emim][Ac] solvent systems.[98] Interestingly, the crystallinity indices of the regener-

Table 1 Regenerated cellulose films from ionic liquids, for applications as structural materials (*e.g.*, packaging). Degree of polymerisation (DP) and crystallinity index (CI in %) of the [a]starting materials, and the [b]regenerated films. [c]Tensile strength in MPa [d](elastic modulus in GPa)

Type of cellulose	DP[a]	CI[a]	Ionic liquid	Cellulose concentration	Dissolution temperature (time)	DP[b]	CI[b]	Mechanical properties	Note	Antisolvent	Ref.
Corn husk-derived	509	59.6	[Emim][Ac]	4 wt%	80 °C (2 h)	370	47.9	47[c] (4.11)[d]	—	Water	88
			[Amim][Cl]	4 wt%	80 °C (4 h)	410	49.5	112[c] (6.01)[d]		Water	
Agave-derived cellulose microfibrils	—	64.4	[Amim][Cl]	4 wt%	80 °C (–)	—	55.9	135[c] (8.15)[d]	Remaining undissolved cellulose microfibrils as "self-reinforcing" agents	Water	89
Cotton linter fiber	920	54	[Amim][Cl]	5 wt%	90 °C (30 min)	—	38	~50[c] (–)[d] No plasticiser	Addition of plasticisers (glycerol, sorbitol, carboxymethyl cellulose).	Water	90
Softwood pulp	1460	77.3	[Bmim][Cl]	6 wt%	80 °C (8 h) with static conditions, then 95 °C (3 h) with stirring	—	32.9	52.8[c] (–)[d] No plasticiser	Effect of plasticiser (glycerol).	1. 10 vol% [Bmim][Cl] in water; 2. film immersed in glycerol/H_2O	91
Microcrystalline	—	—	[Bmim][Cl]	4 wt%	85 °C (7 h)	—	—	1.3[c] (–)[d]	Fluorescent sensing composite	Water	92 and 93
			[Bmim][Ac]	14 wt%	50 °C (7 h)	—	—	12.51[c] (–)[d]	Adsorption study	Water	92
Natural luffa fiber-derived	—	—	[Bmim][Cl]	15 wt%	80 °C (10 h), then 100 °C (5 h, under vacuum)	—	—	—	Nanoporous film	Water	94

Type of cellulose	DP[a]	CI[a]	Ionic liquid	Cellulose concentration	Dissolution temperature (time)	DP[b]	CI[b]	Mechanical properties	Note	Antisolvent	Ref.
Wheat straw-derived	580	—	[Bmim][Cl]	5 wt%	90 °C (12 h)	470	—	170[c] (–)[d]	Effect of dissolution time and temperature	Water	95
Microcrystalline	240	51.36	[Emim][Ac]	5 wt%	Stirring at 80 °C (0.5 h);	145	40.58	69[c] (–)[d]	—	Water	96
Cotton linter	831	54.01			then standing at 80 °C for	570	34.04	~105[c] (–)[d]			
Pine-derived	819	49.02			1 h (for degassing)	559	39.58	120[c] (–)[d]			
Bamboo-derived	625	46.69				460	32.93	~80[c] (–)[d]			
Coniferous dissolving pulp	500	73.8	[Amim][Cl]	3 wt%	90 °C (0.5 h)	354	52.4	152[c] (–)[d]	—	Water	97
			[Bmim][Cl]			400	49.2	75[c] (–)[d]			
			[Emim][Ac]			451	44.8	50[c] (–)[d]			
Cotton linter	920	—	[Emim][Ac]	~5 wt%	80 °C (5 min)	—	34 (no plasticiser)	84.5[c] (–)[d]	Addition of plasticiser (sorbitol, glycerol and CMC)	Water	98
Never dried commercial 96α *Eucalyptus* dissolving pulp	—	—	[Emim][Ac]	4 wt%	Drying overnight at 60 °C, followed by continuous stirring at 60 °C for 2 h	—	—	—	Effect of the coagulation medium	Water/ ethanol/ 1-propanol	99
Microcrystalline cellulose	—	65	[Emim][Ac]	0.1–2 wt%	50 °C (overnight)	—	—	—	Ultrathin 10 nm thick film	Ethanol	100

[a] Degree of polymerisation (DP) and crystallinity index (CI in %) of the starting materials. [b] Degree of polymerisation (DP) and crystallinity index (CI in %) of the regenerated films. [c] Tensile strength in MPa. [d] Elastic modulus in GPa.

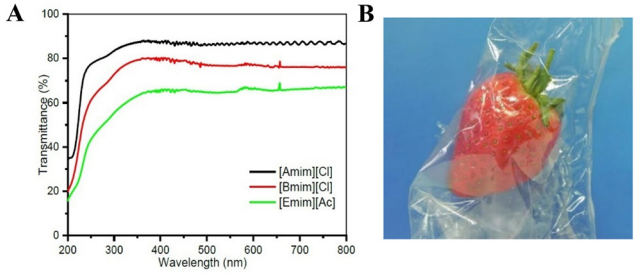

Fig. 6 (A) Transmittance of cellulose films regenerated from ionic liquids in water as coagulant (the film from [Amim][Cl] has transparency of about 90% at 550 nm). Reproduced from ref. 97 with permission from Elsevier, copyright 2018. (B) Transparent regenerated cellulose film for food packaging application (cotton linter cellulose dissolved in [Emim][Ac], containing 25% glycerol as plasticiser). Reproduced from ref. 98 with permission from Springer Nature, copyright 2013.

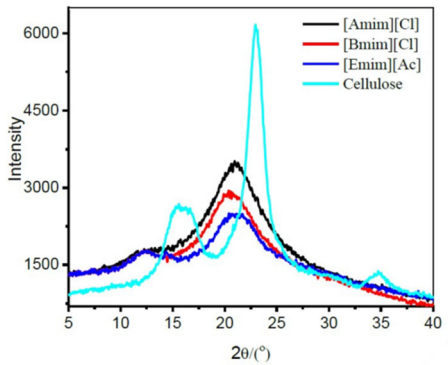

Fig. 7 X-ray diffraction (XRD) patterns of native cellulose (coniferous dissolving pulp), exhibiting typical cellulose I structure, and that of the films regenerated from different ionic liquids in water with XRD profiles typical for a cellulose II structure. Crystallinity index: [Amim][Cl] > [Bmim][Cl] > [Emim][Ac]. Reproduced from ref. 97 with permission from Elsevier, copyright 2018.

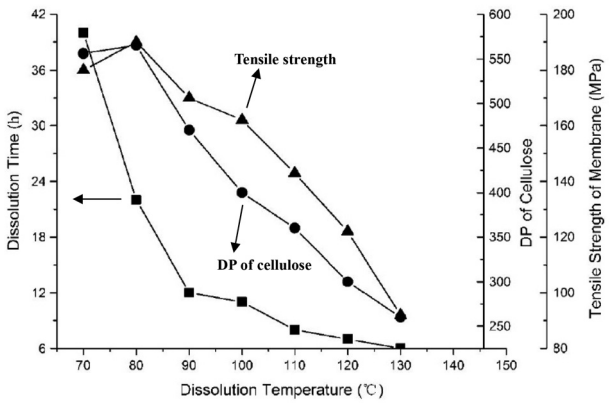

Fig. 8 Effect of dissolution time and temperature on the tensile strength and degree of polymerisation (DP) of regenerated cellulose (dissolved in [Bmim][Cl], regenerated in water). Reproduced from ref. 95 with permission from Wiley, copyright 2012.

ated cellulose films with plasticisers decreased when [Amim][Cl] was used, meanwhile an increase was observed for [Emim][Ac] compared to a control regenerated cellulose film without plasticiser. In all cases, an increase in the tensile strength was observed by the addition of the plasticiser, which was attributed to secondary interactions forming between cellulose and plasticiser molecules. Somewhat different result was obtained when the regenerated film (using [Bmim][Cl]) was immersed in a plasticiser solution as a post-treatment process instead of its direct inclusion in the ionic liquid solution.[91] In this case, tensile strength decreased, while elongation at break increased as an effect of the glycerol plasticiser.

The *hydrophilicity of the surface* is another important parameter for applications, such as for packaging films or thin film substrates. It is known that amorphous regions in regenerated cellulose are prone to swelling, these regions provide sufficient mobility that is advantageous for the orientational requirement of hydrogen bond formation with water molecules.[104,105] Since the crystallinity of the films regenerated from ionic liquids can be controlled to some extent depending on experimental conditions, this provides an opportunity to prepare films with various wettability. Amorphous cellulose film regenerated from [Emim][Ac] solution (DMSO co-solvent, ethanol coagulant) has low static water contact angle (~30°), similarly to amorphous thin films regenerated using other solvent systems.[100] Pang *et al.*[96] prepared regenerated cellulose films using [Emim][Ac] (water coagulant) with various crystallinity depending on the starting cellulose material. They observed high water contact angles (~73° for regenerated microcrystalline cellulose; ~77° for pine-derived regenerated cellulose) for the films with high crystallinity indices (see Table 1). This phenomenon was attributed to the different hydrogen bonding network in crystalline/amorphous samples. It was also demonstrated that plasticisers can also have an effect on the wettability of the surface. Pang *et al.*[90] showed that the presence of sorbitol/glycerol/CMC in the regenerated cellulose film ([Amim][Cl] solvent, water coagulation medium) leads to a significant increase in the recorded water contact angles (59°/74°/75°, respectively). They argued that surface morphology of the films, and interference of the plasticiser molecules with the hydrogen bonding network of cellulose contribute to a reduced surface free energy. Similar result was observed by Hameed *et al.*[106] with poly(3-hydroxybutyrate-*co*-3-hydroxyvalerate) (abbreviated as PHBV, a microbial biopolymer) as additive in regenerated cellulose blends using [Bmim][Cl] (water coagulant). In this case, however, it should be noted that PHBV regenerated from the ionic liquid has already hydrophobic character (with water contact angle of about 97°).

Several studies reported on the formation of a *nanoporous film* upon regeneration from ionic liquid solutions. Wang *et al.*[94] dissolved natural luffa-derived cellulose in [Bmim][Cl], and found that the regenerated film has nanopores with an average pore size of about 18 nm. Östlund *et al.*[99] studied the porosity of regenerated cellulose films ([Emim][Ac] solvent) through NMR cryoporometry, using various coagulation media

(water, ethanol and 1-propanol). In all cases, pores with radius below 15 nm were observed (spherical pore geometry model). It was also possible to obtain uniform porous structure with pore radius centred around 3 nm, using 1-propanol as coagulant, through repeated drying cycles.

Ultrathin regenerated cellulose films could also be prepared from an [Emim][Ac] solution containing 0.1 wt% cellulose (microcrystalline) that was spin-coated on a silicon wafer substrate, and regenerated using ethanol as antisolvent.[100] AFM image of the ultrathin film indicated the presence of fine nanofibrillar cellulose structure on the surface (Fig. 9).

Radiation-curable coating was also developed using *ionic liquid monomers that can dissolve cellulose*, this approach is considered a green alternative to coating systems that apply volatile organic solvents. Isik *et al.*[107,108] synthesised 2-cholinium lactate methacrylate monomer that dissolved 5–10 wt% cellulose. Photopolymerisation at 368 nm in the presence of 2,2-dimethoxy-2-phenylacetophenon photoinitiator afforded a transparent coating film from the 5 wt% cellulose/ionic liquid solution (Fig. 10). Cholinium-based cellulose-dissolving ionic liquids are advantageous due to their low toxicity, biodegradability, and low cost.[109]

The cellulose/ionic liquid system can be used to form regenerated cellulose coating also for *controlled drug release*. Song *et al.*[110] fabricated chitosan hydrogel beads that could be coated with regenerated cellulose by dropping the hydrogels in the cellulose/[Emim][Ac] solution. Regenerated cellulose coating was formed by the diffusion of water from the hydrogel. The fabricated material showed good properties for controlled drug release applications.

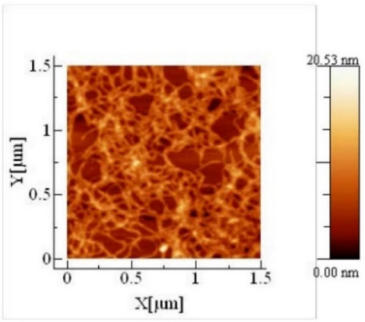

Fig. 9 Atomic force microscopy (AFM) image of cellulose ultrathin film regenerated from [Emim][Ac] solution (0.1 wt% cellulose), using ethanol as coagulant. Reproduced from ref. 100 with permission from Walter de Gruyter GmbH, copyright 2018.

4.2. Thin film filtration membranes

Cellulosic materials have long history in separation science dating back to ancient times (*e.g.*, just think about cotton cloth for filtering particles). Both natural and physically/chemically modified cellulose were shown to be efficient as adsorbent for water, organic solvents, metal ions and organic substances (such as dyes).[111] Furthermore, cellulose can be converted to various forms of activated carbons with high surface area, extending its efficiency and application to other adsorbates (*e.g.*, gases). Among the chemically modified cellulose derivatives, cellulose esters proved particularly successful as membranes in the separation field, basically covering all range of the filtration spectrum including micro-, ultra- and nanofiltration, reverse osmosis and dialysis applications.[74]

The introduction of ionic liquids as solvent of cellulose opened the gates for the preparation of novel thin film membranes directly from the natural polymer.

4.2.1. Regenerated cellulose filtration membranes *via* phase inversion using ionic liquids. Regenerated cellulose films from ionic liquids found applications also in *membrane science*, where *phase inversion* is a well-known way to prepare thin film membranes *via* immersion precipitation.[112] Table 2 shows selected works devoted to the fabrication of regenerated cellulosic membranes using ionic liquids. The first regenerated cellulosic membrane was made by Xing *et al.*[113] using cellulose acetate dissolved in [Bmim][SCN]. The choice of the ionic liquid was based on its low melting point (<−20 °C) and low viscosity (54 cP at 20 °C), enabling fast dissolution and processing of the cellulose derivative at room temperature. They recognised that the morphology of the resulting membrane is very different from membranes prepared using conventional solvents (such as *N*-methyl-2-pyrrolidone (NMP) and acetone in their work). While using the latter systems results in macrovoid formation, the membranes regenerated from ionic liquids have a dense structure full with nodules (Fig. 11A). They hypothesised that the mechanism of phase inversion is different when ionic liquids are used, the sequence of events possibly being nucleation growth and gela-

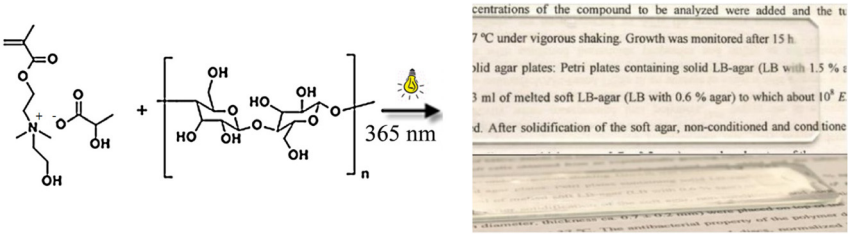

Fig. 10 Photopolymerisable cellulose coating using a cholinium-based ionic liquid methacrylic monomer as both solvent and crosslinker. Reproduced from ref. 107 with permission from the American Chemical Society, copyright 2013. A part reproduced from ref. 108 with permission from Wiley, copyright 2014.

Table 2 Regenerated cellulose separation membranes based on the phase-inversion method using various ionic liquids as solvents

Type of cellulose	Ionic liquid	Cellulose concentration	Dissolution temperature (time)	Membrane properties	Membrane thickness	Membrane performance	Antisolvent	Ref.
Cellulose acetate (39.8% acetyl content)	[Bmim][SCN]	10 wt%	50 °C (5 h)	Dense, macrovoid-free, self-standing membrane with low porosity (~6%)	8.72 μm	Pure water permeability: 114.14 L m^{-2} h^{-1} bar^{-1} (at 0.15 MPa). Mean pore size ~39 nm based on neutral solute rejection experiment (PEG/PEO solute)	Water	113
α-Cellulose (DP 300)	[Amim][Cl]	8 wt%	90 °C (25 min)	Dense, macrovoid-free, layered structure. Film casted on PET non-woven fabric	10.5 μm	Pure water permeability: 128.5 L m^{-2} h^{-1} at 0.4 MPa. Antifouling membrane could be developed for filtration of organic dyes with a MWCO less than 700 Da, and for BSA in PBS	Water	114
Wheat straw-derived (DP 580)	[Bmim][Cl]	5 wt%	90 °C (12 h)	Self-supporting asymmetric porous membrane. Dense thin surface layer with small holes, inner layer with bigger holes. Tensile strength of 170 MPa (6.4% breaking elongation)	~15 μm	Pure water flux of 238.9 L m^{-2} h^{-1} at 0.3 MPa. Rejection of BSA ~97%	Water	95
Bamboo fiber-derived	[Bmim][Cl]	3, 5, 10 wt%	80 °C (8 h)	Self-supporting membranes. Dense, nodular, macrovoid-free structure. Denser membrane fabricated from concentrated solution (10 wt%), showing higher rejection towards organic dyes (best performance)	—	Best performance: pure water-flux: 150 L m^{-2} h^{-1} (0.4 MPa); about 100% flux recovery ratio, good antifouling performance; maximum organic dye rejection: 89% (for crystal violet)	Water	115
Microcrystalline cellulose (M_w 160–560 kDa)	[Emim][Ac]	2, 5, 10 wt%	80 °C (24 h)	Regenerated cellulose membranes on various porous substrates. Self-supporting membrane showing good solvent-tolerance (THF, hexane, DMF, NMP, DMA)	0.4–6.8 μm	Lowest MWCO for the membrane prepared from 10 wt% cellulose solution. MWCO (using PEG) as low as 3000 g mol^{-1} with 13.8 L m^{-2} h^{-1} bar^{-1} at 0.5 MPa (polysulphone (PSU) support)	Water	116
Microcrystalline cellulose (M_w 160–560 kDa)	[Emim][Ac]	2, 5 wt%	60 °C (–)	Dense, selective coating on porous PSU substrate	0.4 μm, 0.9 μm	Oil could be selectively removed from the oil-in-water emulsions. The thin 0.4 μm coating gave the highest permeance and flux recovery – pure water permeance: 150 L m^{-2} h^{-1} at 0.5 MPa (90 L m^{-2} h^{-1} flux recovery for oil-in-water emulsion)	Water	117
Cotton linter	[Emim][Ac] (acetone as cosolvent for some samples)	8, 12, 20 wt%	70 °C or RT, samples with cosolvent	Self-supporting membranes. Dye rejection was correlated with membrane affinity (sorption), attributed to hydrogen-bonding and electrostatic interactions	—	Highest rejection (regenerated from 20 wt% cellulose solution) - 94% for bromothymol blue, with permeance of 0.3 L m^{-2} h^{-1} in ethanol at 0.4 MPa	Water	118
Cotton linter	[Emim][Ac] (DMSO as cosolvent for some samples)	8 wt%	70 °C or RT, samples with cosolvent	Self-supporting membranes. Dense, nodular, macrovoid-free structure. Symmetric morphology	—	Although cellulose membranes with different morphologies could be obtained by using cosolvent and different coagulation baths, the dried membranes performed similarly with high organic dye rejection (over 80%), water permeance 0.5–1 L m^{-2} h^{-1}, and ethanol permeance 0.1–0.3 L m^{-2} h^{-1} at 0.4 MPa	Water/ ethanol	119

Abbreviations: PEG – polyethylene glycol; PEO – polyethylene oxide; MWCO – molecular weight cut-off; BSA – bovine serum albumin; PBS – phosphate-buffered saline; THF – tetrahydrofuran; DMF – *N*,*N*-dimethylformamide; NMP – *N*-methyl-2-pyrrolidone; DMA – dimethylacetamide.

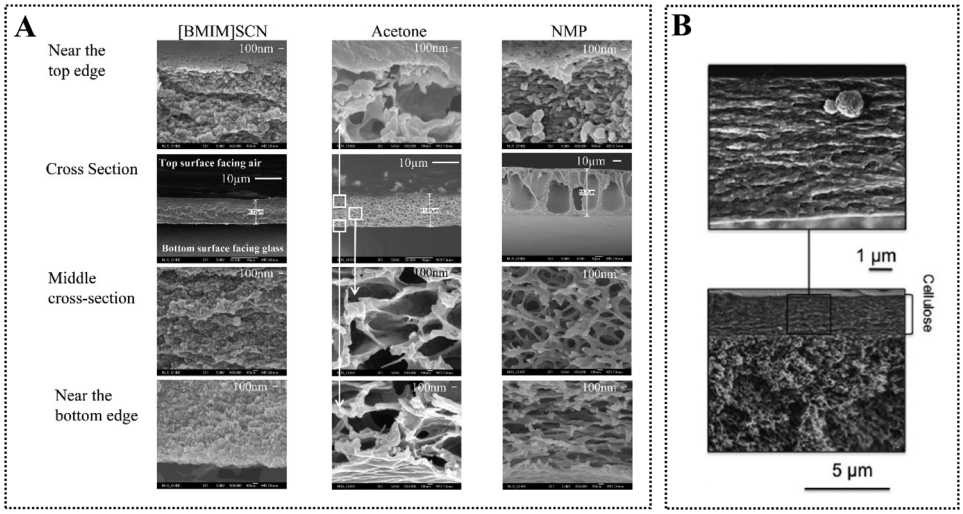

Fig. 11 (A) Morphology of cellulose acetate membranes regenerated from different solvents (10 wt% cellulose acetate solution). Reproduced from ref. 113 with permission from the American Chemical Society, copyright 2010. (B) Morphology of cellulose membrane on porous polysulphone support regenerated from 10 wt% cellulose solution in [Emim][Ac]. Reproduced from ref. 116 with permission from Elsevier, copyright 2015.

tion in the beginning followed by spinodal decomposition. Furthermore, they thought that macrovoid formation can be avoided on account of the slow water inflow into the system together with the high viscosity of the ionic liquid. Similar membrane morphologies were observed later by others using [Amim][Cl],[114] [Bmim][Cl][95,115] and [Emim][Ac][116–119] ionic liquids. The first ionic liquid-assisted regenerated membrane from native cellulose was made by Li *et al.*[114] using [Amim][Cl]. They fabricated the *regenerated cellulose membrane* on a polyethylene terephthalate (PET) non-woven fabric as a *support*. In membrane science, it has been a common strategy to prepare *multilayer membranes* by using a porous material that provides mechanical support without negatively affecting the flux. Nevertheless, it was difficult to prepare multilayer regenerated cellulose membranes in such a way before the discovery of the ionic liquids, due to the lack of cellulose solvent that would not damage the structure of the porous support. Livazovic *et al.*[116] prepared regenerated membranes using [Emim][Ac] on a range of porous substrates including the frequently used polysulphone (PSU); polyetherimide (PEI) and polyester nonwoven supports, demonstrating the versatility of ionic liquids in fabricating *multilayer asymmetric membranes* (Fig. 11B). Furthermore, they showed that the prepared regenerated membrane has excellent solvent resistance against tetrahydrofuran (THF), hexane, DMF, NMP and DMA. Note that *self-supporting membranes* could also be fabricated by others,[95,113,115,116,118,119] similarly to the initial work of Xing *et al.*,[113] in some cases with excellent mechanical characteristics (*e.g.*, the membrane developed by Chen *et al.*[95] had a tensile strength of 170 MPa, and 6.4% breaking elongation). In several works it was observed that by increasing the cellulose concentration in the ionic liquid, denser membranes can be fabricated providing the highest rejection values, and the lowest permeance in organic dye filtration,[115,118] in case of the neutral solute polyethylene glycol/polyethylene oxide,[116] and for oil-in-water emulsions.[117] Furthermore, Sukma and Culfaz-Emecen[118] found that dye rejection is also correlated with membrane affinity (sorption), attributed to hydrogen-bonding and electrostatic interactions.

4.3. Enzyme immobilisation using cellulose/ionic liquid systems

Cellulose, owing to its biologically compatible and nontoxic nature, has received significant interest as a *support material for enzyme immobilisation*. Table 3 shows selected works on enzyme immobilisation using regenerated cellulose films/beads through ionic liquid processing media. Turner *et al.*[120] was the first who studied enzyme encapsulation in regenerated cellulose films using [Bmim][Cl] solvent (*via* a cold processing method to avoid thermal denaturation), and laccase from *Rhus vernificera* as a model enzyme (an oxidoreductase responsible for the biodegradation of *e.g.*, lignin[121]). They observed a significant decrease in laccase activity (18% of the activity compared to the free form) for the enzyme-encapsulated regenerated film. They also realised that a hydrophobic ionic liquid ([Bmim][NTf_2]) "precoating" enables the formation of a more stable microenvironment in the regenerated cellulose film that results in an enhanced enzymatic activity (29% compared to the native form in aqueous solution). It is known that Cl^- in neat ionic liquids can form H-bonds with proteins, which can disturb their secondary structure, leading to denaturation. In addition, several enzymes show higher activity in more hydrophobic ionic liquids.[122] Following the initial experiences on entrapping enzymes in a regenerated cellulose film, Turner *et al.*[123] investigated enzyme immobilisation on the surface of the substrate, a strategy known to increase enzyme stability. They prepared regenerated cellulose/poly(oxyalkeneamine) composites by directly mixing the amine-containing polymer

Table 3 Immobilisation of enzymes using cellulose/ionic liquid systems

Type of cellulose	Ionic liquid	Cellulose concentration	Dissolution temperature (time)	Immobilised enzyme	Immobilisation strategy	Enzyme activity	Antisolvent	Ref.
Microcrystalline cellulose	[Bmim][Cl]	4.75 wt%	Microwave pulse heating	*Rhus vernificera* laccase	Dispersion in the ionic liquid/cellulose solution (at R.T.). A "precoating" step using a hydrophobic ionic liquid improved enzyme activity in the regenerated film	29% ("precoating" strategy) compared to the native form in aqueous solution	Water	120
Microcrystalline cellulose	[Bmim][Cl]	5 wt%	Microwave pulse heating	*Rhus vernificera* laccase	Immobilisation on the surface using pendant amine groups present in the regenerated cellulose/primary-amine polymer composite film. Glutaraldehyde crosslinker	Close to 50% activity retained compared to the native form in aqueous solution	Water	123
Microcrystalline cellulose	[Bmim][Cl]	6.5 wt%	Microwave pulse heating	*Rhus vernificera* laccase	Regenerated cellulose film with polyamidoamine (PAMAM) dendrimer. The crosslinked (using 1,3-phenylene diisocyanate) generation 1 PAMAM dendrimer (lowest amount of amino groups) provided the highest enzyme activity. Covalent attachment *via* crosslinker using glutaraldehyde resulted in a lower enzyme activity	Enhanced enzyme activity compared to the free form	Water	124
Microcrystalline cellulose	[Bmim][Cl]	3.5 wt%	85 °C (6 h)	Horseradish peroxidase and soybean peroxidase	Co-dissolution of the protein with cellulose and the ionic liquid at 85 °C. Immobilised in the regenerated film	Retained more than 50% of their original activity in the regenerated films	Water	125
Dissolving pulp	[Bmim][Cl]	7 wt%	100 °C (30 min)	*Aspergillus niger* glucose oxidase	Cellulose-chitosan microspheres as hydrogels coated on magnetic nanoparticles. Enzyme immobilisation by covalent attachment (*via* chitosan amine group) using glutaraldehyde	Enhanced thermal and storage stability, wider pH optima	Oil with surfactant, addition of ethanol	128
Cellulose acetate	[Bmim][NTf_2]	Around 6 wt% cellulose acetate in acetone; addition of the ionic liquid (around 20 wt% in the final solution)	No heating	*Kluveromyces lactis* β-galactosidase	Immobilisation of β-galactosidase *via* triethylenetetramine anchors on the film using glutaraldehyde crosslinker. Improved flexibility and formability compared to cellulose acetate	60% of the initial enzyme activity could be retained after immobilisation	No antisolvent, acetone was evaporated	126
Microcrystalline cellulose	[Emim][Ac]	6 wt%	70–80 °C (3 h)	*Trametes versiclor* laccase	Crosslinked regenerated cellulose beads. Covalent surface attachment of laccase *via* epoxy groups or catechol moieties (dopamine)	Improved thermal stability and pH tolerance compared to the free form	Water	127
Carboxymethyl cellulose	—	—	—	Porcine pancreatic lipase	Magnetic carboxymethyl cellulose nanoparticles functionalised with an imidazolium ionic liquid bearing carboxyl function (PF_6^- counterion). Enzyme attachment using EDC/NHS activator	Enzyme activity 2.83 folds higher than free lipase (1.43 folds higher without ionic liquid functionalisation)	—	129

Abbreviations: EDC: 1-ethyl-3-(3-dimethylaminopropyl)carbodiimide; NHS: *N*-hydroxysuccinimide

with the cellulose/[Bmim][Cl] solution. When laccase was attached to the surface using glutaraldehyde crosslinker, for one of the examined primary amine-containing polymers the enzyme retained about 50% of its activity. This increase was attributed to the improvement in the flexibility of the enzyme attached to the surface. Further improvement was achieved with regenerated cellulose films by using polyamidoamine (PAMAM) dendrimers dissolved together with cellulose in [Bmim][Cl].[124] Interestingly, the highest enzyme activity was observed when the cellulose-PAMAM matrix was crosslinked with 1,3-phenylene diisocyanate, and surface attachment was done by incubating the enzyme with the regenerated film. This strategy outperformed even the frequently applied method of surface attachment *via* glutaraldehyde crosslinker. Several works prepared bioactive films through similar strategies by directly including horseradish peroxidase/soybean peroxidase in the cellulose/[Bmim][Cl] solution,[125] or by surface attachment of β-galactosidase on regenerated polyamine/cellulose composite films (hydrophobic [Bmim][NTf_2] as solvent – note that cellulose acetate was used here instead of cellulose which does not dissolve in this ionic liquid) postmodified using glutaraldehyde as crosslinker.[126] Regenerated cellulose beads proved also efficient in laccase immobilisation as demonstrated by Gu *et al.*[127] They fabricated crosslinked cellulose beads by dropping a cellulose/[Emim][Ac] solution containing crosslinkers and reactive functions (epoxy and catechol) into water by means of a syringe, and immobilised laccase by simply incubating the enzyme with the prepared beads. Furthermore, *magnetic micro/nanoparticle composites* gained interest in *enzyme immobilisation* as they can be separated easily from the reaction media using a magnet. Liu *et al.*[128] prepared cellulose-chitosan magnetic microspheres (as hydrogels with about 92% water content) using Fe_3O_4 magnetic support in [Bmim][Cl]. The regeneration procedure was different from others in that the [Bmim][Cl] solution was added to an oil-surfactant mixture, followed by the addition of ethanol. The enzyme glucose oxidase (from *Aspergillus niger*) was anchored on the surface of the microspheres through the amine group of chitosan using glutaraldehyde. Enhanced thermal and storage stability, and wider pH tolerance window was reported as a result of the enzyme immobilisation. Recently, Suo *et al.*[129] modified carboxymethyl cellulose-coated magnetic nanoparticles with an imidazolium ionic liquid containing carboxyl function and PF_6^- counterion (Fig. 12). The porcine pancreatic lipase enzyme was immobilised *via* the pendant carboxyl group on the surface of the nanoparticles by applying EDC/NHS coupling protocol. By investigating the structure of the immobilised enzyme, they proposed that the lid of the enzyme active site is open to a higher degree (low α-helix content), and the enzyme has a more rigid structure (high β-sheet content) compared to the free enzyme or enzyme immobilised without the ionic liquid anchor. They concluded that these features can be responsible for the high enzyme activity and stability.

The structure of ionic liquids has a profound impact on enzyme activity, the dominating factors have been comprehensively studied.[122] In case of cellulose/ionic liquid systems, the ionic liquid needs to be both a good solvent of cellulose, and should have ideally a positive effect on enzyme activity and stability.[130,131] There has been great interest in designing novel biocompatible, cellulose-dissolving ionic liquids.[132,133]

4.4. Catalytically active cellulose-based composite materials using ionic liquids

Ionic liquids received great interest as *tunable platform for the synthesis of various metal nanoparticles with controlled size and shape*, sometimes with superior properties compared to those fabricated *via* conventional methods.[134,135] Furthermore, *ionic liquids are flexible media in catalysis* in that they can not only act as solvents, but also as *stabilisers, supports and ligands* in various multiphase catalytic transformations.[134–137]

The first work that described the use of an ionic liquid/metal nanoparticle/cellulose system was from Li *et al.*[138] They studied the *thermally-induced formation of gold microparticles* from an Au(III) salt in BmimCl using *cellulose as the reducing*

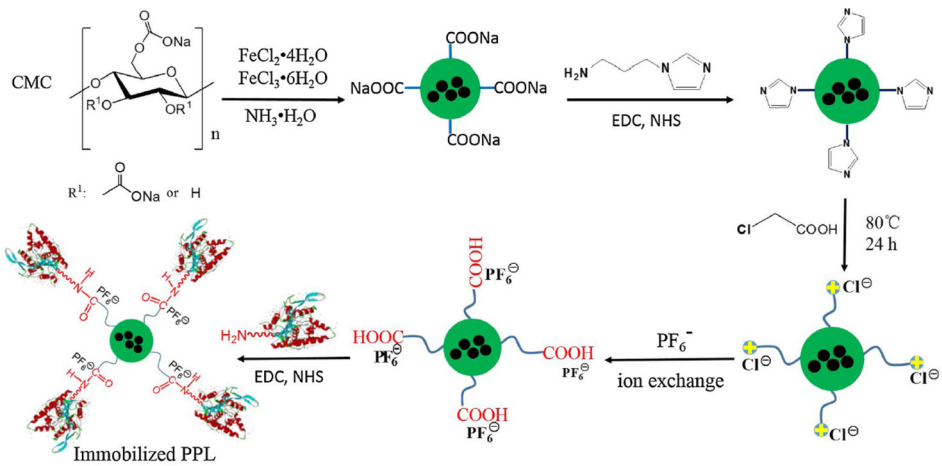

Fig. 12 Enzyme (porcine pancreatic lipase (PPL)) immobilisation on carboxymethylcellulose-coated magnetic nanoparticles *via* an ionic liquid-derived anchor. Reproduced with some modification from ref. 129 with permission from Elsevier, copyright 2020.

agent. Gold microparticles with various sizes and shapes could be obtained by modulating the temperature, owing to the cellulose template and the ionic liquid.

It was Gelesky *et al.*[139] who first recognised the use of *cellulose to prepare catalytic polymeric membranes* through the immobilisation of metal nanoparticles in combination with an ionic liquid. The polymeric support can reduce the loss of the nanoparticles in the course of the process, provides porous contact in gas/liquid multiphase reactions, and prevents agglomeration of the nanoparticles. The latter phenomenon is a well-known limitation when ionic liquids are used in transition metal nanoparticle catalysis.[134,137] Gelesky *et al.*[139] dispersed Pt(0) and Rh(0) nanoparticles in cellulose acetate substrate using [Bmim][NTf_2]/acetone solvent system, and obtained films of various thicknesses (10–40 μm) by evaporating acetone. The cellulose/ionic liquid/Pt(0) 20 μm thick composite film showed much higher catalytic activity (turnover frequency (TOF): 7353 h^{-1}) for the hydrogenation of cyclohexane than the nanoparticles alone in the ionic liquid (TOF: 329 h^{-1}). This phenomenon was attributed to the stabilisation of the nanoparticles in the cellulose substrate, and to the presence of porous regions conducive to the effective gas/liquid contact. They also noted that the presence of ionic liquid confers higher flexibility and formability to the membrane. Since this initial work, several studies have been reported on the fabrication of cellulose/metal nanoparticle composite films/spheres for catalytic applications, a list of selected works can be found in Table 4.

Wittmar *et al.*[140] prepared *TiO_2-doped regenerated cellulose films* using [Bmim][Ac]/[Bmim][Cl] ionic liquids (Fig. 13A). The prepared film showed good *photocatalytic efficiency* in degradation of organic dye when impregnated on the cellulosic substrate. However, the process was less effective in bulk solution of the organic dye, which the authors have attributed to the poor solute diffusion owing to the low porosity of the film. In order to improve the performance of the material, in another study from the same group, TiO_2-doped porous films were prepared *via* a freeze-drying process using [Bmim][Ac] solvent[141] (Fig. 13B). They noted the beneficial effect of DMSO as co-solvent to decrease the viscosity of the ionic liquid, and thereby improve the processability. Interestingly, when irradiated with sunlight, dye decomposition was efficient in case of dye-impregnated films. This feature is promising for application as *"self-cleaning" material under sunlight*. Furthermore, Fe_2O_3–TiO_2 co-doped regenerated porous cellulose film could be also prepared.[142] In this case, it was noted that the presence of magnetite nanoparticle did not affect the photocatalytic activity of TiO_2 (although the activity decreased an order of magnitude compared to TiO_2 powder). The *magnetic, photocatalytically active film* can be easily separated from the reaction solution using a magnet (Fig. 13C), and can be also readily heated by alternating magnetic field (AMF, Fig. 13D). Furthermore, in order to aid the recyclability of the photocatalytic regenerated cellulose material, it was further shaped into porous macrospheres in a recent study.[143] In this case, the superiority of [Bmim][Ac]/DMSO system over [Emim][Ac]/DMSO medium was reported, as it provided a material with higher porosity, and it also dispersed TiO_2 nanoparticles better. In another work by Jo *et al.*,[144] carrageenan, a polysaccharide with sulphate moieties, was added to the TiO_2-doped regenerated films ([Emim][Ac] solvent) that resulted in increased adsorption capacity for the cationic organic dye, and lead to an improved degradation efficiency in the photocatalytic reaction. The compatibility of the cellulose/ionic liquid system for other photocatalytically active nanoparticles, such as Bi_2WO_6, was also demonstrated.[145]

These studies clearly show that ionic liquids provide versatile platform for the fabrication of catalytically active cellulose-based composites with tailored structures and properties.

4.5. Cellulose-based separator membranes and conductive composite films for electronic devices, using ionic liquid processing media

4.5.1. Separators for supercapacitors and batteries. Cellulose has long been used as an *insulating separator material in various energy storage devices*.[146,147] Separators provide ion diffusion paths between the opposite electrodes through their porous structure while help avoiding short-circuit issues owing to their insulating nature. They are essential components to improve operation safety, lifetime and performance of battery and capacitor devices. The first semi-permeable cellulose membrane was applied in commercial alkaline batteries which still represents a dominating market within the battery industry.[146] In lithium-ion batteries, polyolefin-based separators (*e.g.*, polyethylene (PE), polypropylene (PP)) gained dominance, although efforts have been made to develop cellulose-based membranes for this application. As an environmentally friendly, renewable material with advantageous properties, such as chemical and thermal stability, there has been revived interest in using cellulosic materials for developing efficient separators for high-performance energy storage devices.

Ionic liquids provide a versatile platform to prepare nanoporous membranes for energy storage devices from cellulose via the phase inversion method (which we have already mentioned in section 4.2.1). Zhao *et al.*[148] prepared regenerated cellulose film (22 μm-thick) from cellulose/[Bmim][Cl] solution (4 wt% cellulose content) using water as coagulant. They obtained a film (Fig. 14A) with good flexibility and mechanical properties (tensile strength of 171.5 MPa, elastic modulus of 8.93 GPa). The tensile strength is among the highest reported in the literature (see Tables 1 and 2), this may be attributed partly to the starting cellulose that had a high DP of 1484, and to the processing conditions. The regenerated membrane exhibited high porosity (71.78%) with uniformly distributed mesopores having diameters in the range of 5–30 nm (Fig. 14B). The thermal stability, which is an important parameter in separator applications, remained comparable (thermal degradation starts around 275 °C) to commercial cellulose-based separators. The thermal stability of cellulosic membrane is superior compared to commercial polyolefin-based separators (structural changes above 100 °C).[146] Furthermore, high ionic con-

Table 4 Catalytically active regenerated cellulose/metal nanoparticle films/spheres prepared using ionic liquids

Type of cellulose	Ionic liquid	Cellulose concentration	Dissolution temperature (time)	Nanoparticle	Film properties, observations	Catalytic activity	Antisolvent	Ref.
Cellulose acetate	[Bmim][NTf_2]	Around 6 wt% cellulose acetate in acetone; addition of the ionic liquid (around 20 wt% in the final solution)	No heating	Pt(0)/Rh(0)	Metal nanoparticle catalyst immobilisation inside the cellulose acetate-IL composite. Synergistic effect was observed on the catalytic activity of Rh(0) and Pt(0) nanoparticles	Higher catalytic activity of IL/cellulose/nanoparticle composite (TOF 7353 h^{-1}; 20 μm thick film, Pt(0)) than IL/nanoparticle system (TOF 329 h^{-1}, Pt(0)) in hydrogenation of cyclohexane	No antisolvent, acetone was evaporated	139
Microcrystalline cellulose (DP 200)	[Bmim][Ac]	8, 10, 12, 14 wt%	70 °C (1 h)	TiO_2	Higher viscosity results in a more compact film. Dispersion of nanoparticles is negatively affected by increasing viscosity	Photocatalytic activity demonstrated on films impregnated with methylene blue/rhodamine B dye solutions (UV irradiation at 365 nm). Less effective in degradation of dye in solution	Water	140
	[Bmim][Cl]		90 °C (1 h)					
Microcrystalline cellulose (DP 210–230)	[Bmim][Ac] (DMSO co-solvent)	8 wt%	70 °C (5 h)	TiO_2	Porous film could be fabricated *via* freeze-drying. Macrospheres *via* drop-wise addition to the coagulation medium	Wet porous films showed the best photocatalytic activity in dye degradation. Dye adsorbed on porous film could be eliminated by sunlight irradiation in 15 min – self-cleaning surfaces	Water	141
Microcrystalline cellulose (DP 180)	[Bmim][Ac] (IL/DMSO 3/1)	8 wt%	70 °C (5 h)	TiO_2 + Fe_2O_3	Magnetite nanoparticles are more stable in [Emim][Ac]/DMSO system compared to [Bmim][Ac]/DMSO system. Agglomerate size is smaller in the latter one Less macrovoids, denser film	Films have lower photocatalytic activity (about one order of magnitude) compared to TiO_2 powder. Addition of magnetite did not have negative effect on the photocatalytic activity. Degradation of organic dyes	Water	142
	[Emim][Ac] (IL/DMSO 3/1)							
Microcrystalline cellulose (DP 180)	[Bmim][Ac] (IL/DMSO 3/1)	6 wt%	70 °C (–)	TiO_2 + Fe_2O_3	Porous macrospheres. Superior TiO_2 dispersion, higher porosity of the resulting spheres in [Bmim][Ac]/DMSO	Higher photocatalytic activity of the spheres from [Bmim][Ac] solutions. Additional adsorption property for heavy metals (demonstrated on Cu^{2+})	Water	143
	[Emim][Ac] (IL/DMSO 3/1)							
Microcrystalline cellulose (DP 180)	[Emim][Ac]	7 wt%	80 °C (–)	TiO_2	Cellulose/carrageenan/TiO_2 composite film	The negatively charged composite has high adsorption capacity for a cationic dye. Photodegradation efficiency is higher than TiO_2/cellulose composite	Ethanol, water	144
Waste cotton fabric	[Amim][Cl]	~2 wt%	65 °C (1 h)	Bi_2WO_6	IL/cellulose solution added to Bi_2WO_6/DMA solution prior to the regeneration. Good compatibility between cellulose and the nanoparticle. Layered porous film	Good adsorption and photocatalytic activity to remove organic dyes under visible light irradiation	Water	145

Abbreviations: TOF: turnover frequency.

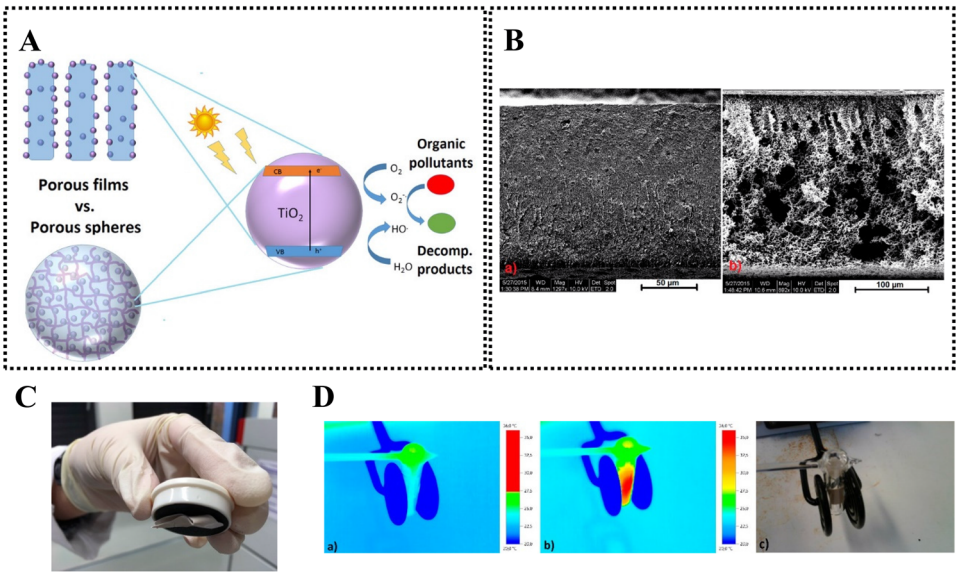

Fig. 13 (A) Preparation of TiO_2-doped regenerated cellulose films for photocatalytic degradation of organic pollutants. (B) Effect of the freeze-drying process on the resulting regenerated cellulose film (left: air drying; right: freeze-drying). (A) and (B) reproduced from ref. 141 with permission from the American Chemical Society, copyright 2017. (C) Magnetic properties of the Fe_2O_3–TiO_2 co-doped regenerated cellulose film. (D) AMF-induced temperature increase of the Fe_2O_3–TiO_2 co-doped regenerated cellulose film. (C) and (D) reproduced from ref. 142 with permission from the American Chemical Society, copyright 2017.

ductivity (0.325 S cm^{-1} after soaking in 6 M KOH) and good electrolyte retention was observed. In line with these excellent characteristics, the assembled solid state supercapacitor (sandwich-like configuration, cellulose separator impregnated with 6 M KOH placed between the activated carbon electrodes) device outperformed other devices based on commercial separators in terms of specific capacitance (110 F g^{-1} at 1 A g^{-1} current density), rate capability (*i.e.*, high capacitance retention at high current density), capacitance retention (84.7% after 10 000 cycles), equivalent series resistance, energy density and power density (energy density more than 1.5-times higher than the performance achieved with commercial cellulose-based separators). Furthermore, the authors also prepared interdigitated finger-type micro-supercapacitors *via* a novel method (Fig. 14C): patterns (PTFE mask and activated carbon powder) were deposited on the cellulose/IL substrate prior to the regeneration step, which represents a simple, cost-effective method without using additives and special tools applied for common patterning methods (photolithography, inprinting, *etc.*). The micro-supercapacitor device showed excellent formability without decrease in capacitance or change in the electric double layer behaviour (see Fig. 14D, similar cyclic voltammograms). The device gave superior energy density and power density compared to the performance of other micro-supercapacitors in the literature (Fig. 14E). In addition, it was demonstrated that the micro-supercapacitor can be connected in series (giving twice the operating voltage) or parallel (giving about twice the current and discharge time), and can drive a digital watch in plane or bent state (Fig. 14F and G).

In another work from the same group,[149] a regenerated cellulose/glass microfiber composite film was prepared and used as a flexible separator for lithium-ion batteries (Fig. 15A). The composite film was prepared by carefully choosing the concentration (1 wt% as optimal), and thus adjusting the viscoelastic property of the cellulose/[Bmim][Cl] solution in order to make it penetrate into the microfiber structure. The presence of cellulose conferred exceptional flexibility and structural stability to the microfiber separator, which could be shaped into various forms without fracture even when wetted with electrolyte (Fig. 15B and C). Furthermore, the composite separator exhibited good thermal stability (200 °C), electrolyte wettability; superior electrolyte retention, ionic conductivity and Li^+ transference number compared to the glass microfiber film as reference. The assembled $LiFePO_4$–Li battery cell showed lower charge transfer resistance (102.2 Ω), higher discharge specific capacitance (160.6 mA h g^{-1} at 0.2 C), better rate capability (145.9 mA h g^{-1} at 2 C) and cycling stability (108.5 mA h g^{-1} after 1000 cycles at 2 C) compared to the reference (Fig. 15D). A pouch cell was also assembled to demonstrate a flexible Li battery application. It was concluded that the inhibition of Li dendrite growth and rapid ion diffusion through the composite membrane contributed to the excellent rate performance and cycling stability.

4.5.2. Conductive composite films. Various works describe the fabrication of conductive regenerated cellulose films by the addition of a conductive filler (Table 5), such as single-walled and multi-walled carbon nanotubes,[150–153] graphene,[153] graphite[154,155] and silver nanowires.[156]

The first work on conductive regenerated cellulose films was done by Pushparaj *et al.*[150] They impregnated vertically aligned multiwalled carbon nanotubes (MWCNTs; grown on a silicon substrate *via* thermal chemical vapor deposition (CVD)

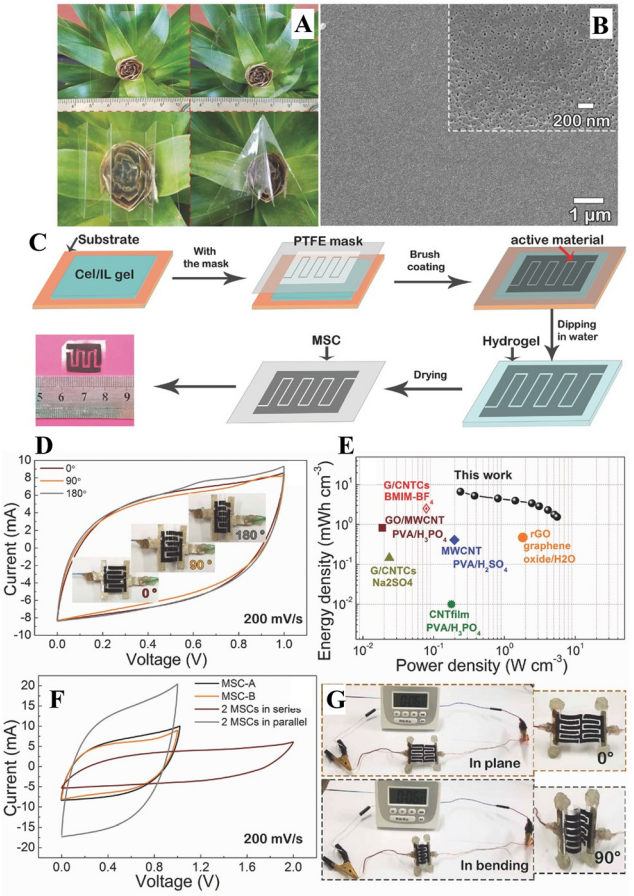

Fig. 14 (A) Photograph showing the regenerated cellulose film with high transparency and flexibility. (B) Scanning electron microscopy (SEM) image about the pore structure. (C) Processing steps for fabricating the interdigitated finger-type electrode. (D) Cyclic voltammograms recorded for different bent states of the flexible micro-supercapacitor. (E) Ragone-plot that compares the performance of the device with others from the literature. (F) Cyclic voltammogram recorded for devices connected in parallel or in series. (G) Micro-capacitor device powering a digital watch. Reproduced from ref. 148 with permission from Wiley, copyright 2017.

technique) with a cellulose/[Bmim][Cl] solution. After immersing in ethanol, the regenerated cellulose/MWCNT film could be peeled off from the substrate. Symmetric *supercapacitor device* was fabricated using the composite film, affording a flexible, thin and lightweight design. An extra thin cellulose layer was used as the separator, and [Bmim][Cl] as electrolyte (see Fig. 16). The supercapacitor showed good performance (≈13 W h kg^{-1} energy density, 1.5 kW kg^{-1} power density), with excellent operating temperature window (195–423 K). The device could be operated with various body fluids as electrolytes (such as body sweat, blood), which is promising for biomedical applications (*e.g.*, biomedical microelectromechanical systems). The authors fabricated *flexible Li-ion battery* using the cellulose/MWCNT composite as cathode. Furthermore, the *supercapacitor and battery* device were also combined to make *hybrid devices*.

Several works prepared conductive filler/regenerated cellulose composite by including the filler in the ionic liquid/cellulose solution prior to the coagulation process. Interestingly, it was observed by Ye *et al.*[157] that graphite can be exfoliated directly in a [Bmim][Cl]/cellulose solution under ultrasonication. They recognised that cellulose can help the exfoliation process, probably through hydrogen bonding between –OH groups of cellulose and the π electrons of graphene. Similar phenomenon was noted later by Zhang *et al.*[155] using [Amim][Cl]. They also observed the positive effect of the presence of small amount of single/multilayer graphene (0.1–1 wt%) on the mechanical properties of the regenerated cellulose film. In the regenerated cellulose film, cellulose nanofibers were observed, the diameter of these fibres were affected by the amount of graphene in the composite. At the lowest graphene loading, graphene was nicely dispersed resulting in small cellulose nanofibers, meanwhile increasing the graphene content resulted in graphene aggregation and larger cellulose nanofibers. Toughness and tensile strength were the highest when cellulose nanofibers had the smallest diameter. Furthermore, Chen *et al.*[154] studied relatively high amount of graphite loading (10–200 wt%) in regenerated cellulose films, which had negative effect on the tensile properties. In this case, graphite flakes were present in the film, exfoliation by *e.g.*, ultrasonication was not done, graphite flakes were only stirred in the ionic liquid. The prepared graphite/regenerated cellulose film coated with a polypyrrole layer showed good properties as an *electromagnetic interference shielding material* (electromagnetic shielding effectiveness: 30 dB). Relatively small loading of single walled carbon nanotubes (SWCNT) had also positive effect on the tensile strength and elongation at break, with an increase in the elastic modulus.[152] Furthermore, Wang *et al.*[151] prepared regenerated cellulose/poly(butylene succinate) composite with improved toughness and ductility (compared to regenerated cellulose), the presence of multiwalled carbon nanotubes (0.5–4 wt%) could further improve the tensile strength of the material. In respect to electronics applications of the films, it was noted in several cases that electrical conductivity is limited by the discontinuity of the conductive filler at low concentrations. At high concentrations, agglomeration limits the continuity, and thus the electric contact between filler segments. In order to prevent graphene restacking, and improve the contact points throughout the cellulose matrix, Zhou *et al.*[153] prepared graphene/MWCNT/cellulose composite using [Emim][DEP] ionic liquid. At optimum graphene/MWCNT/cellulose loading the regenerated film reached a conductivity of 1124 S m^{-1}, which is the highest reported to the best of our knowledge for a conductive regenerated cellulose film prepared *via* ionic liquid processing.

4.6. Regenerated cellulose/biopolymer green composites using ionic liquids

Since a synthetic petroleum-derived polymer additive would compromise the green nature of cellulose-based materials, in order to tailor their properties, several works focused on

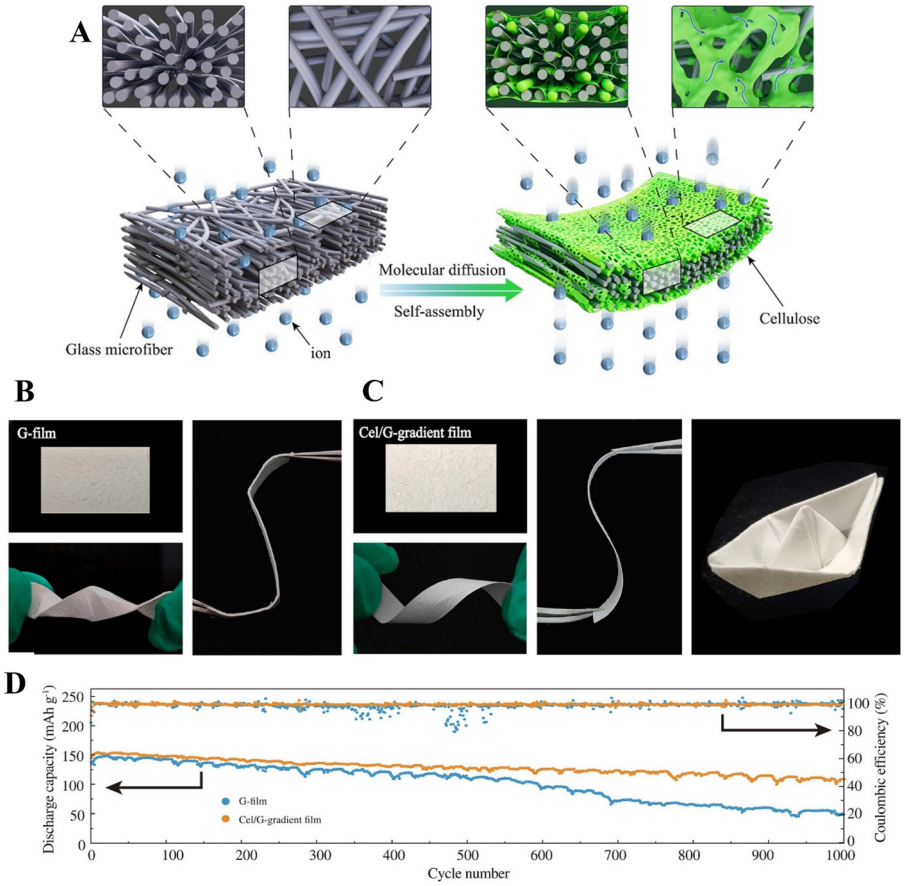

Fig. 15 (A) Fabrication of cellulose/glass microfiber composite film for application as separator in lithium-batteries. (B) Glass microfiber film with poor flexibility. (C) Cellulose/glass microfiber composite film with excellent flexibility and formability. (D) Cycling stability of a $LiFePO_4$/Li cell using glass microfiber (blue line) *vs.* cellulose/glass microfiber composite (orange line) separators. Reproduced from ref. 149, copyright 2021 The Authors.

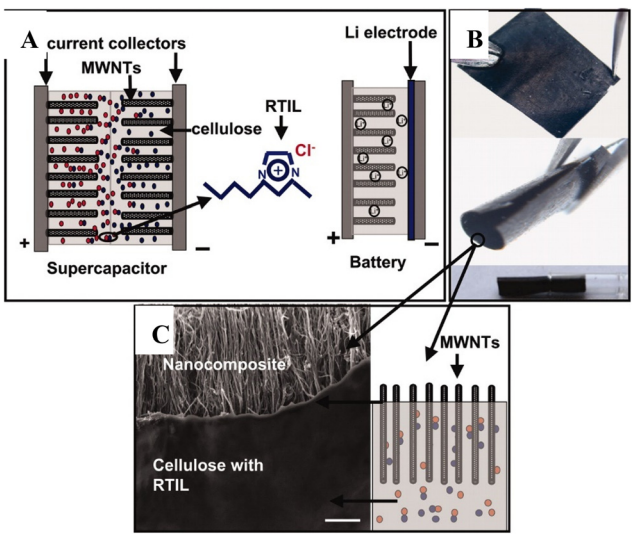

Fig. 16 (A) Supercapacitor and Li-ion battery device fabricated using the regenerated cellulose/MWCNT composite. (B) Demonstration on the flexibility of the composite film. (C) Cross-sectional SEM image of the nanocomposite film. Reproduced from ref. 150 with permission from the National Academy of Sciences, copyright 2007.

blending cellulose with other biopolymers to obtain *tailor-made biocomposites* with improved properties (Tables 6–8). Some ionic liquids that can dissolve cellulose show good ability to dissolve other biopolymers as well, among them are a range of *polysaccharides*: chitin/chitosan, glycosaminoglycans (*e.g.*, heparin), starch, agarose, carrageenan, *etc.*; *proteins*: silk, wool keratin, collagen; and *lignocellulosics*: xylan and lignins, *etc.*[158] This provides unique opportunity to prepare homogeneous blends of cellulose with biopolymers, which lead in several cases to advantageous film properties.

4.6.1. Cellulose/chitin and cellulose/chitosan biocomposites. Several studies considered *chitin* (β-1,4-linked 2-acetamido-D-glucose) as additive (Table 6), being the second most abundant biopolymer on Earth after cellulose. Takegawa *et al.*[159] dissolved cellulose in [Bmim][Cl], and chitin in [Amim][Br] separately, then mixed the two solutions, followed by the common film casting and regeneration step (water coagulation bath) to obtain finally the composite films. They noted that it is difficult to find an ionic liquid that can dissolve both cellulose and chitin at high concentration. They also found that [Amim][Br] can dissolve chitin, a 5 wt% clear solution could be prepared without deacetylation and degra-

Table 5 Conductive regenerated cellulose films using ionic liquid/cellulose processing with conductive fillers

Type of cellulose	Ionic liquid	Cellulose concentration	Dissolution temperature (time)	Conductive filler	Conductivity	Film properties, observations	Application	Antisolvent	Ref.
Unmodified plant cellulose	[Bmim][Cl]	—	—	Vertically aligned multiwalled carbon nanotubes (MWCNTs)	—	Few tens of microns thick film	Ultrathin flexible supercapacitor, Li-ion battery, hybrid supercapacitor-battery	Ethanol	150
Cotton linter pulp	[Bmim][Cl]	~4 wt%	100 °C (–)	Graphite powder in the film. Polypyrrole nanoparticle coating on the film surface	55 S m^{-1} at 200% graphite loading. Conductivity attributed to the polypyrrole coating (graphite forms discontinuous segments)	10–100 μm thick film. Graphene and polypyrrole both improve electromagnetic shielding synergistically	Lightweight electromagnetic interference shielding material	Water	154
Cotton linter pulp	[Amim][Cl]	~5 wt%	PBS (poly (butylene succinate)) dispersed (melt) first at 130 °C (1 h); cellulose added at 90 °C (2 h)	MWCNTs	1.3×10^{-5} S m^{-1} (4 wt% MWCNTs)	PBS particles and MWCNTs uniformly dispersed in the matrix	Presence of PBS could improve toughness and ductility. Elastic modulus and tensile strength increase due to MWCNT	Water	151
α-Cellulose (DP 650)	[Amim][Cl]	—	90 °C (2 h)	Exfoliated graphite (single and multilayers of graphene)	2.5 S m^{-1} (0.3 wt% graphene loading)	Regenerated cellulose nanofibers in the film	Increasing tensile strength and toughness by addition of graphene (0.1–1 wt%)	Water	155
Coniferous dissolving pulp (DP 500)	[Amim][Cl]	3 wt%	90 °C (0.5 h)	Ag nanofiber deposited on the surface	Sheet resistance of 29 Ω $\square^{-1}$	HNO_3 treatment improved the transmittance. Optimal treatment gave 80% transmittance	Perovskite solar cells	Water	156
Microcrystalline cellulose	[Emim][Cl]	6 wt%	90 °C (24 h)	Single-walled carbon nanotubes (SWCNTs)	Maximum electrical conductivity at 2 wt% SWCNT loading (0.3 S m^{-1})	Thickness about 30 μm. Uniformly dispersed SWCNTs	1 wt% SWCNT increases elastic modulus by 188%, tensile strength by 129%, elongation at break by 51%. Improved oxygen barrier and water absorption resistance	Water	152
Wood pulp cellulose (DP 900)	[Emim][DEP]	~1 wt%	90 °C (3 h)	Graphene nanoplatelets (GN) + MWCNTs	Highest: 1124 S m^{-1} (GN : MWCNT : Cellulose 7 : 3 : 2 by weight)	14–83 μm	After carbonisation, application as electrode in Li-ion battery	Water	153

Table 6 Regenerated cellulose/chitin and cellulose/chitosan binary composite films using ionic liquid processing media

Type of cellulose	Ionic liquid	Cellulose concentration	Dissolution temperature (time)	Biopolymer additive	Film properties, observations	Antisolvent	Ref.
Microcrystalline cellulose	[Bmim][Cl]	10 wt%	100 °C (24 h)	Chitin; 5 wt% [Amim][Br] solution, same dissolution procedure as cellulose	Elasticity of the film decreases with increasing chitin content	Water	159
Microcrystalline cellulose (DP 124)	[Bmim][Ac]/ γ-valerolactone 8/1	8 wt%	90 °C (3 h)	Chitin; 2 wt% solution prior to mixing with cellulose/solvent system	Chitin contributes to the elasticity of the composite; hydrophobicity increases with increasing chitin content	Ethanol, soaking for 4 h, then Soxhlet extraction for 24 h	162
Microcrystalline cellulose	[Dmim][Cl]	4 wt%	75 °C (15 min)	Chitosan; 4 wt% using [Dmim][Cl]/ [Hmim][Cl] 9/1	Composite has no porous structure. Chitosan makes the composite brittle; tensile strength improves with cellulose content	Methanol	164
Cellulose pulp (DP 670)	[Bmim][Ac]	6 wt%	85–95 °C (12 h)	Chitosan; 6 wt% 85–95 °C (3–4 days)	Good miscibility without phase separation	Methanol/ water 50/50	165
Cellulose pulp (DP 630)	[Amim][Cl] with 1 wt% Gly·HCl	3–5 wt%	80 °C (12 h)	Chitosan; 2–35 wt% relative to cellulose, simultaneous dissolution of the two polymers	Antibacterial films could be obtained	Water	166

dation.[160] Hence a binary [Bmim][Cl]/[Amim][Br] system was used for the formation of the regenerated cellulose/chitin composite. Increasing the amount of chitin in the film appeared to lead to a decrease in the elasticity. They have further improved the mechanical and thermal properties of the chitin/cellulose composite films by changing the coagulation process (Soxhlet extraction in ethanol and water).[161] The simultaneous dissolution of cellulose and chitin was done using [Bmim][Ac],[162] which can dissolve both biopolymers.[163] The authors used γ-valerolactone as bioresourced co-solvent, in order to improve the environmental footprint of the process. A [Bmim][Ac]/ γ-valerolactone 8/1 ratio proved sufficient to dissolve the two polymers within relatively short time at low temperature (90 °C, 3 h) compared to other systems. The authors observed that chitin contributed to the elastic properties of the composites, and made them more hydrophobic.[162] The degree of acetylation of chitin only slightly decreased as a result of processing. *Chitosan*, the deacetylated derivative of chitin has also received significant interest as an additive to regenerated cellulose (Table 6). Xiao *et al.*[164] investigated different ionic liquid systems for the dissolution of cellulose and chitosan for the preparation of composite blends. They realised that the addition of 1-*H*-methylimidazolium chloride ([Hmim][Cl]) to 1,3-dimethylimidazolium chloride ([Dmim][Cl]) facilitates the dissolution of chitosan. Interestingly, they noted that chitosan may not be present in its protonated form (it is not a polyelectrolyte), but the increased Cl^- concentration may help the dissolution process. They noted that chitosan renders the composites brittle, and the tensile strength increases with increasing cellulose content. Stefanescu *et al.*[165] pointed out the use of [Bmim][Ac] as good solvent of cellulose and for even high molecular weight chitosan, which otherwise does not dissolve in [Bmim][Cl]. The authors observed the good miscibility of the polymers without phase separation, the formation of hydrogen bonds between cellulose and chitosan was proposed. The composite film exhibited a more amorphous structure compared to the individual regenerated polymer films. In another study, Fu *et al.*[166] used [Amim][Cl] with the amino acid based ionic liquid Gly·HCl as co-solvent in order to facilitate chitosan dissolution (with relatively high viscosity average molecular weight of about 630 kDa). It was proposed that at relatively high chitosan loading the chitosan/cellulose film is not homogeneous anymore, which lead to a decline in the mechanical properties and thermal stability. Antibacterial films could be obtained owing to the presence of chitosan, which is known to exert bactericidal/bacteriostatic effects against a range of microorganisms.[167]

4.6.2. Biocomposites prepared using hemicellulose, lignin (synthetic wood), and starch. *Hemicelluloses* are also among the most abundant polysacccharides in nature. Hemicelluloses are heteropolymers with branched structure, they are present in the plant cell wall together with cellulose. Several works considered them as additives for regenerated cellulose blends (Table 7). *Xyloglycan* (1,4-β-glucan backbone with 1,6-α-xylosyl substituents that can be further modified with other monosaccharides) is a major hemicellulose that is known to bind

Table 7 Regenerated cellulose/biopolymer composite films (hemicelluloses, synthetic wood (hemicellulose, lignin), starch, natural rubber, and heparin)

Type of cellulose	Ionic liquid	Cellulose concentration	Dissolution temperature (time)	Biopolymer additive	Film properties, observations	Antisolvent	Ref.
Microcrystalline cellulose	[Emim][Ac]	1 wt%	100 °C (1 h)	Xyloglycan	At certain composition nanostructuration was observed, which resulted in increased tensile strength and strain at break	Water	169
Cellulose from spruce *via* chlorite delignification	[Emim][Ac]	~4 wt%	80 °C (4 days)	Arabinoglucuronoxylan	Addition of xylan increased the stiffness of the composite at relatively low humidity conditions	Ethanol	170
Cellulose solution in [Emim][Ac] (Cellionic™); DP ~ 680	[Emim][Ac]	5 wt%	90 °C (3 h)	Xylan from birch wood; softwood kraft lignin from pine	Synthetic wood composite with enhanced hydrophobicity, thermal stability, tensile strength and UV shielding properties	Water	172
Microcrystalline cellulose	[Emim][Ac]	5 wt%	80 °C (3 h)	Xylan from birch wood; Alkali lignin; 80 °C (2 h) mixing with the cellulose/[Emim][Ac] solution	Synthetic wood composite. Biodegradability (cellulase) was increased with xylan content whereas decreased with lignin addition. Water vapor solubility was positively correlated with xylan content	Water	173
Cellulose bamboo pulp (DP 650)	[Amim][Cl]	~2–5 wt%	80 °C (30 min)	Starch, lignin and cellulose dissolved at a 6 wt% total concentration in [Amim][Cl]	By optimising the ratio of cellulose/lignin/starch, the mechanical properties could be maximised. The biopolymers exert synergistic effects. Gas barrier properties promising for food packaging applications	Water	175
Eucalyptus cellulose (*via* chlorite delignification)	[Bmim][Ac]	5 wt%	100 °C (3 h)	Gutta percha (natural rubber) from *Eucommia ulmoides* Oliver leaves. 5–15 wt% relative to cellulose. Dissolved in chloroform	Enhanced tensile strength and elongation at break. Decreasing oxygen permeability. Increasing hydrophobicity. Food packaging applications	Water	192
Cellulose (not specified)	[Bmim][Cl]	10 wt%	Preheating at 70 °C, then microwave heating	Heparin imidazolium salt dissolved in 1-ethyl-3-methylimidazolium benzoate	Nanoporous, blood compatible membrane for renal dialysis	Ethanol	193

Table 8 Regenerated cellulose/natural protein binary composite films (silk fibroin, wool keratin, collagen)

Type of cellulose	Ionic liquid	Cellulose concentration	Dissolution temperature (time)	Biopolymer additive	Film properties, observations	Antisolvent	Ref.
Microcrystalline cellulose	[Bmim][Cl]	2 wt%	90 °C (–)	Silk fibroin from *Bombix mori*	Enhanced mechanical properties (tensile strength, elongation at break), thermal stability and water resistance. Conformational transition from random coil to β-sheet	Methanol	178
Cotton linter pulp	[Bmim][Cl]	4 wt%	90 °C (–)	Silk fibroin from *Bombix mori*	Detailed solid-state NMR study revealing hydrogen bonding between the biopolymers, cellulose structure and secondary protein structure in the composite	Methanol	180
Microcrystalline cellulose	[Amim][Cl]	10 wt%	85 °C (–)	Silk fibroin from *Bombix mori*	Intra- and intermolecular interactions between the biopolymers that shape the supramolecular structures (studied by small- and wide-angle X-ray scattering) and determine the thermal/physical properties of the composite. These features can be tuned by changing the composition	Water	179
Microcrystalline cellulose	[Bmim][Cl] [Emim][Cl] [Amim][Cl] [Emim][Ac] [Bmim][Br] [Bmim][$MeSO_3$]	10 wt%	100 °C (–)	Silk fibroin from *Bombix mori* (silk fibroin/cellulose fixed at 1/9 weight ratio)	The bulkiness of the anion strongly affects the fraction of β-sheet structure, the highest amount was obtained for [Bmim][Br] and [Bmim][$MeSO_3$]. The highest level of β-sheet configuration also meant the highest thermal stability	Water	181
Microcrystalline cellulose	[Amim][Cl]	5 wt%	103 °C (48 h)	Silk fibroin from *Bombix mori*	Theoretical model to predict the crystallinity, thermal stability and Young's modulus of silk fibroin/cellulose blends	Water	182
Microcrystalline cellulose	[Emim][Ac]	9 wt%	85 °C (24 h)	Silk fibroin from *Bombix mori* (silk fibroin/cellulose fixed at 1/9 weight ratio; 10 wt% total polymer concentration)	Positive correlation between cellulose crystallite size (cellulose II) and H_2O_2 concentration. Protein structure is not much affected by the coagulation process	0–25% aqueous H_2O_2 solution	183
Microcrystalline cellulose	[Emim][Ac] or [Emim][Cl]	5 wt%	85 °C (24 h)	Silk fibroin from *Bombix mori* (silk fibroin/cellulose fixed at 1/1 weight ratio; 10 wt% total polymer concentration)	The anion of the ionic liquid has an effect on the protein structure (a more amorphous structure is obtained when [Emim][Ac] is used)	0–25% aqueous H_2O_2 solution	184
Microgranular cellulose	[Bmim][Cl]	5 wt%	100 °C (–)	Wool keratin. 5 wt% dissolved at 100 °C for 10 h. The cellulose and keratin solutions added at 100 °C, stirred for 12 h	Improved thermal stability and elongation at break compared to the individual biopolymers. Hydrogen bonding interactions between the biopolymers	Water	186
Microcrystalline cellulose	[Emim][Ac]	10 wt% (total polymer)	80 °C (24 h)	Wool keratin (Keratin Azure)	The secondary structure of the protein can be influenced by the coagulation medium. Cellulose crystallinity increased when aqueous 25% H_2O_2 was used as coagulation bath	Aqueous 1% or 25% EtOH and 1% or 25% H_2O_2	187
Cotton cellulose	[Bmim][Cl]	—	100 °C (6 h)	Native skin collagen	—	Water/methanol/ethanol/acetone; at 4 °C	188
Microcrystalline cellulose	[Emim][Ac]	~6 wt%	60 °C (4 h)	Calf skin collagen. Collagen dissolution at 25 °C (6 h)	Hydrogen bonding between the biopolymers. Denaturation temperature increases in the composites (except at high collagen loading, 5/1 cellulose/collagen). High collagen content leads to phase separation and inhomogeneity	Water; at 4 °C	190
				Calf skin collagen. Collagen dissolution at 25 °C (36 h)		10% aqueous ethanol	191

strongly to cellulose microfibrills.[168] Inspired by its strong interaction with cellulose in the plant cell wall, Bendaoud *et al.*[169] simultaneously dissolved xyloglycan and cellulose in [Emim][Ac] and fabricated regenerated composites after immersing the cast films into water bath. Interestingly, the water-soluble xyloglycan mostly remained in the composite following the aqueous washing step (the authors used 3 days immersion), owing to the strong interactions between these two polymers. It was observed that at a certain xyloglycan/cellulose composition (this was 1/1 in their work), maximum tensile stress and strain at break could be obtained. The authors realised phase separation on the nanoscale, with the formation of 10–25 nm domains at this optimal composition (Fig. 17). It was rationalised that the nanostructuration of harder and softer cellulose and xyloglycan domains, respectively, lies behind the synergistic improvement in the mechanical properties. Sundberg *et al.*[170] prepared composites using *arabinoglucuronoxylan* (*xylans* consist of a 1,4-β-xylose backbone that is substituted with other monosaccharides, such as arabinofuranose and glucuronic acid units) – a hemicellulose extracted from spruce wood, with cellulose obtained from the same woody biomass. They dissolved both biopolymers in [Emim][Ac], and fabricated transparent regenerated films by using ethanol as antisolvent. The addition of xylan made the composites stiffer (higher elastic modulus) at relatively low humidity conditions (at 30% relative humidity (RH)). According to their explanation, a regenerated cellulose network may independently form during the coagulation process, and xylan may adhere to this network as a binder. Humidity had a significant effect on the mechanical properties, increasing RH above 30% resulted in a plasticising effect.

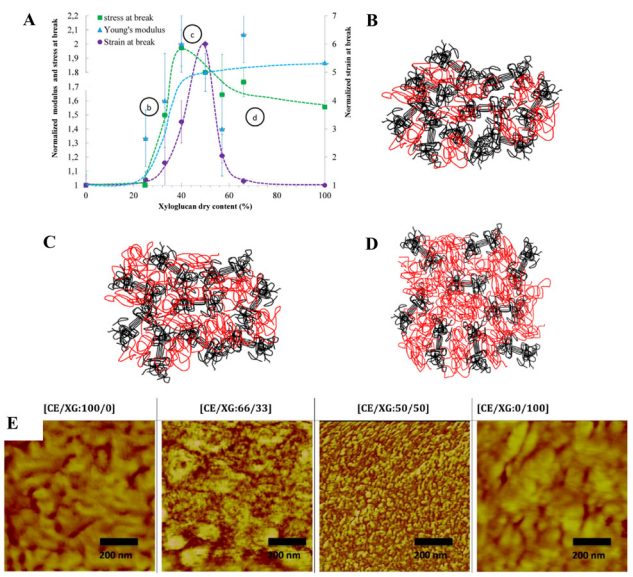

Fig. 17 (A) Normalised tensile properties of the xyloglycan/cellulose blends. Visual models for composites with (B) continuous cellulose matrix (xyloglycan/cellulose <40%), (C) continuous xyloglycan and cellulose matrix – nanostructured composite (xyloglycan/cellulose ~40–50%), (D) continuous xyloglycan matrix (xyloglycan/cellulose >50%). Red line represents amorphous xyloglycan domains, black line indicates cellulose semicrystalline domains. (E) AFM phase contrast images of the composites. Reproduced from ref. 169 with permission from Elsevier, copyright 2017.

Several works prepared so called "*synthetic wood*" composites that contain *lignin* besides *cellulose* and *hemicellulose*, and thus have all the major constituents of lignocellulosic biomass (Table 7). Lignin is the most abundant aromatic biopolymer in nature, it is a heteropolymer made of phenylpropanoid units.[171] Synthetic wood composites based on the tricomponent biopolymer system was studied first by Simmons *et al.*[172] using [Emim][Ac] as solvent, and water as coagulant. The ionic liquid solution contained 5 wt% cellulose, 3 wt% xylan from birch wood and 2 wt% softwood kraft lignin prior to the regeneration process, mimicking wood composition. The regenerated synthetic wood composite was more hydrophobic (water contact angle of 72°) than regenerated cellulose (45°) or cellulose/lignin (54°) composite, which was attributed to the smooth surface of the film (with an average roughness of about 50 nm). In addition, the synthetic wood composite had superior tensile strength (~62 MPa), the synergistic effect may have arisen from the strong hydrogen bonding interactions between the biopolymers. The authors observed also better UV shielding properties and thermal stability compared to the regenerated cellulose film. Furthermore, synthetic wood composites with PEG, chitosan and multiwalled carbon nanotubes were prepared to endow the film with enhanced hydrophilicity, antibacterial properties and with increased dielectric constant, respectively. Kim *et al.*[173] studied later the biodegradability and water vapor solubility of similar synthetic wood films prepared using [Emim][Ac] and water coagulation bath. The authors found that the biodegradability (cellulase test) increased with increasing xylan content, however, decreased with increasing lignin content. The water vapor solubility also increased with the addition of xylan, which may be a reason for the enhanced cellulase activity. The synthetic wood composite was studied further by Lee *et al.*[174] for biomimetic artificial photosynthesis through incorporating light harvesting porphyrins in the composite film (Fig. 18A and B). The porphyrins were solubilised in [Emim][Ac], and then mixed with the synthetic wood solution using the same solvent, prior to the regeneration step in water upon which the porphyrins could be entrapped in the matrix. The synthetic wood composite showed higher level of NADH generation (Fig. 18C), higher photo-to-dark current ratio, and faster response compared to that of the composite based on cellulose only (Fig. 18D). The authors attributed the enhanced charge transfer efficiency to the presence of lignin, which has redox active phenol groups.

Starch (a complex carbohydrate consisting of two types of polysaccharides: amylose (mainly α-1,4-linked D-glucopyranose units) and amylopectin (highly branched polymer, α-1,6-linkages besides the α-1,4-linked D-glucopyranose residues)) has also been considered as a biopolymer additive. Wu *et al.*[175] prepared cellulose/lignin/starch ternary composites *via* simultaneously dissolving the polysaccharides in [Amim][Cl], fol-

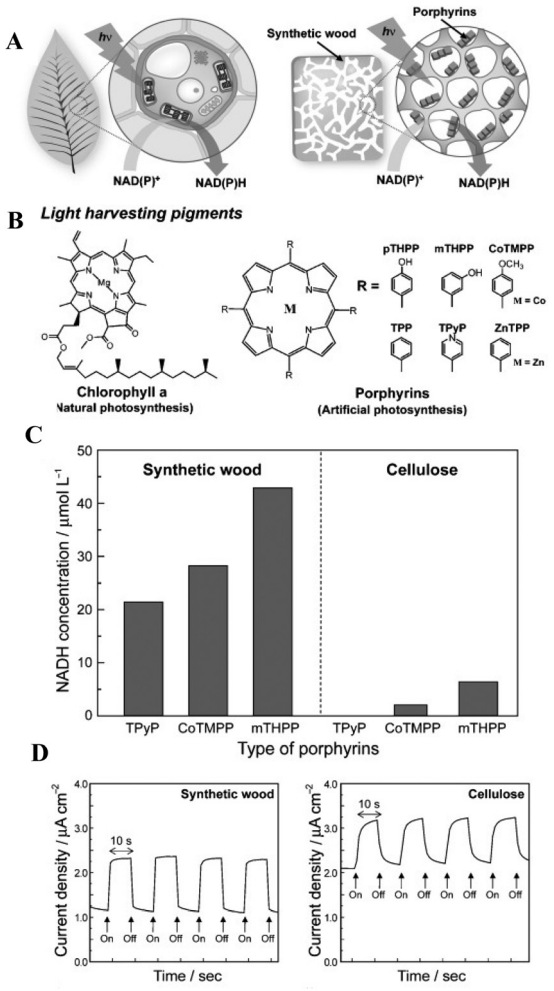

Fig. 18 (A) Light harvesting apparatus of green plants (left) and the concept of using a synthetic wood composite for artificial photosynthesis. (B) The structure of the natural photosynthetic pigment chlorophyll and the studied porphyrins as additives. (C) Photochemical NADH generation using the synthetic wood composite/cellulose with porphyrins, $[Cp^*Rh(bpy)H_2O]^{2+}$ as hydride transfer mediator, and triethanolamine as sacrificial electron donor. (D) Photocurrent generation of the respective composites. Reproduced from ref. 174 with permission from Wiley, copyright 2011.

lowed by regeneration in water. By optimising the amount of each biopolymer in the composite, the mechanical properties (tensile strength, elongation at break) could be greatly enhanced. It appeared that cellulose contributes to the flexibility of the material. The synergistic interaction of the biopolymers could be explained by destruction of the hydrogen bonds between each biopolymer upon dissolving in [Amim][Cl], followed by reconstitution of a hydrogen boding network between the homogeneously dispersed components during the regeneration step. In addition, good gas barrier properties and $CO_2 : O_2$ permeation ratios (1.05–1.67) indicated the applicability of the film for food packaging purposes.

4.6.3. Biocomposites with natural proteins: silk fibroin, wool keratin and collagen. *Natural proteins* have also gained considerable interest for the preparation of binary cellulose/biopolymer composites (Table 8). *Silk fibroin*, which can be obtained from *Bombyx mori* cocoons, has been widely studied as a promising additive. This interest has been fuelled by the excellent biocompatibility and biodegradability of this protein, finding various applications in the biomedical field.[176] Dissolution of silk fibroin in imidazolium-based ionic liquids was first reported in 2004,[177] and regenerated films were also prepared. In this early work, it was already noted that the structure of the regenerated silk fibroin greatly depends on the coagulation solvent and process. Shang *et al.*[178] was the first to study regenerated silk fibroin/cellulose films using [Bmim][Cl] solvent, and methanol coagulation bath. It was recognised that the random coil structure of silk I changes to the β-sheet conformation as a result of the addition of cellulose compared to regenerated silk films, as studied by FTIR spectroscopy. This lead to an increase in the tensile strength of the material, which at a certain composition reached a maximum value (silk fibroin/cellulose 25/75), along with the thermal stability and water resistance. The interesting conformational transition prompted others to further study this binary composite, and find ways to control the developing protein and cellulose structures (most of these works were done by D. Salas-de la Cruz and his co-workers). Stanton *et al.*[179] prepared regenerated silk fibroin/cellulose composite films from [Amim][Cl] solutions of the biopolymers. Their results indicated strong intra- and intermolecular interactions in the blends, which determined the supramolecular assemblies in the matrix as studied by small- and wide-angle X-ray scattering experiments. These features influence the physical and thermal properties of the material. They found that the β-sheet size increases with cellulose content, while increase in silk content results in smaller cellulose microfibril diameter. A more detailed characterisation of the structure and molecular interactions in silk fibroin/cellulose blends (regenerated from [Bmim][Cl] solution) was done by Tian *et al.*[180] through solid-state NMR experiments. Fig. 19 shows the ^{13}C CP/MAS NMR spectra recorded on regenerated silk fibroin, cellulose and cellulose/silk fibroin 3/1 blends as reported in ref. 180. The absence of the peaks at 65 ppm (C6) and 89 ppm (C4), characteristic for crystalline cellulose, indicated the presence of an amorphous cellulose structure. The region between 15–25 ppm is assigned to the Ala C_β (S7) moieties (Fig. 19C), which are sensitive to the secondary protein structure. It can be seen that the amount of well-defined parallel β-sheet increases in the cellulose/silk fibroin blends (see the shoulder around 23 ppm), together with a decrease in the distorted β-turns (peak around 17 ppm). The authors anticipated that the well-defined β-sheet structure could contribute to the enhanced tensile strength and toughness of the binary composite that was widely observed by them and by others in the literature. Furthermore, through ^1H–^{13}C heteronuclear correlation NMR experiments it was revealed that hydrogen bonding between the –NH group of the protein and the hydroxyl groups connected to the C2 and C3 carbons of cellulose is the most favourable. It was also recognised that some water remains bound to the cellulose structure causing nanoheterogeneity in the system. In a later study by Stanton

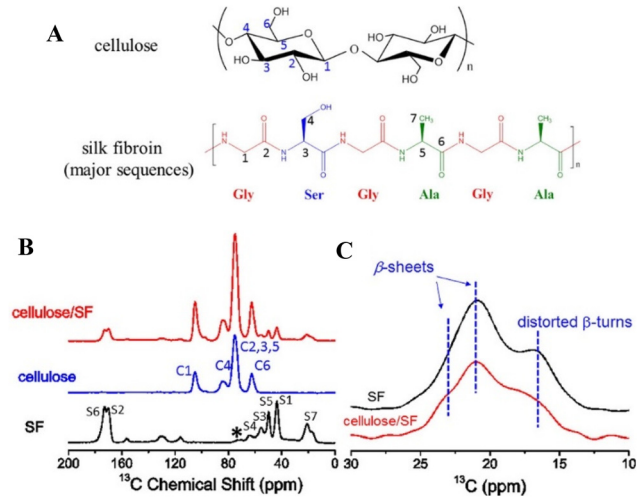

Fig. 19 (A) Structure of cellulose and silk fibroin with numbering for peak assignment (below). (B) ^{13}C CP/MAS NMR spectra of regenerated silk fibroin (SF), cellulose and cellulose/silk fibroin composite (3/1). Asterix indicates spinning sideband. (C) ^{13}C NMR spectra of regenerated SF and cellulose/SF composite in the Ala $^{13}C_{\beta}$ region for comparison. Reproduced from ref. 180 with permission from the American Chemical Society, copyright 2017.

et al.,[181] the effect of ionic liquid on the structure of the silk fibroin/cellulose film was investigated using [Bmim][Cl], [Emim][Cl] and [Amim][Cl] (effect of cation and hydrophobicity), [Emim][Ac], [Bmim][Br] and [Bmim][$MeSO_3$] (effect of the anion), while fixing the silk fibroin/cellulose ratio at 1/9. It was revealed that the level of the β-sheet structure depends significantly on the type of anion, the fraction of this segment was the highest (>50%) for [Bmim][Br] and [Bmim][$MeSO_3$], which have the bulkiest anion. The composite films regenerated from the latter ionic liquids also gave the highest thermal stability. In addition, it was observed that the inter-sheet distance between cellulose microfibrils and β-sheet structure decreases when the cation is changed from allyl-substituted ([Amim][Cl]) to ethyl-substituted ([Emim][Cl]) form. The composite film from [Amim][Cl] had the lowest amount of β-sheet structure. Moreover, theoretical model was also developed to predict the trends in crystallinity, thermal stability and mechanical properties (Young's modulus) of the regenerated silk fibroin/cellulose blends as a function of the composition.[182] This model appeared to describe well the experimental results in the same work (thermal stability), and aligned with other findings in the literature (mechanical properties). It is interesting to note that Love *et al.*[183] found a way to tune the crystallinity of the cellulose in the silk fibroin/cellulose film regenerated from [Emim][Ac] solutions. They observed that cellulose crystallite size increases as the concentration of H_2O_2 increases in the aqueous coagulation bath, while this had only a subtle effect on the structure of silk fibroin in the composite. According to their explanation, this phenomenon may be due to the preference of H_2O_2 to form hydrogen bonds with the cellulose molecules. The material with larger cellulose crystals showed higher thermal stability, as expected. Furthermore, in a later study by the same group,[184] it was revealed that the protein structure can be affected by the type of the anion of the ionic liquid. It appeared that using [Emim][Ac] as solvent leads to the formation of more amorphous protein structure compared to [Emim][Cl].

Wool keratin is another interesting natural protein to consider as additive in cellulose composites. It is an underutilised, low-cost material generated in large quantities as waste by the wool textile industry, and by the food industry through the operation of butcheries. The dissolution of wool keratin in an ionic liquid was first reported by Xie *et al.*[185] using [Bmim][Cl], and regenerated wool keratin and cellulose/wool keratin blends were also fabricated in this work using methanol as coagulation medium. The properties of the cellulose/wool keratin regenerated films were studied later in detail as a function of the composition by Hameed and Guo.[186] The blends showed higher thermal stability and elongation at break compared to the individual components, these properties reached maximum value at a certain composition (cellulose/wool keratin 60/40). It was also observed through FTIR measurements that hydrogen bonding interactions take place between the biopolymers. In a recent study,[187] the effect of the coagulation bath (1% or 25% EtOH and 1% or 25% H_2O_2 aqueous solution) on the structure of cellulose and wool keratin was studied using [Emim][Ac] as solvent. It appeared that the amount of β-sheet and α-helical protein structures can be manipulated by the composition, coagulation bath additive and its concentration. The highest amount of α-helices (34.3%) was obtained for 75/25 wool keratin/cellulose composites using 25% H_2O_2 aqueous solution as coagulation bath, this value is much higher than that of the initial wool keratin sample (8.7%). The highest amount of β-sheets (33.6%) were observed when the coagulation bath was 25% aqueous EtOH solution, this value is close to the initial keratin sample (33.0%). Furthermore, an increase in cellulose crystallinity was observed when higher concentration of H_2O_2 was used.

Type I *collagen* is an abundant protein found in vertebrates, it is widely used for biomedical applications, and in the food and cosmetic industry, owing to its biocompatible, biodegradable and edible character. The processing of collagen in an ionic liquid was reported using [Bmim][Cl] for the first time,[188] the dissolution was done at 100 °C (for 6 h). It was recognised through FTIR and XRD analysis that the triple helical structure of collagen is partly destroyed, random coils are formed and possible degradation may also take place. It was also observed that the secondary structure can be significantly influenced by the type of the coagulant (they used water, ethanol, methanol and acetone). Collagen/cellulose blends could also be prepared and shaped into various forms during the coagulation step (films, gels, fibres). Using this processing system ([Bmim][Cl], 100 °C), Wang *et al.*[189] prepared hydrogel beads by dropping the collagen/cellulose binary solution into water. These beads were used for the adsorption of Cu(II), this process showed a positive correlation with collagen content until a limiting value (a mass ratio of 2/1 collage/cellulose). Zhang *et al.*[190] used [Emim][Ac] as solvent to dissolve

first cellulose at 60 °C (for 4 h), followed by the addition of collagen at room temperature, in order to operate below the denaturation temperature of the protein. They found that the denaturation temperature of the protein increased in the regenerated cellulose/collagen films. Their FTIR results indicated the formation of hydrogen bonds between the polymers. While the addition of relatively small amount of collagen (cellulose/collagen 30/1) increased the thermal stability (maximum decomposition temperature) and mechanical properties (elastic moduli from dynamic mechanical analysis (DMA)), these parameters declined at higher collagen loading (10/1 cellulose/collagen). Cellulose crystallinity also decreased significantly for this higher collagen content. In another study from the same group,[191] it was confirmed that at high collagen loading aggregates exist in the solution (at 10/1 cellulose/collagen; based on dynamic rheology experiments). The lack of homogeneity and phase separation was also observed at high collagen content in the composite films (5/1 cellulose/collagen).

4.6.4. Miscellaneous – biocomposites with various other biopolymers. *Gutta percha*, a *natural rubber* that consists of long chain *trans*-1,4-polyisoprene molecules, was considered as additive by Xu *et al.*[192] Interestingly, this long-chain, high molecular weight polymer was not soluble in the ionic liquid [Bmim][Ac] that was used to dissolve cellulose. Therefore, gutta percha was dissolved first in chloroform, and was then added to the cellulose/ionic liquid solution. Hydrophobicity of the films could be conveniently increased by adding the aliphatic long-chain polyisoprene molecule to the matrix. The prepared composite exhibited maximum tensile strength (about 73% increase compared to regenerated cellulose) and elongation at break at a certain loading of the natural rubber (10% relative to cellulose). At this composition the material showed minimum oxygen permeability (1.87 cm^3 m^{-2} day kPa at 25 °C). These properties make the prepared composite a promising candidate for food packaging applications.

Heparin, is a glycosaminoglycan, a negatively charged polysaccharide that can be found in animals, and is an important medication owing to its anticoagulant properties. Murugesan *et al.*[193] aimed at fabricating blood-compatible dialysis membranes using regenerated cellulose/heparin composites. The imidazolium salt of heparin was first prepared and dissolved in 1-ethyl-3-methylimidazolium benzoate ([Emim][Ba]). Cellulose was separately dissolved in [Bmim][Cl] (10 wt% concentration), and the two solutions were mixed to prepare the binary composite film using ethanol coagulation bath. The successful entrapment of heparin in the matrix was confirmed by leaching test, showing small amount of loss. The excellent blood compatibility of the membrane was demonstrated *via* Activated Partial Thromboplastin Time (APTT) and Thromboelastography (TEG) tests. The composite exhibited a nanoporous structure; in an equilibrium dialysis test urea could diffuse through the membrane while bovine serum albumin (BSA) was mostly retained. This biocompatible membrane is promising for renal dialysis application while avoiding systemic heparinisation and the complications associated with that process.

Park *et al.*[194] in a comprehensive work studied *agar, agarose, arabic gum, bacterial cellulose, chitosan, collagen, β-cyclodextrin, dextran, gelatine, κ-carrageenan, lignin, silk, starch, tragacanth gum, xanthan gum* and *xylan* biopolymers as additives to cellulose, using [Emim][Ac] solvent (dissolution at 60 °C, stirring with cellulose for 3 h), and ethanol as coagulant (cellulose/biopolymer 4/1). The composites had diverse physicochemical properties. The water contact angle varied between 90.1° (cellulose/chitosan) and 33.0° (cellulose/κ-carrageenan), thus more hydrophobic and hydrophilic films could be obtained, respectively, compared to cellulose (water contact angle of 52.8°). The high light barrier properties of the lignin/cellulose blend were noted below 400 nm, indicating good UV-shielding properties (Fig. 20A). The chitosan/cellulose film exhibited excellent adsorption capacity towards organic dyes (9.1-fold and 7.9-fold higher adsorption capacity, respectively, compared to cellulose film). The biopolymer composite films showed enhanced adsorption for the enzyme lysozyme

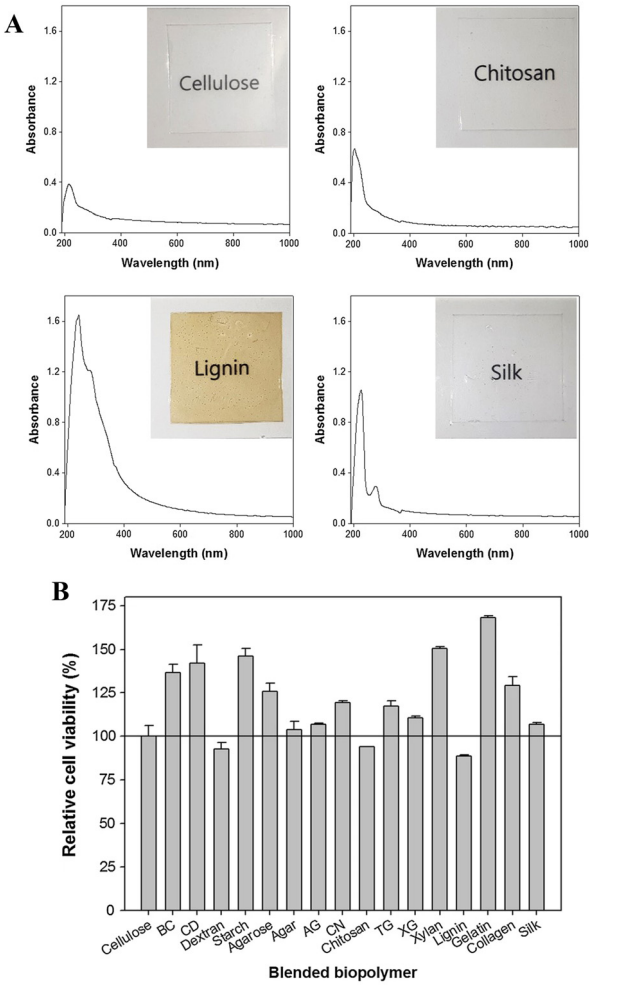

Fig. 20 (A) UV-Vis spectra of regenerated cellulose, cellulose/chitosan, cellulose/lignin and cellulose/silk films with good light barrier properties below 400 nm. (B) Cell viability of TCMK-1 cells cultured on the composite films. Reproduced from ref. 194 with permission from Springer Nature, copyright 2020.

compared to cellulose films, and for the enzyme pepsin some films showed excellent adsorption behaviour exceeding that of cellulose (*e.g.*, for the cellulose/β-cyclodextrin film). Furthermore, outstanding cell viability (TCMK-1 cells) could be observed for some of the films (superior to cellulose), the highest was achieved for the cellulose/gelatine films (Fig. 20B).

4.7. Cellulose-based ionogels, hydrogels and aerogels using ionic liquids

4.7.1. Cellulose-based ionogels. *Ionogel* is a type of gel where ionic liquids are dispersed in a continuous solid matrix. Although they can be found under several names in the literature (such as *ionic gel, ionic liquid gel, ion gel, ion-gel, etc.*), the term ionogel rose in popularity in recent works. Cellulose-based ionogels have gained significant interest for a wide range of applications including sensor, actuator and energy storage devices.[195]

The first cellulose-based *physical ionogel* was reported by Kadokawa *et al.*[196] in 2008. They prepared a concentrated cellulose solution (15 wt%) in [Bmim][Cl] (at 100 °C for 24 h), which was kept between glass slides for 7 days. The obtained gel was washed with ethanol to remove the excluded ionic liquid. Besides the ionic liquid and cellulose, the ionogel contained considerable amount of water as well (in their work water amount was 8.69–16.0 eq. per glucose unit, whereas ionic liquid content was 2.48–4.68 eq. per glucose unit). According to their explanation, the ionogel forms as water slowly diffuses into the ionic liquid/cellulose solution, creating non-crystalline aggregates as physical crosslinking points. Such materials can be classified as *physical ionogels*, as they are generated through reversible non-covalent interactions, in contrast to *chemical ionogels* that contain covalent crosslinks between the polymer chains. The physical ionogel obtained this way can be easily reversed to its original fluid form by heating to 150 °C. Please note that a gel material can be easily identified, and its physical/chemical gel character judged most commonly through oscillatory rheometry or dynamic mechanical analysis (DMA) measurements;[197,198] unfortunately, such characterisation is not always present in the literature. The physical ionogels that were prepared by others through similar strategy to that of the original work of Kadokawa *et al.*[196] by dissolving cellulose, are summarised in Table 9.

Cellulose-based physical ionogels are promising materials for *solid electrolytes* in electrochemical applications. The first study towards this direction was done by Yamazaki *et al.*[199,200] on hybrid cellulose/chitin ionogels for supercapacitor devices. Cellulose was dissolved in [Bmim][Cl], while chitin was dissolved in [Amim][Br]. The two solutions were mixed (to reach a cellulose/chitin weight ratio of 3/1), and ionogel was obtained after leaving the sample at room temperature for 4 days. Additionally, the obtained gel was immersed in H_2SO_4 solution in order to have an acidic cellulose/chitin ionogel. Symmetric two-electrode device was assembled using the ionogel sandwiched between activated carbon fiber cloths as electrodes.

Table 9 Physical ionogels prepared by dissolving cellulose in an ionic liquid

Type of cellulose	Ionic liquid	Cellulose concentration	Dissolution temperature (time)	Properties, observations	Application	Ref.
Microcrystalline cellulose	[Bmim][Cl]	15 wt%	100 °C (24 h)	Solution kept between glass slides for 7 days. Finally washing with ethanol	—	196
Microcrystalline cellulose	[Bmim][Cl]	5 wt% (and 10 wt% chitin solution in [Amim][Br])	100 °C (24 h)	Cellulose/chitin composite ionogel at 3/1 weight ratio (solutions mixed at 100 °C (1 h))	Supercapacitor	199 and 200
Microcrystalline cellulose	[Bmim][Cl]	13 wt% (DMA as plasticiser and co-solvent)	100 °C (15 min)	Performance superior to common dielectric elastomers	Actuator	201
Microcellulose (ARBOCEL® MF 40-7, J. Rettenmaier & Sons)	Phosphonate-based ionic liquid with [Emim] cation/ [Emim][NTf_2]	—	—	[NTf_2] anion helps improving ionic mobility, while the phosphonate anion based ionic liquids form gels with cellulose	Flexible paper-based electronics; electrolyte-gated field-effect transistors (FETs)	202
Cellulose powder (Sigma Aldrich)	1-methyl-3-propylimidazolium iodide ([Mpim][I])/ [Emim][SCN] 1/1	5 wt%	90 °C (24 h)	A maximum photoconversion efficiency of 3.33%	Gel electrolyte for dye-sensitised solar cells	203
Cellulose source not defined	[Bmim][Cl]	8 wt%	Not defined	Dynamic ionogel with tunable properties by adjusting the water content	Demonstrated application as electronic skin (sensing). Other possible applications such as flexible electronics, soft robotics, energy storage and other intelligent devices	205

The *supercapacitor* device exhibited a specific capacitance somewhat higher than the device with H_2SO_4 electrolyte, together with good cycling stability (100 000 cycles, 80% capacitance retention, performed at 5 A g^{-1} current density).[199] The device showed good stability for operating at wide temperature window (−10–60 °C).[200] Furthermore, Kunchornsup and Sirivat[201] fabricated cellulose/[Bmim][Cl]/DMA ionogels as *electro-active paper for actuator applications*.

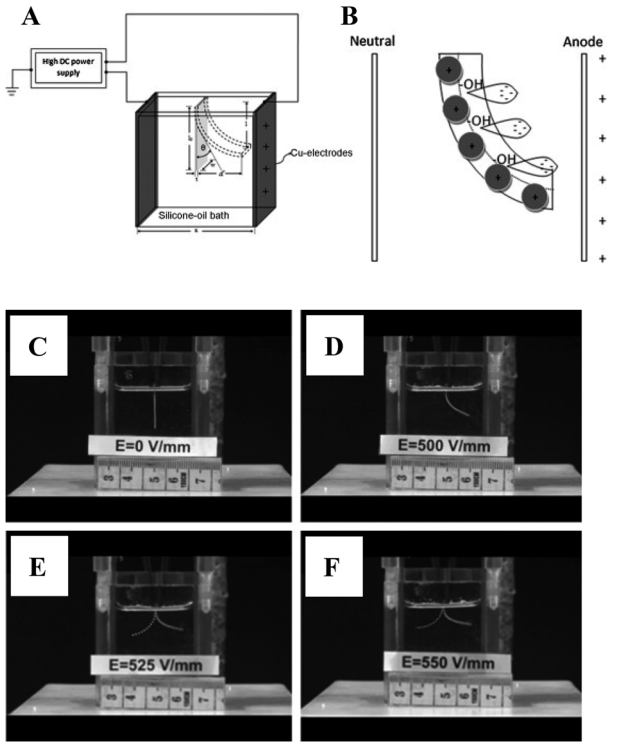

Fig. 21 (A) Experimental setup for studying the bending response of the ionogel under an applied electric field. (B) Schematic representation of the proposed mechanisms of the bending response. (C and D) Deflection and (E and F) swinging movement of the ionogel in response to a ground and positive electric field at room temperature. Reproduced from ref. 201 with permission from Elsevier, copyright 2012.

According to their results, several electromechanical parameters of the ionogel were superior to other studied dielectric elastomers at room temperature. However, they identified the slow response speed of the ionogel as a limiting parameter, which should be improved in the future. Fig. 21A shows the experimental setup to study the response of the ionogel towards an applied electric field. According to the authors' explanation, ionic polarisation of the imidazolium cations, together with polarisation of the hydroxyl groups of the cellulose structure cause the movement (Fig. 21B). Images of the bending and swinging responses are shown in Fig. 21C–F.

Thiemann *et al.*[202] developed cellulose ionogels for *flexible electronics* application. They fabricated electrolyte gated *field-effect transistors (FETs)*, using multilayer coated flexible paper substrate in one of the devices (Fig. 22A and B). In their work, microcellulose (ARBOCEL® MF 40-7, from J. Rettenmaier & Sons) was casted on a glass slide first, followed by dropping ionic liquid on the film to obtain an ionogel (with cellulose/ionic liquid mass ratio of 3/70). They used ionic liquids that are based on [Emim] cations and methylphosphonate anions or their mixture with [Emim][NTf_2] (Fig. 22C, note that TFSI = [NTf_2]). [Emim] cations with methylphosphonate anions show good ability to dissolve/gelate cellulose, while [Emim][NTf_2] is a non-dissolving ionic liquid that does not interact with cellulose, and its main role in the system is to increase ionic mobility. It was found that the highest specific capacitance (18.4 μF cm^{-2} determined *via* impedance spectroscopy measurement) was obtained for a binary system with [Emim][MeAc(Me)PO_3] (where [MeAc(Me)PO_3] is 2-methoxy-2-oxoethyl methylphosphonate anion)/[Emim][NTf_2] at 9/1 ratio. These ionogels with high ionic mobility performed well for side-gated FET devices. The authors noted that by increasing the bulkiness of the anion (increasing ethylene glycol chain length) of the ionic liquid, the specific capacitance of the ionogel decreases. These ionogels with lower ionic mobility gave rise to higher electron mobility in spray-coated ZnO FETs.

Salvador *et al.*[203] studied the application of cellulose-based ionogels as electrolytes for *dye-sensitised solar cells*. They used a mixture of two ionic liquids: 1-methyl-3-propylimidazolium iodide ([Mpim][I]) that can supply ions for the iodide/triiodide

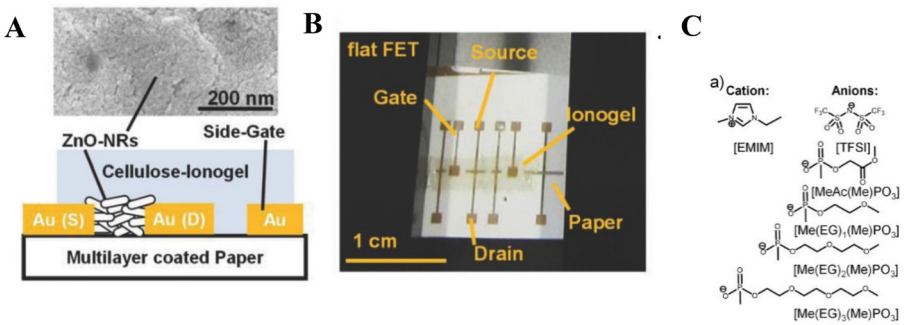

Fig. 22 (A) The structure of the ionic liquids used to fabricate the ionogels for electrolyte-gated field-effect transistor (FET) devices. (B) Schematic description of the flexible FET device with ZnO nanorods (NRs; an SEM image is shown above the device) and cellulose ionogel. (C) Photograph of the flexible paper-based FET. Reproduced from ref. 202 with permission from Wiley, copyright 2013.

redox couple, a mediator in mesoscopic dye-sensitised solar cells;[204] and [Emim][SCN] which helps decreasing the high viscosity of the [Mpim][I]/cellulose system, thereby increasing ionic mobility. They found that a 50/50 mixture of the two ionic liquids provides the best photovoltaic performance. Increasing cellulose concentration had a positive effect on the photocurrent and photovoltage, reaching a plateau at 5 wt% cellulose loading. Dissolution of cellulose was done in the ionic liquid mixture together with other electrolyte components (LiI and I_2) at 90 °C (24 h), followed by gelation at room temperature for one day. 4-*tert*-Butylpyridine, another important component for the electrolytes of mesoscopic dye-sensitised solar cells, was added after the gelation process due to its volatile nature. A maximum photoconversion efficiency of 3.33% could be achieved with the fabricated dye-sensitised solar cell containing the quasi-solid electrolyte. Interestingly, the authors observed that the photovoltaic performance increases in the beginning of the operation, and reaches a plateau at a later time. According to their explanation, the movement of ions are hindered by the forming hydrogen bonds with the hydroxyl groups of cellulose. During operation, through the energy input, the energy barrier of these interactions can be overcome, releasing free iodide ions that can contribute to the improvement of the photovoltaic performance.

Zhao *et al.*[205] developed a dynamic gel based on the [Bmim][Cl]/cellulose type ionogel. They realised that the ionogel exhibits tunable, and reversible dynamic properties based on the water content (Fig. 23A). At low water content (6 wt%), hydrogen bonds are generated between water and the cellulose molecules leading to a loosely packed Turing type topological network. In this system, ions exhibit low mobility, leading to low ionic conductivity. In addition, this ionogel exhibits excellent self-healing properties owing to the reversibility of the hydrogen bonds, and can adhere strongly to various substrates, *e.g.*, glass, plastics and metals (it can lift more than 30 times its weight ones adhered to the metal substrate). At high water content (32 wt%), more hydrogen bonds are formed and a denser Turing microstructure is generated that exhibits robust toughness with excellent strength and formability (*e.g.*, withstanding repeated rolling and folding). This system contains more hydrated ions with enhanced mobility, leading to a high ionic conductivity (a maximum of 40 mS cm^{-1}). Switching between the two topological networks can be reversibly done by adjusting the water content of the ionogel (drying or increasing the relative humidity), with arriving at the original properties as demonstrated by the authors. Such dynamic ionogel can be useful for a range of applications such as *soft robotics and flexible electronics*. The authors demonstrated the application for *electronic skin* (e-skin, see Fig. 23B). The e-skin device was fabricated by sandwiching conductors between two ionogels (by taking advantage of the self-healing property of the material). The e-skin device can be applied for sensing various external stimuli such as breathing patterns, air flow and touching.

We would like to note that the *ionic diffusion* process that determines the conductivity in [Bmim][Cl]/cellulose type ionogels has been studied in detail by NMR spectroscopy.[206] It was revealed that two cation diffusion processes can be identified in the matrix: (1) a fast translational diffusion in the pores where the ionic liquid behaves similarly to its bulk structure, and (2) a slow ion diffusion close to the surface of cellulose owing to secondary interactions. The authors noted that the small difference between the ionic conductivity of the ionogel and the bulk ionic liquid can be explained by the presence of the fast, unrestricted diffusion process supplying ions through the channels within the matrix.

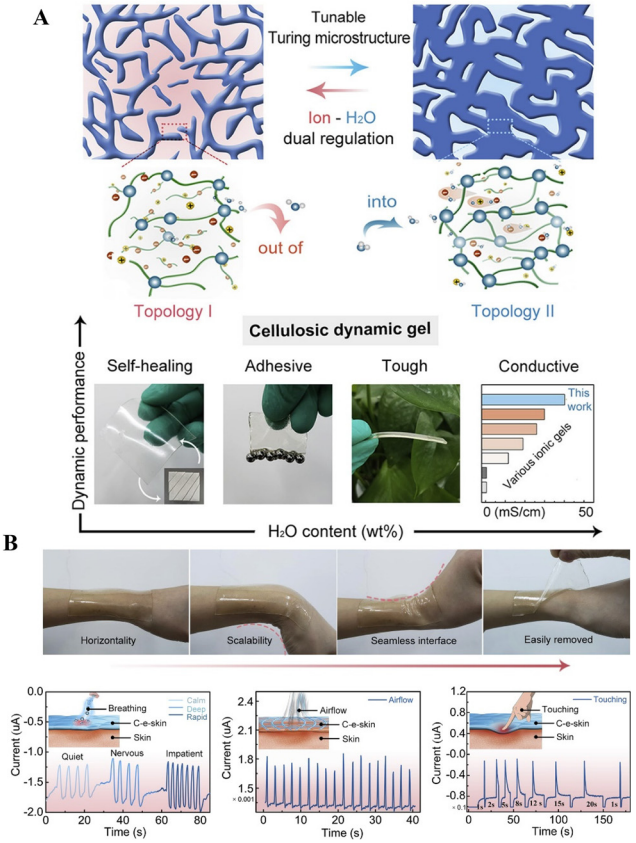

Fig. 23 (A) Transition between two topological networks by adjusting the water content of a cellulose/[Bmim][Cl] ionogel. The ionogel thus exhibits tunable dynamic properties as shown in the bottom of the figure. (B) Application of the dynamic ionogel in an electronic skin device that can be used for sensing *e.g.*, breathing pattern, airflow and touching. Reproduced from ref. 205 with permission from Elsevier, copyright 2019.

Besides common unmodified cellulose starting materials, several works used *bacterial cellulose*,[207] *methylcellulose*[208–210] and *nanocellulose*[211] that have already been proven excellent for the preparation of other types of hydrogels (Table 10). The preparation of the physical ionogel is different in these works compared to previous studies discussed above, in that they do not follow the usual dissolution – gelation strategy. Bacterial cellulose is interesting in that it has high water absorption capacity, a hydrogel can have as high as 99 wt% water content. In the work of Smith *et al.*,[207] a *bacterial cellulose* hydrogel was first prepared, followed by a solvent exchange process with

Table 10 Physical ionogels prepared using non-dissolving (cellulose) ionic liquids and cellulose materials that can form gels

Type of cellulose	Ionic liquid	Maximum ionic liquid content	Preparation method	Properties, observations	Application	Ref.
Bacterial cellulose	[Emim][NTf_2] or [Bmpy][NTf_2] or [$P_{14,6,6,6}$][NTf_2]	99 wt%	First hydrogel, then alcogel after solvent exchange with ethanol. Ionic liquid incorporation *via* co-solvent assisted diffusion and then co-solvent evaporation gives the ionogel	Ionogels of various shapes and thicknesses can be fabricated by using a template during culturing	Incorporation of chemosensory molecules (*via* co-solvent assisted diffusion) for ammonia and H_2S detection	207
Methylcellulose	[Bmpy][NTf_2]	97 wt%	Methylcellulose and [Bmpy][NTf_2] dissolved in DMF, then mixed. Gelation occurs after a heating–cooling (up to 90 °C) cycle. DMF removed by vacuum drying	Flexible ionogel with high ionic conductivity (3.3 mS cm^{-1} at 30 °C), wide electrochemical stability window (5.6 V). Thermally stable (no thermoreversible sol–gel transition) until degradation (around 300 °C)	Solid state electrolyte	208
Methylcellulose	[Emim][NTf_2]	95 wt%	Same as previous procedure, using DMF as co-solvent	Soft, but mechanically strong (5 MPa storage modulus) gel with good compatibility for the porous carbon nanofiber electrode. High ionic conductivity (5.7 mS cm^{-1} at 25 °C)	Self-standing solid-state supercapacitor	209
Methylcellulose	[G_4Li][NTf_2]	90 wt%	Same as previous procedure, using DMF as co-solvent	High ionic conductivity (0.4 mS cm^{-1} at 30 °C) and storage modulus (60 MPa) at R.T. High thermal (up to 200 °C) and anodic stability (up to 5 V). Li^0/iongel/$LiFePO_4$ coin cell with performance comparable to that of the liquid electrolyte	Lithium metal battery	210
Cellulose nanocrystals (CNC)	Hyperbranched polymeric ionic liquid (PIL) + [Emim][NTf_2]	95 wt% [Emim][NTf_2]	CNC/PIL aqueous suspension first, then solvent exchange with ethanol. [Emim][NTf_2]/ethanol diffusion into gel, followed by evaporation of ethanol	High compressive elastic modulus (5.6 MPa) and ionic conductivity (7.8 mS cm^{-1} at 30 °C)	—	211

ethanol to obtain an alcogel. Ionic liquid/ethanol mixture was added to this alcogel, and after evaporating ethanol, an ionogel could form. In a similar fashion, through co-solvent assisted diffusion (using ethanol, which is then evaporated), chemosensory molecules could also be incorporated in the ionogels for NH_3 sensing and H_2S detection. This bacterial cellulose ionogel was capable of hosting 99 wt% ionic liquid, which is an outstanding performance compared to other ionogels. The authors selected ionic liquids with [NTf_2] anion and [Emim], 1-butyl-1-methylpyrrolidinium ([Bmpy]) and trihexyltetradecylphosphonium ([$P_{14,6,6,6}$]) cations, which are non-dissolving ionic liquids for cellulose. *Methylcellulose* is another intriguing gelator for the preparation of physical ionogels. It is known that fibrillar methylcellulose can dissolve in water, and upon a heating–cooling cycle it reforms the nanofibrils which eventually generate an interconnected fibrillar network leading to gelation.[212] The same phenomenon occurs when methylcellulose is dissolved in DMF.[213] In the work of Mantravadi *et al.*,[208] [Bmpy][NTf_2] was used as ionic liquid to fabricate ionogels using methylcellulose. [Bmpy][NTf_2] does not dissolve methylcellulose, the ionic liquid and methylcellulose was first dissolved separately in DMF. After mixing these solutions at certain ratios, gel formation was achieved by a thermal heating–cooling cycle (heating to 90 °C, cooling to room temperature; gelation occurs due to the presence of DMF). After removing DMF, an ionogel could be obtained with high 97 wt% ionic liquid content. This ionogel did not show thermoreversible sol–gel transition anymore, it remains solid until decomposition occurs (at around 300 °C). The authors highlighted that the film is self-standing and flexible with high moduli (>100 MPa) and high ionic conductivity (>10^{-3} S cm^{-1}, room temperature). This procedure was later adapted to

prepare [Emim][NTf_2]/methyl cellulose ionogels with 95 wt% ionic liquid content.[209] This ionogel was used as solid electrolyte for symmetric supercapacitors with activated porous carbon nanofiber electrodes. The supercapacitor device exhibited a wide operation window (3.5 V) owing to the ionic liquid, and high gravimetric capacitance (153 F g^{-1}), energy density (around 65 W h kg^{-1} at 1150 W kg^{-1} power density) and cycling stability (4% capacitance loss after 20 000 charge–discharge cycles at 1 A g^{-1} current density) were reported. In the same way of preparation, a solvate (or chelate) ionic liquid/methylcellulose ionogel was also prepared, where the ionic liquid was [G_4Li][NTf_2] (G_4 means tetraglyme here, with 1/1 molar ratio in respect to the Li^+; 90 wt% ionic liquid content).[210] Glymes can wrap around the Li^+ ions, resulting in a stable complex; the resulting ionic liquid when combined with [NTf_2] anion has high anodic stability (4.5 V), and exhibits high lithium ion transference number ($t_{Li^+} \approx 0.5$; fraction of electric current derived from lithium ions in respect to the total current, it indicates the mobility of lithium ions in the electrolyte). Interestingly, the electrochemical working window of the [G_4Li][NTf_2]/methylcellulose ionogel is about 5 V, somewhat higher than the liquid electrolyte [G_4Li][NTf_2]. The authors attributed this phenomenon to the forming hydrogen bonds between the oxygen groups of glyme and cellulose, thereby protecting them against oxidation. In addition, the ionogel showed high ionic conductivity (4×10^{-4} S cm^{-1}, 30 °C), storage modulus (60 MPa) and thermal stability (>200 °C). The assembled Li^0/ionogel/$LiFePO_4$ coin cell showed comparable performance to that of the cell with the pure [G_4Li][NTf_2] ionic liquid.

Cellulose nanocrystals (CNC) have also been used to prepare ionogels. Lee *et al.*[211] developed a system that contains a polymeric hyperbranched ionic liquid (PIL; see Fig. 24) and cellulose nanocrystals in order to create a mechanically persistent (high compressive modulus of 5.6 MPa) ionogel that can hold 95 wt% [Emim][NTf_2]. The ionogel exhibited also high ionic conductivity owing to the continuous nanoporous network structure that enables efficient transport of ions throughout the structure. For preparing the ionogel, the authors used similar solvent exchange strategy we discussed above for bacterial cellulose. First, a CNC and PIL binary suspension was prepared in aqueous medium, followed by a solvent exchange process with ethanol. An ionic liquid/ethanol solution was then added, which slowly diffused into the gel. After evaporating the co-solvent ethanol, an ionogel was obtained (4.5 wt% CNC content, 0–2 wt% PIL content).

Chemical ionogels were prepared for example by crosslinking the cellulose solution in ionic liquids using glutaraldehyde (HCl catalyst) crosslinker (in [Bmim][Cl]);[214] *via* acrylic acid monomer (AIBN initiator) grafting/*in situ* polymerisation in cellulose/[Bmim][I] solution (for dye-sensitised solar cell with quasi-solid-state electrolyte);[215] and through ionising radiation (γ-rays) induced crosslinking of cellulose/[Emim][Ac] or cellulose/*N*,*N*-diethyl-*N*-methyl-*N*-(2-methoxyethyl)ammonium (DEMA)-formate in the presence of water.[216] Furthermore, as another strategy, dual network structure ionogel can also be prepared by polymerising a monomer in the presence of cellulose as it was shown by Rana *et al.*[217] In their work, cellulose was dissolved in the ionic liquid 1,3-dimethylimidazolium methyl phosphite [DMIM][MeO(H)PO_3] containing small amount of [Bmim][NTf_2] (9/1 weight ratio). During the dissolution process, the hydroxyl groups connected to the C6 carbon atoms get phosphorylated in [DMIM][MeO(H)PO_3] (Fig. 25A). While the role of [DMIM][MeO(H)PO_3] is to dissolve cellulose, [Bmim][NTf_2] increases the conductivity of the ionogel due to the presence of [NTf_2] anion that does not interact with polar groups and exhibits high mobility in the system. The use of [NTf_2] anion is a common strategy seen in the literature to ensure the good ionic conductivity of the ionogels. After the dissolution/modification process, 2-hydroxyethyl methacrylate (HEMA) monomer was polymerised using *N*,*N*′-methylenebisacrylamide crosslinker and benzoyl peroxide as initiator (Fig. 25B). The ionogel was used to fabricate flexible symmetric supercapacitors by sandwiching one between two activated carbon electrodes. The flexible supercapacitor device

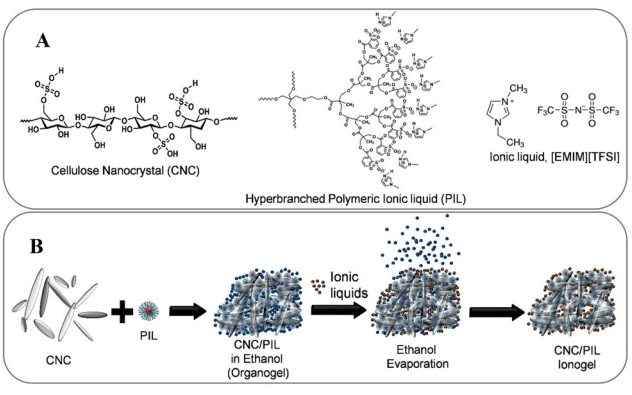

Fig. 24 (A) Ionogel containing cellulose nanocrystals, hyperbranched polymeric ionic liquid and [Emim][NTf_2]. (B) Method to prepared the CNC/PIL ionogel containing [Emim][NTf_2]. Note that TFSI = NTf_2. Reproduced from ref. 211 with permission from Wiley, copyright 2021.

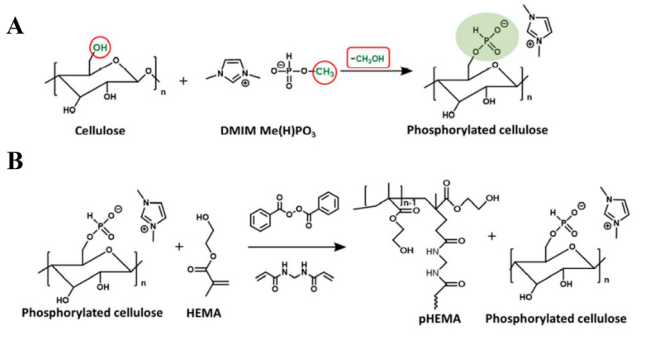

Fig. 25 (A) Cellulose dissolution and modification in [DMIM][MeO(H)PO_3] ionic liquid. (B) Polymerisation of HEMA in the presence of phosphorylated cellulose in order to obtain a dual network ionogel. Reproduced from ref. 217 with permission from Elsevier, copyright 2019.

could be operated at 2.5 V within wide temperature range (30–120 °C), exhibiting good performance.

4.7.2. Cellulose-based hydrogels through ionic liquid processing. *Hydrogels* can be prepared from the corresponding ionogels by simple solvent exchange process with water, when the ionic liquid is water-soluble. In such a way, cellulose physical hydrogels were obtained from [Amim][Cl],[218] [Bmim][Ac]/DMSO,[219] [Emim][Ac],[220] and [Bmim][Cl][221] solutions. Furthermore, in the work of Kimura *et al.*,[222] 1-ethyl-3-methylimidazolium methylphosphonate ([Emim][(MeO)(H)PO_2]) ionic liquid was used to dissolve cellulose, followed by a coagulation process with methanol, and then solvent exchange with water to obtain the physical hydrogel. Temperature- (*e.g.*, shape is retained in boiling water, no sol–gel transition observed), pH- and solvent-resistant, tough hydrogels could be prepared in this way, even with micrometer-sized patterns by using an appropriate mold. The hydrogel could be post-modified with amino groups, which allowed the immobilisation of negatively charged photoresponsive porphyrin molecules (namely tetrakis(4-sulfonatophenyl)porphyrin) inside the hydrogel *via* electrostatic interactions.

Cellulose/biopolymer binary hydrogels have also been prepared using polysaccharide additives such as κ-carrageenan, chitosan, guar gum and starch.[223] In the latter work, cellulose sample was extracted from spent tea leaves, and [Amim][Cl] was used as solvent to dissolve cellulose together with the other polysaccharide additives. All of the composites showed cell compatibility without cytotoxicity, and some biopolymer-specific functional properties (such as specific mechanical and physicochemical characteristics) could be also observed. Furthermore, okara-derived (food residue from soybean industry) cellulose hydrogels containing hemicellulose (remained after the extraction process) were prepared by Wu *et al.*[224] They reported on an improvement in the performance of the hydrogel (*e.g.*, gelling behaviour, mechanical properties) upon TEMPO oxidation of the extracted okara cellulose.

Ionic liquids can be also useful for dissolving drugs and cellulose together in order to obtain *drug-loaded hydrogels* after the gelation and solvent exchange process. The use of ionic liquids can be especially advantageous for drugs with poor solubility profile in other common solvents. As an example, Santra and Sen[225] dissolved cellulose and selenourea in [Emim][Ac]/DMSO solvent (1/2) system, in some cases together with tannic acid or L-methionine, to obtain drug-loaded hydrogels with promising sustained release profile.

Hydrogels obtained *via* ionic liquid processing can be *hosts for catalytic nanoparticles*. Su *et al.*[226] prepared wheat straw *cellulose/feather protein physical hydrogel* after dropping their [Bmim][Cl] solution into water. Magnetic hydrogel was then obtained by a co-precipitation technique using mixed solution of Fe^{2+} and Fe^{3+}. Subsequently, the hydrogels were immersed in a solution of copper salt in order to obtain a magnetic hydrogel loaded with Cu nanoparticles after *in situ* reduction with $NaBH_4$. The magnetic hydrogel showed good catalytic activity for the reduction of 2-nitrobenzoic acid. The hydrophilic functional groups of cellulose and the feather protein (*e.g.*, –OH, $–NH_2$, –COOH) may have helped the immobilisation of the metal nanoparticles in this case. FTIR results indicated for example the presence of coordination between $–COO^-$ groups and Cu^{2+}. In addition, Li *et al.*[227] dissolved cellulose (cotton pulp) in the 1,1,3,3-tetramethyl guanidine [TMG]/DMSO/CO_2 superbase solvent system. Subsequently, cellulose was acylated with cyclic anhydrides (succinic anhydride and pyromellitic dianhydride), in this process 1,1,3,3-tetramethyl guanidine acted as a catalyst and provided the positive counter ion for the forming carboxylate group (Fig. 26). The addition of bicyclic anhydrides was essential to the formation of a chemically crosslinked 3D network leading to a *chemical hydrogel*. The guanidine moiety is known to exhibit good coordination ability with transition metals. Pd nanoparticles were immobilised in the hydrogel by soaking in the solution of the metal salt ($PdCl_2$), followed by a reduction step ($NaBH_4$). The hydrogel showed good catalytic activity and reusability in the reduction of 4-nitrophenol. The authors attributed the absorption, dispersion, and stabilisation ability of the hydrogel for hosting Pd nanoparticles to the presence of the guanidine moiety.

Conductive chemical hydrogels were fabricated by Liang *et al.*[228] using [Bmim][Cl]. Cellulose/[Bmim][Cl] solution was crosslinked with *N*,*N*-methylene bisarcylamide (benzoyl peroxide initiator), followed by solvent exchange with water to form the chemical hydrogel. Polypyrrole was *in situ* polymerised in the hydrogel that was soaked in ferric chloride/sodium *p*-toluenesulfonate solution (TsONa) first, followed by the addition of the monomer pyrrole. The hydrogel doped with TsONa exhibited good electrical conductivity (~8 mS cm^{-1}, RT).

Highly tough *cellulose/reduced graphene oxide physical hydrogels* were prepared by Xu *et al.*[229] In their work, cellulose was dissolved in [Bmim][Cl], while in a separate experiment graphene oxide was reduced in [Bmim][Cl] using ascorbic acid. The two liquids were mixed and then regenerated in water in

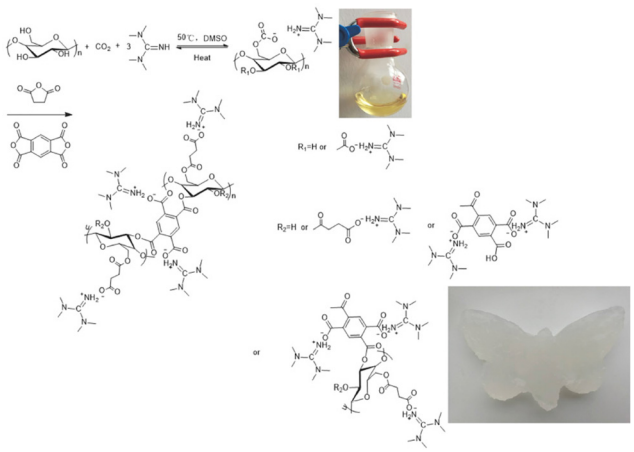

Fig. 26 Synthesis of hydrogel with 1,1,3,3-tetramethylguanidinium-based protic ionic liquid. Reproduced from ref. 227 with permission from Elsevier, copyright 2019.

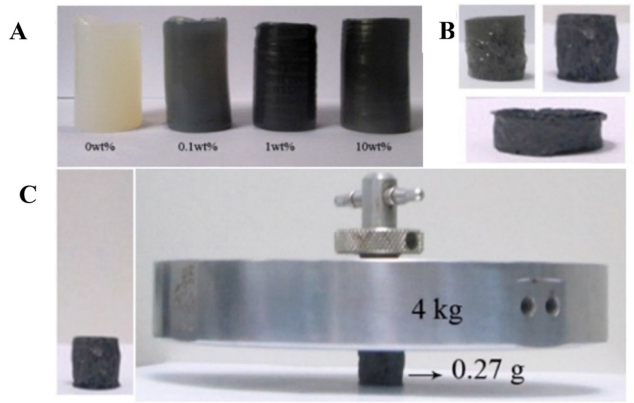

Fig. 27 (A) Cellulose/reduced graphene oxide (rGO) hydrogels with varying rGO content. (B) Aerogels obtained after freeze-drying process. (C) Demonstration of the mechanical strength of the aerogel. Reproduced from ref. 229 with permission from Elsevier, copyright 2015.

order to obtain the hydrogel by complete solvent exchange (Fig. 27A). At a certain reduced graphene oxide content (0.5 wt%), high compression modulus was observed (~19 MPa) compared to the reference cellulose hydrogel (~5 MPa). After freeze-drying process, mechanically strong cellulose/reduced graphene oxide aerogels could be obtained (Fig. 27B and C).

4.7.3. Cellulose-based aerogels through ionic liquid processing. *Cellulose aerogels/foams* can be obtained after removing the liquid from the gels. The removal process has been shown to have a critical impact on the developing porous architecture. Tsioptsias *et al.*[230] developed a high-pressure CO_2 processing technique for foaming of a cellulose hydrogel regenerated from [Amim][Cl] solution. After the foaming process, the material was subjected to a freeze-drying step at −2 °C, affording an aerogel with micrometer-size pores. Through another strategy, a methanogel was prepared first, after coagulating the cellulose/[Amim][Cl] solution in methanol, and removing the ionic liquid. Methanol was removed from the gel *via* supercritical CO_2 drying. This process yielded a nanoporous aerogel with pore sizes falling in the micro (<2 nm) and mesopore range (2–50 nm). Furthermore, *nanoporous aerogels* could be obtained later by Deng *et al.*[231] using a fast cooling process with liquid nitrogen on a regenerated hydrogel (from cellulose/[Bmim][Cl] system), followed by lyophilisation. The obtained aerogel had mainly mesopores (2–50 nm). The authors pointed out that a slow freezing process at 0 °C does not yield nanoporous material due to the formation of larger ice crystals. Oven drying does not yield a porous material either. It was also shown that the *mechanical properties* of the aerogels are dependent on the starting cellulose material; for example, when cellulose pulp is used with high *degree of polymerisation*, the aerogel can have significantly higher compression modulus compared to a sample prepared using microcrystalline cellulose.[232] *In general, freeze drying and supercritical CO_2 drying methods are widely used in the literature to prepare aerogels.*[233]

The prepared cellulose aerogels have usually no directional ordering, they possess an isotropic structure. Hierarchically assembled, ordered structures are omnipresent in nature, such features are known to give extraordinary functionality and mechanical properties to these materials, a good example for this is bamboo.[234] Design of *anisotropic gels and aerogels* is of great interest as it could allow the directional control on *e.g.*, cell growth, mechanical properties, and other physical phenomena (*e.g.*, diffusion of molecules, propagation of light, *etc.*). Efforts towards anisotropic cellulose gels/aerogels regenerated from ionic liquid solution have been made by Plappert *et al.*[235] They dissolved cellulose in the superbase-derived ionic liquid 1,1,3,3-tetramethylguanidinium acetate ([TMGH][Ac]). Cellulose was dissolved in [TMGH][Ac] at 100 °C, and poured into porous molds to allow the homogeneous diffusion of ethanol into the [TMGH][Ac]/cellulose system at 20 °C. Under this condition, the ionic liquid is in a "supercooled" state (melting point of [TMGH][Ac] is ~90–97 °C), exhibiting highly viscous glassy state. Therefore, the diffusion of the antisolvent ethanol is significantly decelerated compared to other systems. Furthermore, [TMGH][Ac] has poor miscibility with ethanol, which also contributes to the slow decelerated de-mixing of cellulose and the ionic liquid. There is a diffusion zone that slowly progresses as antisolvent induced de-mixing occurs at the interface, where cellulose supramolecular assembly takes place as it slowly coagulates. This process results in onion-like concentrical cellulose layers with higher degree of orientation of the fibrillar network structure from the core towards the skin layer (Fig. 28). The obtained aerogels after the supercritical CO_2 drying process have high crystallinity index (~72%; cellulose II polymorph), with a fibrillar strut size of about 2.5 nm. The orientation-dependent compression properties of the obtained aerogels have been also studied.[236] When compression test was done parallel to network orientation, the aerogel exhibited more resilience compared to the perpendicular direction.

Addition of a surfactant to the cellulose/ionic liquid solution can help the formation of large μm-sized pores, as reported by

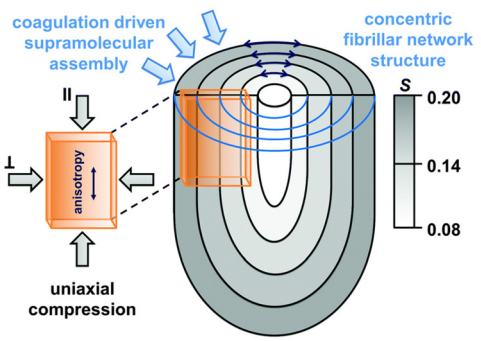

Fig. 28 Cellulose gel with concentric onion-like layers that have different level of ordering as shown with the *S* parameter, which indicates higher degree of ordering from the core towards the skin layer. Reproduced from ref. 236 with permission from The Royal Society of Chemistry, copyright 2019.

An *et al.*[237] In their work, cellulose was dissolved in [Amim][Cl], followed by the addition of sodium dodecyl sulphate (SDS) and vigorous stirring to facilitate foaming. By adjusting the cellulose concentration and the amount of the air phase, a stable biphasic system could be obtained. After the regeneration process with water and freeze-drying, ionic liquid was added to the system again (to a final concentration of 50.1 wt%). The presence of the ionic liquid imparted exceptional superelasticity and ionic conductivity to the system. The authors demonstrated the application of this flexible *cellulose/ionic liquid aerogel* as a wearable *sensing device monitoring motions* such as pulse, walking, speaking, *etc.*

Lignocellulose aerogels have also been fabricated using ionic liquids, these composites contain lignin and hemicellulose fraction in addition to cellulose.[238–240] Please note that in other works such composition is referred as "synthetic wood",[165,166] there is a discussion about these composites above in section 4.6 (regenerated cellulose/biopolymer green composites using ionic liquids). The first work in this topic was done by Aaltonen and Jauhiainen.[238] They prepared cellulose, sodalignin, cellulose/sodalignin, cellulose/sodalignin/xylan and spruce wood aerogels using [Bmim][Cl] as solvent, and aqueous ethanol coagulation bath. They pointed out that gels could be obtained at specific biopolymer compositions, and the dissolution time and ethanol concentration in the bath appeared to be also important for the gelation process. The aerogels were then produced after solvent exchange with ethanol, followed by drying with supercritical CO_2. The aerogels had an open pore structure with various morphologies (macropore size depending on the composition), and contained also mesopores. In an interesting work by Li *et al.*,[239] a cyclic freezing-thawing process (from −20 °C to 20 °C) was applied on the wood/[Amim][Cl] solution, followed by coagulation in water bath, and solvent exchange with acetone prior to a supercritical CO_2 drying process. They noted that the freezing-thawing process was important to obtain a gel that can keep its form. According to their explanation, the cyclic freezing–thawing process acts as a physical crosslinker to form a continuous 3D network. Later, an ultralow freezing-thawing process was also developed using liquid nitrogen (from −196 °C to 20 °C), in this way a mesoporous lignocellulose aerogel could be obtained.[240] Th authors argued that the formation of smaller ionic liquid crystals during the fast ultralow freezing process compared to the other freezing process (from −20 °C to 20 °C) facilitates the development of the 3D fibrillar network with mesopores. The fabricated lignocellulose aerogel showed good thermal insulating properties, and exhibited also good performance for noise reduction.

Cellulose aerogels have found application as *adsorbent materials*.[232] In order to develop an aerogel with selective adsorption to specific contaminants, the surface of the aerogel can be further modified. As an example, Zhang *et al.*[241] developed superhydrophobic and superoelophilic aerogel by plasma treatment followed by silanisation of the cellulose hydroxyl groups.

Various nanomaterials can be also incorporated into the cellulose/ionic liquid system to impart additional functions to the aerogels, such as improved thermal insulation by developing cellulose/nanosilica composite aerogels,[242] or incorporating quantum dots to obtain gels/aerogels with photoluminescence properties.[243] In the latter case, the photoluminescence wavelength could be controlled in the visible light spectrum, thus gels/aerogels with colour-tuned photoluminescence could be developed.

It should be noted that the cellulose aerogels can be converted to *carbon aerogels* through thermal treatment.[233] Carbon aerogels have various applications in energy storage, catalysis, water treatment, gas storage/separation and thermal management.[244]

4.8. Cellulose-based fibres from ionic liquid solutions

Fibres fulfil important functions in living systems,[234] and have been used by humans for creating structural materials since prehistoric times. These high aspect ratio structures possess intriguing properties for materials science, such as a combination of flexibility with strength (exceptional formability), high surface area, network formation possibilities, and small defect size, just to mention a few.[245] Recently, smart textiles comprising of fibres with functional properties came into the forefront, which may change our approach towards personalised healthcare,[246] and the way we communicate with electronic devices[247] in the future.

Textile fibre filaments used in cloths and for households have a diameter of about 5–50 μm, although finer fibres with diameters down to about 3 μm have been also achieved with common spinning techniques, they are referred to as microfibers in the literature.[245] Nanofibers with sub-micrometer diameters can be produced through electrospinning technique (some common spinning techniques are illustrated in Fig. 29), which usually yields nonwoven fabrics (random web structure with intertwined filaments).

Synthetic and natural cellulose fibres make up a large share of the textile market. The textile industry is continuously growing, and so is the demand for cellulosic fabrics. Since the production of cotton has several limitations, man-made synthetic cellulosic fibres are expected to fill the gap to meet the market demand in the future.[248,249]

4.8.1. Conventional processing systems to fabricate synthetic cellulose fibres. Synthetic cellulose fibres are generally fabricated by dissolving cellulose in a certain solvent, followed by a spinning method where the solution is pumped through a spinneret into a coagulation bath. Commercial synthetic cellulose fibres for the textile industry are predominantly produced through the *viscose process* using a *wet-spinning technique* (Fig. 29). In this process, cellulose is reacted with CS_2 to form cellulose xanthate that can be dissolved in aqueous sodium hydroxide. This solution is spun directly into an acidic coagulation bath containing zinc salts resulting in the decomposition of the metastable intermediate cellulose xanthate and the formation of high-quality pure cellulose fibres. The viscose process generates large amount of hazar-

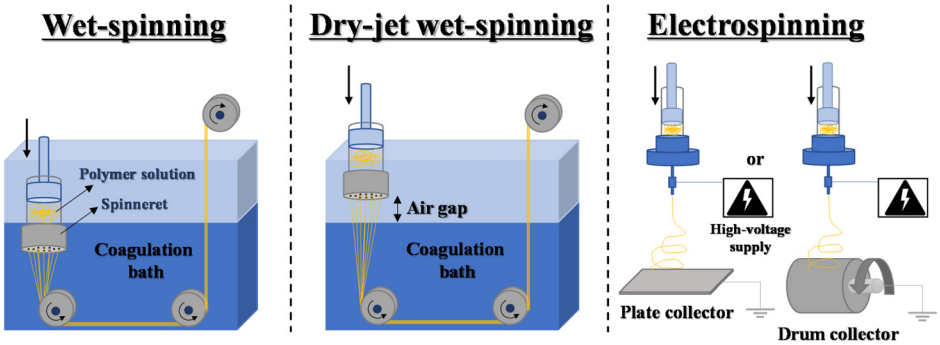

Fig. 29 Common spinning techniques for fabricating synthetic cellulose fibres from solutions. Other methods, such as dry-jet spinning uses no coagulation bath, and for melt spinning the polymer melt is extruded through the spinneret (note that this is not possible for cellulose itself).

dous waste (various sulphur byproducts such as H_2S, and heavy metals), and therefore, environmentally more benign technologies should be promoted. Thus, technologies that are based on non-derivatising solvents have gained interest to avoid the generation of byproducts. Among these methods, the *Lyocell process* gained importance – this technology is already applied for commercial production. In the Lyocell process, cellulose is dissolved in *N*-methylmorpholine-*N*-oxide (NMMO) monohydrate (a water content of 13.3 wt%) as solvent, and fibres are produced *via* a *dry-jet wet spinning process* (an air-gap exists between the spinneret and the coagulation medium, see Fig. 29) using water coagulation bath.[73] As a significant achievement, the solvent recovery of the industrial process is close to 100%, making it a practically emission-free technique. Although considered environmentally more friendly than the viscose process, there are still drawbacks arising from the instability of the solvent which necessitates the use of stabilisers and some basic safety measures. Hence, there is still need for direct cellulose solvents that can overcome the problems associated with the viscose and Lyocell processes. In this regards, ionic liquids came into the limelight in the past decade. Several comprehensive reviews were published on the production of fibres from cellulose/ionic liquid solutions, we recommend the one published by Hummel *et al.*[250] in 2016, and by Hermanutz *et al.*[251] in 2019. We will give a brief overview here on the state-of-the-art.

4.8.2. Ionic liquid/cellulose solution for fibre production. Early works on fibre spinning using ionic liquid/cellulose systems focused on halide-based first-generation ionic liquids, such as [Bmim][Cl] and [Amim][Cl].[252,253] By using a dry-jet wet spinning process (like the Lyocell process), fibres with high tenacity (textile strength) could be obtained compared to Lyocell fibres. Nevertheless, several disadvantages of these systems were recognised: high processing temperatures result in cellulose degradation; and the corrosive nature of the chloride ion poses problems for the spinning apparatus. Later, the use of acetate-based ionic liquids appeared to be a better choice. Kosan *et al.*[254] studied the dry-jet wet spinning of cellulose using [Bmim][Cl], [Emim][Cl], [Bmim][Ac] and [Emim][Ac] ionic liquids. They noted that the viscosity of the [Bmim][Ac] and [Emim][Ac] solutions are much lower compared to the other systems (Lyocell process, [Bmim][Cl] and [Emim][Cl]), and compensated the difference by increasing the loading of cellulose (to about 20 wt%; *e.g.*, this is 13.5 wt% for the Lyocell process). Although the tenacity of the fibres prepared using [Emim][Ac] and [Bmim][Ac] remained lower compared to [Bmim][Cl]/[Emim][Cl], the values were still somewhat above that of Lyocell fibres. 1-Ethyl-3-methyl imidazolium diethyl phosphate ([Emim][DEP]) was also studied as a promising solvent for fibre spinning.[255] When dry-jet wet spinning was used to fabricate the fibres, unlike Lyocell fibres and those produced from [Emim][Ac], the fibres obtained using [Emim][DEP] did not show the typical fibrillation behaviour in the wet state. Dry-jet wet spinning process yields fibres with high crystallinity in contrast to fibres obtained *via* the wet-spinning process. The interactions between the crystallites are not strong in the lateral direction, which results in the typical fibrillation of such (dry-jet spun) fibres in the wet state. Interestingly, Zhu *et al.*[256] could prepare mechanically strong fibres *via* dry-jet wet spinning from microcrystalline cellulose (DP: 200–220) using [Emim][DEP]. Microcrytalline cellulose is mostly used for applications that do not require high mechanical performance, due to the low molecular weight of this type of cellulose. They used high cellulose concentration (>12 wt%) in [Emim][DEP] where the solution showed anisotropic behaviour. Recently, wood pulp cellulose was spun into filaments on laboratory-scale fibre production line (composed of a dissolving and spinning kettle, multihole spinneret, coagulation bath, stretching bath, washing bath, dryer, winder) with the dry-jet wet spinning method using [Emim][DEP].[257] The authors used relatively low cellulose concentration (8 wt%, 90 °C spinning temperature), and obtained mechanically strong fibres by adjusting the draw ratios (three stretching draws). Furthermore, Zhang *et al.*[258] compared [Bmim][Cl], [Emim][DEP] and NMMO.H_2O in a dry-jet wet spinning process using dissolving pulp. According to their results, the fibrillation resistance was as follows: [BMIM][Cl] > [Emim][DEP] > NMMO.H_2O. They noted that fibres with denser structure and higher mechanical strength could form from [Bmim][Cl].

Thus far, the most successful ionic liquid for the production of synthetic cellulose fibres has been 1,5-diazabicyclo [4.3.0]non-5-enium acetate ([DBNH][Ac]), a non-imidazolium superbase-derived ionic liquid introduced by researchers from Aalto University and Helsinki University.[259–261] The process, denoted as *Ioncell-F*, produces fibres *via* a dry-jet wet spinning process with properties better or comparable to that of Lyocell fibres. [DBNH][Ac] is excellent solvent of cellulose allowing low processing temperatures to avoid cellulose and solvent degradation. Furthermore, due to the low viscosity of the system, relatively high spinning dope concentrations can be applied (*e.g.*, 10–17 wt% (ref. 254)). This technique has been studied in detail over the years to optimise the spinning parameters.[262] The influence of cellulose structure (molecular weight, polydispersity) on the spinnability was also investigated,[263] and it was demonstrated that even waste papers and cardboards can be upcycled into textiles (Fig. 30).[264] Recycled newspapers could be also spun into Ioncell-F fibres after deinking and alkaline glycerol pulping processes.[265] As a notable achievement, even coloured textile waste could be recycled using the Ioncell-F process, the colour of the dyes could be sufficiently retained in the new textile products in most of the cases.[266] Since recycling of the ionic liquid is crucial for the industrialisation of the technique in order to compete with the Lyocell process (with a closed-loop system, recycling almost 100% of the solvent), recyclability of the solvent has been studied,[267] and a spinning bath setup for a closed loop operation has also been suggested.[268] Ioncell-F fibres were demonstrated to be suitable for the production of printed fabrics. The technology entered the upscaling phase for commercialisation.

As we have discussed earlier, several other biopolymers can be dissolved in ionic liquids (polysaccharides, proteins, *etc.*), which enables the preparation of *cellulose composite fibres* by properly choosing the ionic liquid system (see section 4.6). Sun *et al.*[269] directly dissolved lignocellulosic biomass (southern yellow pine and bagasse) in [Emim][Ac] and prepared *all-wood composite fibres via* a dry-jet wet spinning process. The authors highlighted the importance of high temperature and short dissolution time (175 °C, 30 min) as a prerequisite for the preparation of continuous filaments from dissolved wood. Furthermore, Nypelö *et al.*[270] prepared *cellulose/lignin*, *cellulose/xylan* and *cellulose/lignin/xylan* all-wood composite fibres based on the Ioncell-F method. *Chitosan/cellulose* fibres could be also prepared *via* the Ioncell-F process.[271] *Chitin/cellulose* fibres were obtained *via* a wet and dry-jet wet spinning method using [Emim][OPr] ([OPr] – propionate) as solvent.[272] *Cellulose/lignin* composite fibres have also gained interest, they have been fabricated using the Ioncell-F process,[273] or using [Emim][Ac] as solvent.[274]

Cellulose/lignin fibres gained interest as precursors for the preparation of *carbon fibres*, in order to improve the carbon yield which is generally low for carbon fibres prepared using only cellulose as precursor.[275] Cellulose/lignin filaments from the Ioncell-F process,[276–281] and from a process that uses [Emim][Ac],[282–286] were studied in detail for this purpose. Interestingly, *cellulose/chitosan* fibres also gave higher carbon yield compared to pure cellulose precursors due to the intimate connection of the two biopolymers.[271,287]

Various *organic and inorganic additives* can be included in the cellulose/ionic liquid system to prepare *functional fibres*. By loading *magnetite* into cellulose/[Emim][Ac] solution magnetic fibres were produced *via* a dry-jet wet spinning process.[288] In a similar manner, *cellulose/TiO_2 composite fibres* could also be fabricated from [Emim][Cl] solution.[289] Fibres with improved tensile properties could be prepared *via* dry-jet wet spinning using *nano-SiO_2 additive* included in the cellulose/[Amim][Cl] solution.[290] *Cellulose/multiwalled carbon nanotube* composite fibres fabricated through a dry-jet wet spinning process from [Amim][Cl] showed also better mechanical and thermal properties compared to pure synthetic cellulose fibres.[291] Similar results were reported by Rahatekar *et al.*[292] using [Emim][Ac]. The Ioncell-F process was also used to fabricate functional fibres. *Silver and gold nanoparticles* could be incorporated into the [DBNH][Ac] solution to obtain fibres with promising *UV-shielding properties*.[293] Furthermore, by adding the nature-derived *plant-based water repellents betulin and betulinic acid* to the spinning dope, *hydrophobic fabrics* could be obtained

Fig. 30 (Left) Ioncell-F fibres produced using bleached pulp (white), cardboard (beige) and pulp with lignin as colorant additive (brown). (Right) Fabrics produced from the upcycled Ioncell-F fibres. Reproduced from ref. 264 with permission, copyright 2016 The Authors. Design: Marjaana Tanttu; photos: Eeva Suorlahti.

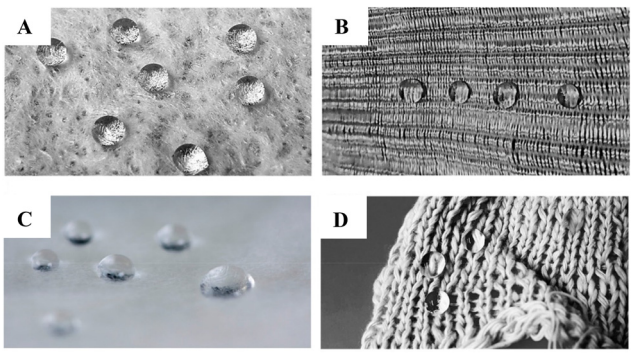

Fig. 31 Hydrophobic Ioncel-F fibres with 10 wt% (A and B) betulin and betulinic acid (C and D). Left pictures are nonwovens, right pictures are hand loomed/knitted fabrics. Reproduced from ref. 294, copyright 2021 The Authors.

(Fig. 31).[294] Ioncell-F fibres with *carbon nanotube* and *graphene oxide* additives were also reported.[295]

Electrospinning technology has also been applied to prepare cellulose nanofibers using ionic liquids. This topic has been comprehensively reviewed in recent works.[296,297] The use of pure ionic liquid/cellulose solutions is rather difficult for this process on account of the low volatility of the solvent (usually the solvent evaporates during electrospinning), together with its high ionic strength. Xu *et al.*[298] for example used the co-solvent DMSO for [Amim][Cl] to decrease surface tension and viscosity, and employed a high humidity chamber for electrospinning in order to solidify the fibres. The electrospun fibres were washed with ethanol to remove the residual solvent. Furthermore, a wet electrospinning process was also introduced by Quan *et al.*,[299] in this case fibres were directly electrospun from [Bmim][Cl] solution at 100 °C into a water bath as "collector".

5. Critical outlook on the future of cellulose processing in ionic liquids for material fabrication

Ionic liquids are considered green solvents based on their non-volatile character, with chemical and thermal stability. They gained popularity as designer solvents – their physicochemical properties can be tuned with the cation–anion combination. These features have nevertheless sparked significant interest into their environmental fate, biodegradability and toxicity profile, with several comprehensive reviews published to date.[3,300–304] As a result of continuing efforts, several ways to produce *non-toxic and biodegradable ionic liquids* have been introduced.[3] It became apparent that not only the *ionic liquid* itself but the *preparation method* also needs to be placed under scrutiny for a more holistic picture (*cradle-to-gate assessment*), if they are to be considered green solvents.[305] We expect to see more research on using non-toxic, biodegradable ionic liquids for cellulose processing and material fabrication in the future. We would like to highlight here that *machine learning* approaches could provide time- and cost-effective ways to navigate within the large chemical space of ionic liquids,[306] in order to design optimal processing media for material fabrication. We believe that designing ionic liquids that can tolerate high water content (present typically in biomass) while dissolving cellulose is an important direction for practical applications.[307]

Furthermore, for the economic viability of the technology, the *cost of the ionic liquid* and its *recyclability* need to be considered. In particular, the ionic liquid needs to be recovered and recycled with favourable energy consumption that will not compromise the economics of the technology. For the recyclability, possible side reactions with cellulose (which has been seen for *e.g.*, [Emim][Ac][43]) need to be avoided. In cellulose processing with ionic liquids, some efforts have been made to recycle the solvent, for example during the production of Ioncel-F fibres using the distillable non-derivatising ionic liquid [DBNH][Ac].[267,268] We hope to see more development in this field. Furthermore, to understand the real cost of ionic liquids, it is important to perform *life cycle assessment (LCA)*. LCA considers the cradle, production, uses, disposal, and environmental impact of the chemicals.[308] IL have been seen as expensive chemicals partly owing to the lack of comprehensive LCA data. The LCA data of IL can help understand the process improvement when these solvents are used. There are only few LCA reports on IL, based on these works, IL can be very competitive with common organic solvents. Baaqel *et al.*[309] for example applied monetisation method which combines LCA and process simulation on protic ionic liquids used for lignocellulose pretreatment (delignification, cellulose non-dissolving ionic liquids). They found that triethylammonium hydrogen sulfate ([TEA][HSO_4]) had the lowest cost among the studied systems (four systems were taken into consideration: [TEA][HSO_4], 1-methylimidazolium hydrogen sulfate ([Hmim][HSO_4]), acetone, and glycerol for cost comparison) for pretreatment of lignocellulose. In a previous report,[39] technoeconomic assessment indicated that the cost of these ionic liquids could be below that of common organic solvents (about 1.24 $ per kg, compared to the price of acetone/ethyl acetate being around 1.3–1.4 $ per kg). It was also found that in biomass pretreatment, imidazole-based IL ([Emim][Ac]) for example have higher cost mainly due to their multistep synthesis process.[310,311] However, on bulk scale the regeneration and recycling process of IL can eventually make them cost effective, thus emphasising the importance of this issue for the economic viability of the technique. At last, we should mention that although ionic liquids are sometimes denoted as expensive solvents of cellulose, when we consider alternative petroleum-derived materials with large carbon footprint – in light of the carbon pricing, advocating the "high" cost of ionic liquids for cellulose processing may be misguiding. When comparing different technologies and materials, a more holistic assessment is necessary, as we pointed out on using LCA.

In addition, the *energetics of cellulose dissolution* should not be neglected either – it must be minimised. Ionic liquids with low melting point and viscosity may be preferred, to perform the mixing with low energy input at low temperatures. Alternative heating methods, such as microwave-heating[1] and ultrasonication[312,313] may facilitate the dissolution process (decrease dissolution time), and lower the energy requirements. Cellulose degradation under such conditions must be avoided. There may be other ways to decrease the energy consumption of the dissolution step, this issue needs to be addressed more in detail in the future. Recently, *reactive extrusion (REX)* has proven to be a fast and efficient technology for cellulose dissolution and modification using ionic liquids.[314,315] Cellulose chemical modification in ionic liquids *via* REX can outpace the conventional heterogeneous batch process due to the continuous flow, scalability and higher cellulose concentration. Moreover, the combination of homogeneous dissolution of cellulose in ionic liquids with efficient

mixing in an extruder can yield a desired product within minutes of reaction time.[316,317]

Regarding the *choice and structure of the ionic liquid*, the most popular ones for material fabrication are first generation ionic liquids based on dialkylimidazolium cations, such as [Emim][Ac], [Amim][Cl] and [Bmim][Cl]. While in many cases an ionic liquid with good dissolution power proved sufficient to fulfill the target purpose (*e.g.*, for thin film and coating applications), there are cases where *the structure of ionic liquid could substantially influence the performance for the application*. We showed that the choice of the ionic liquid can have a substantial impact on the mechanical properties of regenerated cellulose films (section 4.1), by influencing the crystallinity index and degree of polymerisation of the final material. Some studies suggested that [Amim][Cl] is superior compared to other ionic liquids (*e.g.*, [Emim][Ac], [Bmim][Cl]).[88,97] More studies are needed involving other types of ionic liquids as well, to have a clear picture on the influence of ionic liquid structure on the mechanical properties. The dissolution conditions (temperature and time) also need to be considered to avoid cellulose degradation. Furthermore, we think that by tuning the structure of the ionic liquid, the structure of the obtained membrane (section 4.2), such as its porosity, could be tailored during the phase inversion process.[116] It is needless to say that the porosity of the membrane is crucial for filtration performance. We expect to see more progress in this field. Furthermore, it is also important to consider the structure of ionic liquid when adding enzymes to the system (section 4.3): in order to maintain the activity of the enzyme the interactions between the ionic liquid and the protein must be considered. It was shown for example that the addition of a hydrophobic ionic liquid ([Bmim][NTf_2]) to [Bmim][Cl]/cellulose system can have a beneficial effect on enzyme activity, by providing a better environment to accommodate the protein.[120] More understanding is needed to tailor enzyme/ionic liquid/cellulose ternary systems. When cellulose composites are prepared with other biopolymers (section 4.4), the solubility of the other biopolymer in the ionic liquid needs to be considered, and binary ionic liquid systems might be necessary, as we could see with cellulose/chitin composites.[161] We would like to highlight here the nice work done on cellulose/natural protein composites, with valuable studies focusing on how the structure of the ionic liquid can be used to tailor the nanostructure of the material.[181] Ionogels gained substantial interest as solid state electrolytes (section 4.7). It was shown that addition of ionic liquid, which does not interact with cellulose ([Bmim][NTf_2]), can improve ionic mobility within the ionogel, beneficial for various electronic applications. Thiemann *et al.*[202] showed that increasing bulkiness of the anion can lead to a decrease in ionic mobility, and pointed out the superiority of [NTf_2] to improve this property. We think that more research could be done to tailor the ionic mobility in these materials. For fiber fabrication (section 4.8), the viscosity of the system and processing temperature are crucial parameters with a focus on avoiding cellulose and solvent degradation, and thereby enabling solvent recycling with advantageous energetics. In this field, the superbase ionic liquid [DBNH][Ac] came to the forefront. It is clear that more research is needed to understand the influence of ionic liquid structure on the properties of the fabricated materials for the target applications. Studies should go beyond the use of common first generation dialkylimidazolium cation based ionic liquids, and should more eagerly involve the large chemical space of ionic liquids. Computational methods may be involved here to replace time and resource consuming screening processes, as discussed in a recent comprehensive review by Koutsoukos *et al.*[306] Machine learning can be a very helpful tool in various aspects. It could be used to develop ionic liquids with good ability to dissolve cellulose, and together with life cycle assessment, aid the realisation of cost-effective systems. Furthermore, it could also help designing ionic liquids for achieving specific material properties, an approach sometimes referred to as *machine learning-assisted materials design*. Recent advancement can be taken as example from ongoing efforts on tailoring organic molecule and polymer properties *via* machine learning algorithms.[318]

As of similarities in selecting an ionic liquid for material fabrication, when mechanical properties are important, ionic liquids that can process cellulose without appreciable degradation at low temperature with acceptable viscosities are preferred. Furthermore, the recyclability of the system necessitates the use of non-derivatising ionic liquids that can be recycled with favourable energetics. The latter is especially important when studies go beyond laboratory experiments, and industrial scale realisation is the target. This issue came to the fore especially for fiber formation processes. So far, the dialkylimidazolium cation based ionic liquid [Amim][Cl], and the superbase derived ionic liquid [DBNH][Ac] are the most promising choices. We need to emphasise here that more studies are needed since our knowledge on other types of ionic liquids is very limited. As of differences between ionic liquid systems, we would like to draw attention to physical ionogels as promising materials for solid state electrolytes. In this specific case, the use of non-dissolving ionic liquids, with anions that would interact with cellulose the least ([Bmim][NTf_2]), are preferred. This is due to the high ionic mobility required within the gelous network for achieving high ionic conductivity. This is in contrast to the requirements when cellulose solvents are considered.

The *purity of the final regenerated cellulose material* is not examined in most of the studies, although the purity of the ionic liquid itself has been the focus of more intense investigation among works that study solvent recyclability. It can be expected that remaining ionic liquid in the final product could have a considerable impact on mechanical as well as other properties (*e.g.*, ionic liquids have been reported as plasticiser additives,[319,320] and other functions have also also been revealed when added to various polymer matrices[321]) important for the target application. Therefore, we highly recommend future studies to address this issue. It is clear that even small amount of impurities from the ionic liquid could have a devastating effect on the recycling step on an industrial

scale, compromising the economics of the whole process. Therefore, it is crucial to optimise the regeneration step. We have to note here that purity assessment solely based on ^{1}H-NMR analysis may not be sufficient enough in some cases, and more sensitive analysis (*e.g.*, more sensitive HPLC techniques) may be required to claim the purity of the final material, especially when the target application is *e.g.*, food packaging, biomedical sensing (*i.e.*, artificial skin), *etc.*

Another issue is related to the prudent *choice of the technical cellulose*. Many studies focus on the commercially available microcrystalline cellulose. From a technological point of view, however, the use of industrially relevant technical celluloses such as dissolving pulp would be preferred (*e.g.*, if we think about packaging application). This should be considered in the first place, and the use of a certain grade of technical cellulose should be justified (to be necessary for the material to fulfill its function/property). Dissolving pulp has high degree of polymerisation and therefore, a viscose solution may be obtained in some cases that can be more difficult to process. Handling of microcrystalline cellulose is although easier, it has higher cost that may jeopardise the economics of the technology, and its conversion from the raw cellulose will certainly increase the ecological footprint of the process.

We would also like to raise attention to the *source of cellulose*, in particular to the importance of *upcycling agri-food losses and wastes into value-added materials* for a *circular economy*. This topic has been comprehensively addressed in a recent review.[322] These resources can represent sustainable alternatives, as they can be readily available. A good example is banana stem – banana can grow fast, and once yielding fruits, the stalk is cut back and the stem is disposed, representing an untapped source of agri-food residue derived cellulose.[323,324] There are many more examples of agri-food wastes produced annually at millions of tons of quantities,[322] such as the sugar beet pulp, which contains about 22–30% cellulose (on a dry weight basis). Furthermore, sugar beet pulp has a comparatively low lignin content (about 3 wt%) with respect to other lignocellulosic materials (*e.g.*, wheat straw has about 15 wt% lignin), making it an exciting biomass to study for cellulose valorisation. Sugarcane bagasse is considered the most abundant biomass waste on Earth and it consists of 40–50 wt% cellulose – making it a material with a huge potential for obtaining cellulosic pulp for industrial applications. Recently, brewer's spent grain from the brewing industry (cellulose content around 16–25 wt%) has also emerged as a new source of cellulose. Upcycling agri-food waste could also make local communities and industries more prosperous and resilient. *We believe that technological innovations in the near future will provide farmers and related businesses with both economic and social incentives to fully take advantage of the chemical diversity present in the biomass they grow.*

Finally, as a goal of a tutorial review, we would really like to encourage those who have not necessarily worked with ionic liquids before, to explore this promising area of green chemistry. Although we do not really see any problems in preparing these materials, for starting practitioners, there may be some difficulties in the dissolution step of cellulose, due to the high viscosity of the solution in some cases. Handling of such solution may need some practice, and proper machinery. Furthermore, we need to note that most of the ionic liquid systems available at present do not tolerate water impurities present in raw cellulose materials or in the ionic liquid itself, so the starting materials must be dried before any processing. As we have noted above, development of ionic liquid systems that can tolerate high water content is underway. We hope to see many more interesting cellulose-based functional materials created *via* ionic liquid processing systems in the near future.

Conflicts of interest

The authors declare no conflict of interest.

Acknowledgements

L. Szabó would like to thank the support from the International Center for Young Scientists (ICYS) in the National Institute for Materials Science (NIMS; budget code: QN3360, ICYS25). K. Takahashi would like to acknowledge the Center of Innovation (COI) program on open innovation platform for industry academia co-creation (COI-NEXT) supported by the Japan Science and Technology Agency (JST, JPMJPF2102).

References

1 R. P. Swatloski, S. K. Spear, J. D. Holbrey and R. D. Rogers, Dissolution of cellulose with ionic liquids, *J. Am. Chem. Soc.*, 2002, **124**, 4974–4975.
2 F. Endres and S. Z. El Abedin, Air and water stable ionic liquids in physical chemistry, *Phys. Chem. Chem. Phys.*, 2006, **8**, 2101–2116.
3 C. J. Clarke, W.-C. Tu, O. Levers, A. Bröhl and J. P. Hallett, Green and sustainable solvents in chemical processes, *Chem. Rev.*, 2018, **118**, 747–800.
4 K. N. Onwukamike, S. Grelier, E. Grau, H. Cramail and M. A. R. Meier, Critical review on sustainable homogeneous cellulose modification: why renewability is not enough, *ACS Sustainable Chem. Eng.*, 2019, **7**, 1826.
5 A. Cabiac, E. Guillon, F. Chambon, C. Pinel, F. Rataboul and N. Essayem, Cellulose reactivity and glycosidic bond cleavage in aqueous phase by catalytic and non catalytic transformations, *Appl. Catal., A*, 2011, **402**, 1–10.
6 M. Koyama, W. Helbert, T. Imai, J. Sugiyama and B. Henrissat, Parallel-up structure evidences the molecular directionality during biosynthesis of bacterial cellulose, *Proc. Natl. Acad. Sci. U. S. A.*, 1997, **94**, 9091–9095.
7 K. Heise, G. Delepierre, A. W. T. King, M. A. Kostiainen, J. Zoppe, C. Weder and E. Kontturi, Chemical modifi-

cation of reducing end-groups in cellulose nanocrystal, *Angew. Chem., Int. Ed.*, 2021, **60**, 66–87.
8 J. Shen and Y. Okamoto, Efficient separation of enantiomers using stereoregular chiral polymers, *Chem. Rev.*, 2016, **116**, 1094–1138.
9 P. Zugenmeier, Order in cellulosics: a historical review of crystal structure research on cellulose, *Carbohydr. Polym.*, 2021, **254**, 117417.
10 M. Makarem, C. M. Lee, K. Kafle, S. Huang, I. Chae, H. Yang, J. D. Kubicki and S. H. Kim, Probing cellulose structures with vibrational spectroscopy, *Cellulose*, 2019, **26**, 35–79.
11 Y. Nishiyama, P. Langan and H. Chanzy, Crystal structure and hydrogen-bonding system in cellulose Iβ from synchrotron X-ray and neutron fiber diffraction, *J. Am. Chem. Soc.*, 2002, **124**, 9074–9082.
12 P. Langan, Y. Nihsiyama and H. Chanzy, A revised structure and hydrogen-bonding system in cellulose II from a neutron fiber diffraction analysis, *J. Am. Chem. Soc.*, 1999, **121**, 9940–9946.
13 R. N. Goldberg, J. Schliesser, A. Mittal, S. R. Decker, A. F. L. O. M. Santos, V. L. S. Freitas, A. Urbas, B. E. Lang, C. Heiss, M. D. M. C. Ribeiro da Silva, B. F. Woodfield, R. Katahira, W. Wang and D. K. Johnson, A thermodynamic investigation of the cellulose allomorphs: cellulose (am), cellulose Iβ(cr), cellulose II(cr), and cellulose III(cr), *J. Chem. Thermodyn.*, 2015, **81**, 184–226.
14 M. Wada, L. Heux and J. Sugiyama, Polymorphism of cellulose I family: reinvestigation of cellulose IVI, *Biomacromolecules*, 2004, **5**, 1385–1391.
15 K. Igarashi, M. Wada and M. Samejima, Activation of crystalline cellulose to cellulose IIII results in efficient hydrolysis by cellobiohydrolase, *FEBS J.*, 2007, **274**, 1785–1792.
16 C. Yamane, T. Aoyagi, M. Ago, K. Sato, K. Okajima and T. Takahashi, Two different surface properties of regenerated cellulose due to structural anisotropy, *Polym. J.*, 2006, **38**, 819–826.
17 H. Seddiqi, E. Oliaei, H. Honarkar, J. Jin, L. C. Geonzon, R. G. Bacabac and J. Klein-Nulend, Cellulose and its derivatives: towards biomedical applications, *Cellulose*, 2021, **28**, 1893–1931.
18 N. Terinte, R. Ibbet and K. C. Schuster, Overview on native cellulose and microcrystalline cellulose structure studied by X-ray diffraction (WAXD): comparison between measurement techniques, *Lenzinger Ber.*, 2011, **89**, 118–131.
19 Y.-L. Hsieh, Chemical structure and properties of cotton, in *Cotton: Science and Technology*, ed. S. Gordon and Y.-L. Hsieh, Woodhead Publishing Series in Textiles, Woodhead Publishing Limited, Cambridge, England, 2007, pp. 3–34.
20 L. E. Hessler, G. V. Merola and E. E. Berkley, Degree of polymerization of cellulose in cotton fibers, *Text. Res. J.*, 1948, **18**, 628–634.
21 L. Urbina, M.Á Corcuera, N. Gabilondo, A. Eceiza and A. Retegi, A review of bacterial cellulose: sustainable production from agricultural waste and applications in various fields, *Cellulose*, 2021, **28**, 8229–8253.
22 N. Tahara, M. Tabuchi, K. Watanabe, H. Yano, Y. Morinaga and F. Yoshinaga, Degree of polymerization of cellulose from Acetohacter xylinum BPR2001 decreased by cellulase produced by the strain, *Biosci., Biotechnol., Biochem.*, 1997, **61**, 1862–1865.
23 T. Heinze and T. Liebert, Celluloses and polyoses/hemicelluloses, in *Polymer Science: A Comprehensive Reference, Volume 10: Polymers for a Sustainable Environment and Green Energy*, 2012, 83–152.
24 G. A. S. Haron, H. Mahmood, M. H. Noh, Z. Alam and M. Moniruzzaman, Ionic liquids as a sustainable platform for nanocellulose processing from bioresources: overview and current status, *ACS Sustainable Chem. Eng.*, 2021, **9**, 1008–1034.
25 H. Wang, G. Gurau and R. D. Rogers, Ionic liquid processing of cellulose, *Chem. Soc. Rev.*, 2012, **41**, 1519–1537.
26 K. Jedvert and T. Heinze, Cellulose modification and shaping – a review, *J. Polym. Eng.*, 2017, **37**, 845–860.
27 J. Zhang, Q. Ren and J. S. He, *CN Patent*, ZL02155945, 2002.
28 H. Zhang, J. Wu, J. Zhang and J. He, 1-Allyl-3-methylimidazolium chloride room temperature ionic liquid: a new and powerful nonderivatizing solvent for cellulose, *Macromolecules*, 2005, **38**, 8272–8277.
29 J. Zhang, J. Wu, J. Yu, X. Zhang, J. He and J. Zhang, Application of ionic liquids for dissolving cellulose and fabricating cellulose-based materials: state of the art and future trends, *Mater. Chem. Front.*, 2017, **1**, 1273–1290.
30 A. Brandt, J. Gräsvik, J. P. Hallett and T. Welton, Deconstruction of lignocellulosic biomass with ionic liquids, *Green Chem.*, 2013, **15**, 550–583.
31 Y. Fukaya, A. Sugimoto and H. Ohno, Superior solubility of polysaccharides in low viscosity, polar, and halogen-free 1,3-dialkylimidazolium formates, *Biomacromolecules*, 2006, **7**, 3295–3297.
32 A. Xu, J. Wang and H. Wang, Effects of anionic structure and lithium salts addition on the dissolution of cellulose in 1-butyl-3-methylimidazolium-based ionic liquid solvent systems, *Green Chem.*, 2010, **12**, 268–275.
33 B. Zhao, L. Greiner and W. Leitner, Cellulose solubilities in carboxylate-based ionic liquids, *RSC Adv.*, 2012, **2**, 2476–2479.
34 Y. Zhang, A. Xu, B. Lu, Z. Li and J. Wang, Dissolution of cellulose in 1-allyl-3-methylimizodalium carboxylates at room temperature: A structure-property relationship study, *Carbohydr. Polym.*, 2015, **117**, 666–672.
35 K. Ohira, Y. Abe, M. Kawatsura, K. Suzuki, M. Mizuno, Y. Amano and T. Itoh, Design of cellulose dissolving ionic liquids inspired by nature, *ChemSusChem*, 2012, **5**, 388–391.
36 Y. Fukaya, K. Hayashi, M. Wada and H. Ohno, Cellulose dissolution with polar ionic liquids under mild conditions: required factors for anions, *Green Chem.*, 2008, **10**, 44–46.

37 A. Brandt, M. J. Ray, T. Q. To, D. J. Leak, R. J. Murphy and T. Welton, Ionic liquid pretreatment of lignocellulosic biomass with ionic liquid-water mixtures, *Green Chem.*, 2011, **13**, 2489–2499.
38 P. Verdía, A. Brandt, J. P. Hallett, M. J. Ray and T. Welton, Fractionation of lignocellulosic biomass with the ionic liquid 1-butylimidazolium hydrogen sulfate, *Green Chem.*, 2014, **16**, 1617–1627.
39 L. Chen, M. Sharifzadeh, N. M. Dowell, T. Welton, N. Shah and J. P. Hallett, Inexpensive ionic liquids: HSO4-based solvent production at bulk scale, *Green Chem.*, 2014, **16**, 3098–3106.
40 A. George, A. Brandt, K. Tran, S. M. S. N. S. Zahari, D. Klein-Marcuschamer, N. Sun, N. Sathitsuksanoh, J. Shi, V. Stavila, R. Parthasarathi, S. Singh, B. M. Holmes, T. Welton, B. A. Simmons and J. P. Hallett, Design of low-cost ionic liquids for lignocellulosic biomass pretreatment, *Green Chem.*, 2015, **17**, 1728–1734.
41 H. Zhao, G. A. Baker, Z. Song, O. Olubajo, T. Crittle and D. Peters, Designing enzyme-compatible ionic liquids that can dissolve carbohydrates, *Green Chem.*, 2008, **10**, 696–705.
42 A. Pinkert, K. M. Marsh and S. Pang, Reflections on the solubility of cellulose, *Ind. Eng. Chem. Res.*, 2010, **49**, 11121–11130.
43 M. T. Clough, K. Geyer, P. A. Hunt, S. Son, U. Vagt and T. Welton, Ionic liquids: not always innocent solvents for cellulose, *Green Chem.*, 2015, **17**, 231–243.
44 T. Heinze, K. Schwikal and S. Barthel, Ionic liquids as reaction medium in cellulose functionalization, *Macromol. Biosci.*, 2005, **5**, 520–525.
45 E. S. Sashina, D. A. Kashirskii, M. Zaborski and S. Jankowski, Synthesis and dissolving power of 1-alkyl-3-methylpyridinium-based ionic liquids, *Russ. J. Gen. Chem.*, 2012, **82**, 2040–2045.
46 A. Miyata and H. Miyafuji, Reaction behavior of cellulose in various pyridinium-based ionic liquids, *J. Wood Sci.*, 2014, **60**, 438–445.
47 J. Pernak, R. Kordala, B. Markiewicz, F. Walkiewicz, M. Popławski, A. Fabiańska, S. Jankowski and M. Łożyński, Synthesis and properties of ammonium ionic liquids with cyclohexyl substituent and dissolution of cellulose, *RSC Adv.*, 2012, **2**, 8429–8438.
48 Z. Chen, S. Liu, Z. Li, Q. Zhang and Y. Deng, Dialkoxy functionalized quaternary ammonium ionic liquids as potential electrolytes and cellulose solvents, *New J. Chem.*, 2011, **35**, 1596–1606.
49 S. Tang, G. A. Baker, S. Ravula, J. E. Jones and H. Zhao, PEG-functionalized ionic liquids for cellulose dissolution and saccharification, *Green Chem.*, 2012, **14**, 2922–2932.
50 Y.-H. Tseng, Y.-Y. Lee and S.-H. Chen, Synthesis of quaternary ammonium room-temperature ionic liquids and their application in the dissolution of cellulose, *Appl. Sci.*, 2019, **9**, 1750.
51 V. Diez, A. DeWeese, R. S. Kalb, D. N. Blauch and A. M. Socha, Cellulose dissolution and biomass pretreatment using quaternary ammonium ionic liquids prepared from H-, G-, and S–type lignin derived benzaldehydes and dimethyl carbonate, *Ind. Eng. Chem. Res.*, 2019, **58**, 16009–16017.
52 J. Pernak, N. Borucka, F. F. Walkiewicz, B. Markiewicz, P. Fochtman, S. Stolte, S. Steudte and P. Stepnowski, Synthesis, toxicity, biodegradability and physicochemical properties of 4-benzyl-4-methylmorpholinium-based ionic liquids, *Green Chem.*, 2011, **13**, 2901–2910.
53 D. G. Raut, O. Sundman, W. Su, P. Virtanen, Y. Sugano, K. Kordas and J.-P. Mikkola, A morpholinium ionic liquid for cellulose dissolution, *Carbohydr. Polym.*, 2015, **130**, 18–25.
54 H.-W. Ren, Q.-H. Wang, S.-H. Guo, D.-S. Zhao and C.-M. Chen, The role and potential of morpholinium-based ionic liquids in dissolution of cellulose, *Eur. Polym. J.*, 2017, **92**, 204–212.
55 D. Giovanni, S. Laszlo, M. Klemens and S. Veit, Ionic liquids for solubilizing polymers, *PCT Patent*, WO2008043837, 2006.
56 A. Parviainen, A. W. T. King, I. Mutikainen, M. Hummel, C. Selg, L. K. J. Hauru, H. Sixta and I. Kilpeläinen, Predicting cellulose solvating capabilities of acid-base conjugate ionic liquids, *ChemSusChem*, 2013, **6**, 2161–2169.
57 A. W. T. King, J. Asikkala, I. Mutikainen, P. Järvi and I. Kilpeläinen, Distillable acid-base ionic liquids for cellulose dissolution and processing, *Angew. Chem., Int. Ed.*, 2011, **50**, 6301–6305.
58 J. Miao, H. Sun, Y. Yu, X. Song and L. Zhang, Quaternary ammonium acetate: an efficient ionic liquid for the dissolution and regeneration of cellulose, *RSC Adv.*, 2014, **4**, 36721–36724.
59 D. L. Minnick, R. A. Flores, M. R. DeStefano and A. M. Scurto, Cellulose solubility in ionic liquid mixtures: temperature, cosolvent and antisolvent effects, *J. Phys. Chem. B*, 2016, **120**, 7906–7919.
60 J.-M. Andanson, E. Bordes, J. Devémy, F. Leroux, A. A. H. Pádua and M. F. C. Gomes, Understanding the role of co-solvents in the dissolution of cellulose in ionic liquids, *Green Chem.*, 2014, **16**, 2528–2538.
61 L. Zhang, C. Huang, C. Zhang and H. Pan, Swelling and dissolution of cellulose in binary systems of three ionic liquids and three co-solvents, *Cellulose*, 2021, **28**, 4643–4653.
62 Y. Meng, Z. Pang and C. Dong, Enhancing cellulose dissolution in ionic liquid by solid acid addition, *Carbohydr. Polym.*, 2017, **163**, 317–323.
63 X. Li, H. Li, T. You, X. Chen, S. Ramaswamy, Y.-Y. Wu and F. Xu, Enhanced dissolution of cotton cellulose in 1-allyl-3-methylimidazolium chloride by the addition of metal chlorides, *ACS Sustainable Chem. Eng.*, 2019, **7**, 19176–19184.
64 J. Yang, X. Lu, X. Yao, Y. Li, Y. Yang, Q. Zhou and S. Zhang, Inhibiting degradation of cellulose dissolved in ionic liquid via amino acids, *Green Chem.*, 2019, **21**, 2777–2787.

65 Y. Li, J. Wang, X. Liu and S. Zhang, Towards a molecular understanding of cellulose dissolution in ionic liquids: anion/cation effect, synergistic mechanism and physicochemical aspects, *Chem. Sci.*, 2018, **9**, 4027–4043.
66 L. Berga, I. Bruce, T. W. J. Nicol, A. J. Holding, N. Isobe, S. Shimizu, A. J. Walker and J. E. S. J. Reid, Cellulose dissolution and regeneration using a non-aqueous, non-stoichiometric protic ionic liquid system, *Cellulose*, 2020, **27**, 9593–9603.
67 M. Abe, Y. Fukaya and H. Ohno, Fast and facile dissolution of cellulose with tetrabutylphosphonium hydroxide containing 40 wt% water, *Chem. Commun.*, 2012, **48**, 1808–1810.
68 A. Tsurumaki, M. Tajima, M. Abe, D. Sato and H. Ohno, Effect of cation structure on cellulose dissolution in aqueous solutions of organic onium hydroxides, *Phys. Chem. Chem. Phys.*, 2020, **22**, 22602–22608.
69 Eastman Corporate Headquarters, Eastman cellulose esters for formulated products – enhancing performance, productivity, and appearance, **https://www.eastman.com/Literature_Center/E/E325.pdf** (last accessed on 16/03/2022).
70 European Commission, The VOC solvents emissions directive, **https://ec.europa.eu/environment/archives/air/stationary/solvents/legislation.htm** (last accessed on 16/03/2022).
71 US Environmental Protection Agency, National volatile organic compound emission standards for consumer and commercial products, **https://www.govinfo.gov/content/pkg/CFR-2019-title40-vol6/xml/CFR-2019-title40-vol6-part59.xml** (last accessed on 16/03/2022).
72 D. Klemm, B. Philipp, T. Heinze, U. Heinze and W. Wagenknecht, *Comprehensive Cellulose Chemistry*, Wiley-VCH, Weinheim, 1st edn, 1998, vol. 1, pp. 17–27.
73 D. Klemm, B. Heublein, H.-P. Fink and A. Bohn, Cellulose: fascinating biopolymer and sustainable raw material, *Angew. Chem., Int. Ed.*, 2005, **44**, 3358–3393.
74 K. J. Edgar, C. M. Buchanan, J. S. Debenham, P. A. Rundquist, B. D. Seiler, M. C. Shelton and D. Tindall, Advances in cellulose ester performance and application, *Prog. Polym. Sci.*, 2001, **26**, 1605–1688.
75 J. D. Posey-Dowty, K. S. Seo, K. R. Walker and A. K. Wilson, Carboxymethylcellulose acetate butyrate in water-based automotive paints, *Surf. Coat. Int., Part B*, 2002, **85**, 203–208.
76 C. J. Tristram, J. M. Mason, D. B. G. Williams and S. F. R. Hinkley, Doubly renewable cellulose polymer for water-based coatings, *ChemSusChem*, 2015, **8**, 63–66.
77 M. Pei, X. Peng, Y. Shen, Y. Yang, Y. Guo, Q. Zheng, H. Xie and H. Sun, Synthesis of water-soluble, fully biobased cellulose levulinate esters through the reaction of cellulose and alpha-angelica lactone in a DBU/CO2/DMSO solvent system, *Green Chem.*, 2020, **22**, 707–717.
78 M. Yamaguchi, K. Songsurang, H. Shimada, S. Nobukawa and M. E. A. Manaf, Novel methods to control the optical anisotropy of cellulose esters, in *Pulp Production and Processing - High-Tech Applications*, ed. V. I. Popa, De Gruyter, 2020.
79 S. C. Gondhalekar, P. J. Pawar, S. S. Dhumal and S. Thakre, Fate of CS2 in viscose process: a chemistry perspective, *Cellulose*, 2022, **9**, 1451–1461.
80 D. M. Rock and A. Grady, *Zinc Precipitation and Recovery from Viscose Rayon Waste Water, Water Pollution Control Research Series*, US Environmental Protection Agency, Water Quality Office, Washington, 1971.
81 S. Paunonen, Strength and barrier enhancement of cellophane and cellulose derivative films: a review, *BioResources*, 2013, **8**, 3098–3121.
82 S. S. Ahankari, A. R. Subhedar, S. S. Bhadauria and A. Dufresne, Nanocellulose in food packaging: a review, *Carbohydr. Polym.*, 2021, **255**, 117479.
83 H.-P. Fink, J. Ganster and A. Lehmann, Progress in cellulose shaping: 20 years industrial case studies at Fraunhofer IAO, *Cellulose*, 2014, **21**, 31–51.
84 H. C. Arca, L. I. Mosquera-Giraldo, V. Bi, D. Xu, L. S. Taylor and K. J. Edgar, Pharmaceutical applications of cellulose ethers and cellulose ether esters, *Biomacromolecules*, 2018, **19**, 2351–2376.
85 A. Sheikhi, J. Hayashi, J. Eichenbaum, M. Gutin, N. Kuntjoro, D. Khorsandi and A. Khademhosseini, Recent advances in nanoengineering cellulose for cargo delivery, *J. Controlled Release*, 2019, **294**, 53–76.
86 S. Bhaladhare and D. Das, Cellulose: a fascinating biopolymer for hydrogel synthesis, *J. Mater. Chem. B*, 2022, **10**, 1923–1945.
87 L. Pang, Z. Gao, H. Feng, S. Wang and Q. Wang, Cellulose based materials for controlled release formulations of agrochemicals: a review of modifications and applications, *J. Controlled Release*, 2019, **316**, 105–115.
88 Y. Cao, H. Li, Y. Zhang, J. Zhang and J. He, Structure and properties of novel regenerated cellulose films prepared from cornhusk cellulose in room temperature ionic liquids, *J. Appl. Polym. Sci.*, 2010, **116**, 547–554.
89 K. O. Reddy, J. Zhang, J. Zhang and A. V. Rajulu, Preparation and properties of self-reinforced cellulose composite films from Agave microfibrils using an ionic liquid, *Carbohydr. Polym.*, 2014, **114**, 537–545.
90 J. Pang, X. Liu, X. Zhang, Y. Wu and R. C. Sun, Fabrication of cellulose film with enhanced mechanical properties in ionic liquid 1-allyl-3-methylimidaxolium chloride (AmimCl), *Materials*, 2013, **6**, 1270–1284.
91 Z. Jin, S. Wang, J. Wang and M. Zhao, Effect of plasticization conditions on the structures and properties of cellulose packaging films from ionic liquid BMIMCl, *J. Appl. Polym. Sci.*, 2012, **125**, 704–709.
92 S. V. Muginova, D. A. Myasnikova, S. G. Kazarian and T. N. Shekhovtsova, Evaluation of novel applications of cellulose hydrogel films reconstituted from acetate and chloride of 1-butyl-3-methylimidazolium by comparing their optical, mechanical, and adsorption properties, *Mater. Today Commun.*, 2016, **8**, 108–117.

93 S. V. Muginova, E. S. Vakhranyova, D. A. Myasnikova, S. G. Kazarian and T. N. Shekhovtsova, Fluorescence-based artemisinin sensing using a pyronin B-doped cellulose film reconstituted from ionic liquid, *Anal. Lett.*, 2018, **51**, 870–891.

94 Y. Wang, Y.-C. Ji, L. Wei, Q.-G. Wang and H. Li, Dissolution and regeneration in films of natural luffa in 1-butyl-3-methylimidazolium chloride, *J. Macromol. Sci. Phys.*, 2015, **54**, 571–580.

95 H.-Z. Chen, N. Wang and L.-Y. Liu, Regenerated cellulose membrane prepared with ionic liquid 1-butyl-3-methylimidazolium chloride as solvent using wheat straw, *J. Chem. Technol. Biotechnol.*, 2012, **87**, 1634–1640.

96 J. H. Pang, M. Wu, Q. H. Zhang, X. Tan, F. Xu, X. M. Zhang and R. C. Sun, Comparison of physical properties of regenerated cellulose films fabricated with different cellulose feedstocks in ionic liquid, *Carbohydr. Polym.*, 2015, **121**, 71–78.

97 X. Zheng, F. Huang, L. Chen, L. Huang, S. Cao and X. Ma, Preparation of transparent film via cellulose regeneration: correlations between ionic liquid and film properties, *Carbohydr. Polym.*, 2019, **203**, 214–218.

98 X. Liu, J. Pang, X. Zhang, Y. Wu and R. C. Sun, Regenerated cellulose film with enhanced tensile strength prepared with ionic liquid 1-ethyl-3-methylimidazolium acetate (EMIMAc), *Cellulose*, 2013, **20**, 1391–1399.

99 A. Östlund, A. Idström, C. Olsson, P. T. Larsson and L. Nordstierna, Modification of crystallinity and pore size distribution in coagulated cellulose films, *Cellulose*, 2013, **20**, 1657–1667.

100 R. Kargl, T. Mohan, V. Ribitsch, B. Saake, J. Puls and K. S. Kleinschek, Cellulose thin films from ionic liquid solutions, *Nord. Pulp Pap. Res. J.*, 2015, **30**, 6–13.

101 N. Luo, K. Varaprasad, G. V. S. Reddy, A. V. Rajulu and J. Zhang, Preparation and characterization of cellulose/curcumin composite films, *RSC Adv.*, 2012, **2**, 8483–8488.

102 X. Huang, Y. Ji, L. Guo, Q. Xu, L. Jin, Y. Fu and Y. Wang, Incorporating tannin onto regenerated cellulose film towards sustainable active packaging, *Ind. Crops Prod.*, 2022, **180**, 114710.

103 Y. Hu, Q. Guo, P. Liu, R. Zhu, F. Lu, S. Ramaswamy, Y. Wu, F. Xu and X. Zhang, Fabrication of novel cellulose-based antibacterial film loaded with poacic acid against Staphylococcus aureus, *J. Polym. Environ.*, 2021, **29**, 745–754.

104 S. M. Notley, M. Eriksson, L. Wågberg, S. Beck and D. G. Gray, Surface forces measurements of spin-coated cellulose thin films with different crystallinity, *Langmuir*, 2006, **22**, 3154–3160.

105 C. Aulin, S. Ahola, P. Josefsson, T. Nishino, Y. Hirose, M. Österberg and L. Wågberg, Nanoscale cellulose films with different crystallinities and mesostructures – their surface properties and interaction with water, *Langmuir*, 2009, **25**, 7675–7685.

106 N. Hameed, Q. Guo, F. H. Tay and S. G. Kazarian, Blends of cellulose and poly(3-hydroxybutyrate-co-3-hydroxyvalerate) prepared from the ionic liquid 1-butyl-3-methylimidazolium chloride, *Carbohydr. Polym.*, 2011, **86**, 94–104.

107 M. Isik, R. Garcia, L. C. Kollnus, L. C. Tomé, I. M. Marrucho and D. Mecerreyes, Cholinium-based poly(ionic liquid)s: synthesis, characterization, and application as biocompatible ion gels and cellulose coatings, *ACS Macro Lett.*, 2013, **2**, 975–979.

108 M. Isik, R. Garcia, L. C. Kollnus, L. C. Tomé, I. M. Marrucho and D. Mecerreyes, Cholinium lactate methacrylate: ionic liquid monomer for cellulose composites and biocompatible ion gels, *Macromol. Symp.*, 2014, **342**, 21–24.

109 Q. Zhang, M. Benoit, K. D. O. Vigier, J. Barrault and F. Jérôme, Green and inexpensive choline-derived solvents for cellulose decrystallization, *Chem. – Eur. J.*, 2012, **18**, 1043–1046.

110 M.-H. Song, T. P. T. Pham and Y.-S. Yun, Ionic liquid-assisted cellulose coating of chitosan hydrogel beads and their application as drug carriers, *Sci. Rep.*, 2020, **10**, 13905.

111 Suhas, V. K. Gupta, P. J. M. Carrott, R. Singh, M. Chaudhary and S. Kushwaha, Cellulose: a review as natural, modified and activated carbon adsorbent, *Bioresour. Technol.*, 2016, **216**, 1066–1076.

112 A. K. Hołda and I. F. J. Vankelecom, Understanding and guiding the phase inversion process for synthesis of solvent resistant nanofiltration membranes, *J. Appl. Polym. Sci.*, 2015, **132**, 42130.

113 D. Y. Xing, N. Peng and T.-S. Chung, Formation of cellulose acetate membranes via phase inversion using ionic liquid, BMIMSCN, as the solvent, *Ind. Eng. Chem. Res.*, 2010, **49**, 8761–8769.

114 X.-L. Li, L.-P. Zhu, B.-K. Zhu and Y. Y. Xu, High-flux and anti-fouling cellulose nanofiltration membranes prepared via phase inversion with ionic liquid as solvent, *Sep. Purif. Technol.*, 2011, **83**, 66–73.

115 M. R. Esfahani, A. Taylor, N. Serwinowski, Z. J. Parkerson, M. P. Confer, I. Kammakakam, J. E. Bara, A. R. Esfahani, S. N. Mahmoodi, N. Koutahzadeh and M. Z. Hu, Sustainable novel bamboo-based membranes for water treatment fabricated by regeneration of bamboo waste fibers, *ACS Sustainable Chem. Eng.*, 2020, **8**, 4225–4235.

116 S. Livazovic, Z. Li, A. R. Behzad, K.-V. Peinemann and S. P. Nunes, Cellulose multilayer membranes manufactured with ionic liquid, *J. Membr. Sci.*, 2015, **490**, 282–293.

117 D. Kim, S. Livazovic, G. Falca and S. P. Nunes, Oil-water separation using membranes manufactures from cellulose/ionic liquid solutions, *ACS Sustainable Chem. Eng.*, 2019, **7**, 5649–5659.

118 F. M. Sukma and P. Z. Culfaz-Emecen, Cellulose membranes for organic solvent nanofiltration, *J. Membr. Sci.*, 2018, **545**, 329–336.

119 E. N. Durmaz and P. Z. Culfaz-Emecen, Cellulose-based membranes via phase inversion using EMIMOAc-DMSO mixtures as solvent, *Chem. Eng. Sci.*, 2018, **178**, 93–103.

120 M. B. Turner, S. K. Spear, J. D. Holbrey and R. D. Rogers, Production of bioactive cellulose films reconstituted from ionic liquids, *Biomacromolecules*, 2004, **5**, 1379–1384.
121 R. Mehra, J. Muschiol, A. S. Meyer and K. P. Kepp, A structural-chemical explanation of fungal laccase activity, *Sci. Rep.*, 2018, **8**, 17285.
122 H. Zhao, Protein stabilization and enzyme activation in ionic liquids: specific ion effects, *J. Chem. Technol. Biotechnol.*, 2016, **91**, 25–50.
123 M. B. Turner, S. K. Spear, J. D. Holbrey, D. T. Daly and R. D. Rogers, Ionic liquid-reconstituted cellulose composites as solid support matrices for biocatalyst immobilization, *Biomacromolecules*, 2005, **6**, 2497–2502.
124 M. Bagheri, H. Rodríguez, R. P. Swatloski, S. K. Spear, D. T. Daly and R. D. Rogers, Ionic liquid-based preparation of cellulose-dendrimer films as solid supports for enzyme immobilization, *Biomacromolecules*, 2008, **9**, 381–387.
125 S. V. Muginova, D. A. Myasnikova, A. E. Polyakov and T. N. Shekhovtsova, Immobilization of plant peroxidases in cellulose-ionic liquid films, *Mendeleev Commun.*, 2013, **23**, 74–75.
126 M. P. Klein, C. W. Scheeren, A. S. G. Lorenzoni, J. Dupont, J. Frazzon and P. F. Hertz, Ionic liquid-cellulose film for enzyme immobilization, *Process Biochem.*, 2011, **46**, 1375–1379.
127 Y. Gu, P. Xue and K. Shi, A novel support of sponge-like cellulose composite polymer for immobilizing laccase and its application in nitrogenous organics biodegradation, *J. Porous Mater.*, 2020, **27**, 73–82.
128 Z. Liu, H. Wang, B. Li, C. Liu, Y. Jiang, G. Yu and X. Mu, Biocompatible magnetic cellulose-chitosan hybrid gel microspheres reconstituted from ionic liquids for enzyme immobilization, *J. Mater. Chem.*, 2012, **22**, 15085–15091.
129 H. Suo, L. Xu, Y. Xue, X. Qiu, H. Huang and Y. Hu, Ionic liquids-modified cellulose coated magnetic nanoparticles for enzyme immobilization: improvement of catalytic performance, *Carbohydr. Polym.*, 2020, **234**, 115914.
130 H. Zhao, G. A. Baker, Z. Song, O. Olubajo, T. Crittle and D. Peters, Designing enzyme-compatible ionic liquids that can dissolve carbohydrates, *Green Chem.*, 2008, **10**, 696–705.
131 R. A. Sheldon, Biocatalysis in ionic liquids: state-of-the-union, *Green Chem.*, 2021, **23**, 8406–8427.
132 K. Kuroda, H. Satria, K. Miyamura, Y. Tsuge, K. Ninomiya and K. Takahashi, Design of wall-desctructive but membrane-compatible solvents, *J. Am. Chem. Soc.*, 2017, **139**(45), 16052–16055.
133 G. Sharma, Y. Kato, A. Hachisu, K. Ishibashi, K. Ninomiya, K. Takahashi, E. Hirata and K. Kuroda, Synthesis of a cellulose dissolving liquid zwitterion from general and low-cost reagents, *Cellulose*, 2022, **29**, 3017–3024.
134 P. Migowski and J. Dupont, Catalytic applications of metal nanoparticles in imidazolium ionic liquids, *Chem. – Eur. J.*, 2007, **13**, 32–39.
135 M. M. Seitkalieva, D. E. Samoylenko, K. A. Lotsman, K. S. Rodygin and V. P. Ananikov, Metal nanoparticles in ionic liquids: synthesis and catalytic applications, *Coord. Chem. Rev.*, 2021, **445**, 213982.
136 J. Dupont, G. S. Fonseca, A. P. Umpierre, P. F. P. Fichtner and S. R. Teixeira, Transition-metal nanoparticles in imidazolium ionic liquids: recyclable catalysts for biphasic hydrogenation reactions, *J. Am. Chem. Soc.*, 2002, **124**, 4228–4229.
137 J. D. Scholten, B. C. Leal and J. Dupont, Transition metal nanoparticle catalysis in ionic liquids, *ACS Catal.*, 2012, **2**, 184–200.
138 Z. Li, A. Friedrich and A. Taubert, Gold microcrystal synthesis via reduction of HAuCl4 by cellulose in the ionic liquid 1-butyl-3-methyl imidazolium chloride, *J. Mater. Chem.*, 2008, **18**, 1008–1014.
139 M. A. Gelesky, C. W. Scheeren, L. Foppa, F. A. Pavan, S. L. P. Dias and J. Dupont, Metal nanoparticle/ionic liquid/cellulose: new catalytically active membrane materials for hydrogenation reactions, *Biomacromolecules*, 2009, **10**, 1888–1893.
140 A. Wittmar, H. Thierfeld, S. Köcher and M. Ulbricht, Routes towards catalytically active TiO2 doped porous cellulose, *RSC Adv.*, 2015, **5**, 35866–35873.
141 A. S. M. Wittmar and M. Ulbricht, Ionic liquid-based route for the preparation of catalytically active cellulose-TiO2 porous films and spheres, *Ind. Eng. Chem. Res.*, 2017, **56**, 2967–2975.
142 A. S. M. Wittmar, Q. Fu and M. Ulbricht, Photocatalytic and magnetic porous cellulose-based nanocomposite films prepared by a green method, *ACS Sustainable Chem. Eng.*, 2017, **5**, 9858–9868.
143 A. S. M. Wittmar, Q. Fu and M. Ulbricht, Photocatalytic and magnetic porous cellulose macrospheres for water purification, *Cellulose*, 2019, **26**, 4563–4578.
144 S. Jo, Y. Oh, S. Park, E. Kan and S. H. Lee, Cellulose/carrageenan/TiO2 nanocomposite for adsorption and photodegradation of cationic dye, *Biotechnol. Bioprocess Eng.*, 2017, **22**, 734–738.
145 Q. Qin, R. Guo, S. Lin, S. Jiang, J. Lan, X. Lai, C. Cui, H. Xiao and Y. Zhang, Waste cotton fiber/Bi2WO6 composite film for dye removal, *Cellulose*, 2019, **26**, 3909–3922.
146 L. Zhang, Z. Liu, G. Cui and L. Chen, Biomass-derived materials for electrochemical energy storages, *Prog. Polym. Sci.*, 2015, **43**, 136–164.
147 M. M. Pérez-Madrigal, M. G. Edo and C. Alamán, Powering the future: application of cellulose-based materials for supercapacitors, *Green Chem.*, 2016, **18**, 5930–5956.
148 D. Zhao, C. Chen, Q. Zhang, W. Chen, S. Liu, Q. Wang, Y. Liu, J. Li and H. Yu, High performance, flexible, solid-state supercapacitor based on a renewable and biodegradable mesoporous cellulose membrane, *Adv. Energy Mater.*, 2017, **7**, 1700739.
149 Y. Zhu, K. Cao, W. Cheng, S. Zeng, S. Dou, W. Chen, D. Zhao and H. Yu, A non-Newtonian fluidic cellulose-

modified glass microfiber separator for flexible lithium-ion batteries, *EcoMat*, 2021, **3**, e12126.

150 V. L. Pushparaj, M. M. Shaijumon, A. Kumar, S. Murugesan, L. Ci, R. Vajtai, R. J. Linhardt, O. Nalamasu and P. M. Ajayan, Flexible energy storage devices based on nanocomposite paper, *Proc. Natl. Acad. Sci. U. S. A.*, 2007, **104**, 13574–13577.

151 H. Wang, P.-G. Ren, C.-Y. Liu, L. Xu and Z.-M. Li, Enhanced toughness and strength of conductive cellulose-poly(butylene succinate) films filled with multi-walled carbon nanotubes, *Cellulose*, 2014, **21**, 1803–1812.

152 M. Soheilmoghaddam, H. Adelnia, G. Sharifzadeh, M. U. Wahit, T. W. Wong and A. A. Yussuf, Bionanocomposite regenerated cellulose/single-walled carbon nanotube films prepared using ionic liquid solvent, *Cellulose*, 2017, **24**, 811–822.

153 L. Zhou, F. Pan, S. Zeng, Q. Li, L. Bai, Y. Liu and Y. Nie, Ionic liquid assisted fabrication of cellulose-based conductive films for Li-ion battery, *J. Appl. Polym. Sci.*, 2020, **137**, e49430.

154 J. Chen, J. Xu, K. Wang, X. Qian and R. C. Sun, Highly thermostable, flexible, and conductive films prepared from cellulose, graphite, and polypyrrole nanoparticles, *ACS Appl. Mater. Interfaces*, 2015, **7**, 15641–15648.

155 T. Zhang, X. Zhang, Y. Chen, Y. Duan and J. Zhang, Green fabrication of regenerated cellulose/graphene films with simultaneous improvement of strength and toughness by tailoring the nanofiber diameter, *ACS Sustainable Chem. Eng.*, 2018, **6**, 1271–1278.

156 X. Ma, Q. Deng, L. Wang, X. Zheng, S. Wang, Q. Wang, L. Chen, L. Huang, X. Ouyang and S. Cao, Cellulose transparent conductive film and its feasible use in perovskite solar cells, *RSC Adv.*, 2019, **9**, 9348–9353.

157 W. Ye, X. Li, H. Zhu, X. Wang, S. Wang, H. Wang and R. C. Sun, Green fabrication of cellulose/graphene composite in ionic liquid and its electrochemical and photothermal properties, *Chem. Eng. J.*, 2016, **299**, 45–55.

158 S. Park, K. K. Oh and S. H. Lee, Biopolymer-based composite materials prepared using ionic liquids, *Adv. Biochem. Eng./Biotechnol.*, 2019, **168**, 133–176.

159 A. Takegawa, M. Murakami, Y. Kaneko and J. Kadokawa, Preparation of chitin/cellulose composite gels and films with ionic liquids, *Carbohydr. Polym.*, 2010, **79**, 85–90.

160 K. Prasad, M. Murakami, Y. Kaneko, A. Takada, Y. Nakamura and J. Kadokawa, Weak gel of chitin with ionic liquid, 1-allyl-3-methylimidazolium bromide, *Int. J. Biol. Macromol.*, 2009, **45**, 221–225.

161 J. Kadokawa, K. Hirohama, S. Mine, T. Kato and K. Yamamoto, Facile preparation of chitin/cellulose composite films using ionic liquids, *J. Polym. Environ.*, 2012, **20**, 37–42.

162 Y. Duan, A. Freyburger, W. Kunz and C. Zollfrank, Cellulose and chitin composite materials from an ionic liquid and a green solvent, *Carbohydr. Polym.*, 2018, **192**, 159–165.

163 Y. Wu, T. Sasaki, S. Irie and K. Sakurai, A novel biomass-ionic liquid platform for the utilization of native chitin, *Polymer*, 2008, **49**, 2321–2327.

164 W. Xiao, Q. Chen, Y. Wu, T. Wu and L. Dai, Dissolution and blending of chitosan using 1,3-dimethylimidazolium chloride and 1-H-3-methylimidazolium chloride binary ionic liquid solvent, *Carbohydr. Polym.*, 2011, **83**, 233–238.

165 C. Stefanescu, W. H. Daly and I. I. Negulescu, Biocomposite films prepared from ionic liquid solutions of chitosan and cellulose, *Carbohydr. Polym.*, 2012, **87**, 435–443.

166 R. Fu, X. Ji, Y. Ren, G. Wang and B. Cheng, Antibacterial blend films of cellulose and chitosan prepared from binary ionic liquid system, *Fibers Polym.*, 2017, **18**, 852–858.

167 C. Ardean, C. M. Davidescu, N. S. Nemeș, A. Negrea, M. Ciopec, N. Duteanu, P. Negrea, D. Duda-Seiman and V. Musta, Factors influencing the antibacterial activity of chitosan and chitosan modified by functionalization, *Int. J. Mol. Sci.*, 2021, **22**, 7449.

168 T. Hayashi and R. Kaida, Functions of xyloglucan in plant cells, *Mol. Plant*, 2011, **4**, 17–24.

169 A. Bendaoud, R. Kehrbusch, A. Baranov, B. Duchemin, J. E. Maigret, X. Falourd, M. P. Staiger, B. Cathala, D. Lourdin and E. Leroy, Nanostructured cellulose-xyloglycan blends via ionic liquid/water processing, *Carbohydr. Polym.*, 2017, **168**, 163–172.

170 J. Sundberg, G. Toriz and P. Gatenholm, Effect of xylan content on mechanical properties in regenerated cellulose/xylan blend films from ionic liquid, *Cellulose*, 2015, **22**, 1943–1953.

171 B. M. Upton and A. M. Kasko, Strategies for the conversion of lignin to high-value polymeric materials: review and perspective, *Chem. Rev.*, 2016, **116**, 2275–2306.

172 T. J. Simmons, S. H. Lee, J. Miao, M. Miyauchi, T.-J. Park, S. S. Bale, R. Pangule, J. Bult, J. G. Martin, J. S. Dordick and R. J. Linhardt, Preparation of synthetic wood composites using ionic liquids, *Wood Sci. Technol.*, 2011, **45**, 719–733.

173 S. H. Kim, M. H. Kim, J. H. Kim, S. Park, H. Kim, K. Won and S. H. Lee, Preparation of artificial wood films with controlled biodegradability, *J. Appl. Polym. Sci.*, 2015, **132**, 42109.

174 M. Lee, J. H. Kim, S. H. Lee, S. H. Lee and C. B. Park, Biomimetic artificial photosynthesis by light-harvesting synthetic wood, *ChemSusChem*, 2011, **4**, 581–586.

175 R.-L. Wu, X.-L. Wang, F. Li, H.-Z. Li and Y.-Z. Wang, Green composite films prepared from cellulose, starch, and lignin in room-temperature ionic liquid, *Bioresour. Technol.*, 2009, **100**, 2569–2574.

176 L.-D. Koh, Y. Cheng, C.-P. Teng, Y.-W. Khin, X.-J. Loh, S.-Y. Tee, M. Low, E. Ye, H.-D. Yu, Y.-W. Zhang and M.-Y. Han, Structures, mechanical properties and applications of silk fibroin materials, *Prog. Polym. Sci.*, 2015, **46**, 86–110.

177 D. M. Philips, L. F. Drummy, D. G. Conrady, D. M. Fox, R. R. Naik, M. O. Stone, P. C. Trulove, H. C. De Long and R. A. Mantz, Dissolution and regeneration of Bombyx mori silk fibroin using ionic liquids, *J. Am. Chem. Soc.*, 2004, **126**, 14350–14351.

178 S. Shang, L. Zhu and J. Fan, Physical properties of silk fibroin/cellulose blend films regenerated from the hydrophilic ionic liquid, *Carbohydr. Polym.*, 2011, **86**, 462–468.

179 J. Stanton, Y. Xue, J. C. Waters, A. Lewis, D. Cowan, X. Hu and D. Salas-de la Cruz, Structure-property relationships of blended polysaccharide and protein biomaterials in ionic liquid, *Cellulose*, 2017, **24**, 1775–1789.

180 D. Tian, T. Li, R. Zhang, Q. Wu, T. Chen, P. Sun and A. Ramamoorthy, Conformations and intermolecular interactions in cellulose/silk fibroin blend films: a solid-state NMR perspective, *J. Phys. Chem. B*, 2017, **121**, 6108–6116.

181 J. Stanton, Y. Xue, P. Pandher, L. Malek, T. Brown, X. Hu and D. Salas-de la Cruz, Impact of ionic liquid type on the structure, morphology and properties of silk-cellulose biocomposite materials, *Int. J. Biol. Macromol.*, 2018, **108**, 333–341.

182 A. Hadadi, J. W. Whittaker, D. E. Verrill, X. Hu, L. Larini and D. Salas-de la Cruz, A hierarchical model to understand the processing of polysaccharides/protein-based films in ionic liquids, *Biomacromolecules*, 2018, **19**, 3970–3982.

183 S. A. Love, E. Popov, K. Rybacki, X. Hu and D. Salas-de la Cruz, Facile treatment to fine-tune cellulose crystals in cellulose-silk biocomposites through hydrogen peroxide, *Int. J. Biol. Macromol.*, 2020, **147**, 569–575.

184 S. A. Love, X. Hu and D. Salas-de la Cruz, Controlling the structure and properties of semi-crystalline cellulose/silk fibroin biocomposites by ionic liquid type and hydrogen peroxide concentration, *Carbohydr. Polym. Technol. Appl.*, 2022, **3**, 100193.

185 H. Xie, S. Li and S. Zhang, Ionic liquids as novel solvents for the dissolution and blending of wool keratin fibers, *Green Chem.*, 2005, **7**, 606–608.

186 N. Hameed and Q. Guo, Blend films of natural wool and cellulose prepared from an ionic liquid, *Cellulose*, 2010, **17**, 803–813.

187 K. Rybacki, S. A. Love, B. Blessing, A. Morales, E. McDermott, K. Cai, X. Hu and D. Salas-de la Cruz, Structural and morphological properties of wool keratin and cellulose biocomposites fabricated using ionic liquids, *ACS Mater. Au*, 2022, **2**, 21–32.

188 Z. Meng, X. Zheng, K. Tang, J. Liu, Z. Ma and Q. Zhao, Dissolution and regeneration of collagen fibers using ionic liquid, *Int. J. Biol. Macromol.*, 2012, **51**, 440–448.

189 J. Wang, L. Wei, Y. Ma, K. Li, M. Li, Y. Yu, L. Wang and H. Qiu, Collagen/cellulose beads reconstituted from ionic liquid solution for Cu(II) adsorption, *Carbohydr. Polym.*, 2013, **98**, 736–743.

190 M. Zhang, C. Ding, L. Chen and L. Huang, The preparation of cellulose/collagen composite films using 1-ethyl-3-methylimidazolium acetate as a solvent, *BioResources*, 2014, **9**, 756–771.

191 M. Zhang, C. Ding, L. Huang, L. Chen and H. Yang, Interactions of collagen and cellulose in their blends with 1-ethyl-3-methylimidazolium acetate as solvent, *Cellulose*, 2014, **21**, 3311–3322.

192 J. Xu, B. Liu, J. Hu and H. Hou, Ionic liquid mediated technology for fabrication of cellulose film using gutta percha as an additive, *Ind. Crops Prod.*, 2017, **108**, 140–148.

193 S. Murugesan, S. Mousa, A. Vijayaraghavan, P. M. Ajayan and R. J. Linhardt, Ionic liquid-derived blood-compatible composite membranes for kidney dialysis, *J. Biomed. Mater. Res., Part B*, 2006, **79**, 298–304.

194 S. Park, Y. Oh, J. Yun, E. Yoo, D. Jung, K. S. Park, K. K. Oh and S. H. Lee, Characterization of blended cellulose/biopolymer films prepared using ionic liquid, *Cellulose*, 2020, **27**, 5101–5119.

195 C. Hopson, M. M. Villar-Chavero, J. C. Domínguez, M. V. Alonso, M. Oliet and F. Rodriguez, Cellulose ionogels, a perspective of the last decade: a review, *Carbohydr. Polym.*, 2021, **274**, 118663.

196 J. Kadokawa, M. Murakami and Y. Kaneko, A facile preparation of gel materials from a solution of cellulose in ionic liquid, *Carbohydr. Res.*, 2008, **343**, 769–772.

197 G. M. Kavanagh and S. B. Ross-Murphy, Rheological characterisation of polymer gels, *Prog. Polym. Sci.*, 1998, **23**, 533–562.

198 T. K. L. Meyvis, B. G. Stubbe, M. J. Van Steenbergen, W. E. Hennink, S. C. De Smedt and J. Demeester, A comparison between the use of dynamic mechanical analysis and oscillatory shear rheometry for the characterisation of hydrogels, *Int. J. Pharm.*, 2002, **244**, 163–168.

199 S. Yamazaki, A. Takegawa, Y. Kaneko, J. Kadokawa, M. Yamagata and M. Ishikawa, An acidic cellulose-chitin hybrid gel as novel electrolyte for an electric double layer capacitor, *Electrochem. Commun.*, 2009, **11**, 68–70.

200 S. Yamazaki, A. Takegawa, Y. Kaneko, J. Kadokawa, M. Yamagata and M. Ishikawa, High/low temperature operation of electric double layer capacitor utilizing acidic cellulose-chitin hybrid gel electrolyte, *J. Power Sources*, 2010, **195**, 6245–6249.

201 W. Kunchornsup and A. Sirivat, Physically cross-linked cellulosic gel via 1-butyl-3-methylimidazolium chloride ionic liquid and its electrochemical responses, *Sens. Actuators, A*, 2012, **175**, 155–164.

202 S. Thiemann, S. J. Sachnov, F. Pettersson, R. Bollström, R. Österbacka, P. Wasserscheid and J. Zaumseil, Cellulose-based ionogels for paper electronics, *Adv. Funct. Mater.*, 2014, **24**, 625–634.

203 G. P. Salvador, D. Pugliese, F. Bella, A. Chiappone, A. Sacco, S. Bianco and M. Quaglio, New insights in long-term photovoltaic performance characterization of cellulose-based gel electrolytes for stable dye-sensitized solar cells, *Electrochim. Acta*, 2014, **146**, 44–51.

204 Y. Cao, J. Zhang, Y. Bai, R. Li, S. M. Zakeeruddin, M. Grätzel and P. Wang, Dye-sensitized solar cells with solvent-free ionic liquid electrolytes, *J. Phys. Chem. C*, 2008, **112**, 13775–12781.

205 D. Zhao, Y. Zhu, W. Cheng, G. Xu, Q. Wang, S. Liu, J. Li, C. Chen, H. Yu and L. Hu, A dynamic gel with reversible and tunable topological networks and performances, *Matter*, 2020, **2**, 390–403.

206 J. Kaszyńska, A. Rachocki, M. Bielejewski and J. Tritt-Goc, Influence of cellulose gel matrix on BMIMCl ionic liquid dynamics and conductivity, *Cellulose*, 2017, **24**, 1641–1655.

207 C. J. Smith II, D. V. Wagle, H. M. O'Neill, B. R. Evans, S. N. Baker and G. A. Baker, Bacterial cellulose ionogels as chemosensory support, *ACS Appl. Mater. Interfaces*, 2017, **9**, 38042–38051.

208 R. Mantravadi, P. R. Chinnam, D. A. Dikin and S. L. Wunder, High conductivity, high strength solid electrolytes formed by in situ encapsulation of ionic liquids in nanofibrillar methyl cellulose networks, *ACS Appl. Mater. Interfaces*, 2016, **8**, 13426–13436.

209 S. K. Simotwo, P. R. Chinnam, S. L. Wunder and V. Kalra, Highly durable, self-standing solid-state supercapacitor based on an ionic liquid-rich ionogel and porous carbon nanofiber electrodes, *ACS Appl. Mater. Interfaces*, 2017, **9**, 33749–33757.

210 S. Chereddy, J. Aguirre, D. Dikin, S. L. Wunder and P. R. Chinnam, Gel electrolyte comprising solvate ionic liquid and methyl cellulose, *ACS Appl. Energy Mater.*, 2020, **3**, 279–289.

211 H. Lee, A. Erwin, M. L. Buxton, M. Kim, A. V. Stryutsky, V. V. Shevchenko, A. P. Sokolov and V. V. Tsukruk, Shape persistent, highly conductive ionigels from ionic liquids reinforced with cellulose nanocrystal network, *Adv. Funct. Mater.*, 2021, **31**, 2103083.

212 P. W. Schmidt, S. Morozova, S. P. Ertem, M. L. Coughlin, I. Davidovich, Y. Talmon, T. M. Reineke, F. S. Bates and T. P. Lodge, Internal structure of methylcellulose fibrils, *Macromolecules*, 2020, **53**, 398–405.

213 R. P. Singh and P. P. Kundu, DSC and micro structural studies of methylcellulose gels in N,N-dimethylformamide, *J. Polym. Res.*, 2013, **20**, 226.

214 W. Kunchornsup and A. Sirivat, Effects of crosslinking ratio and aging time on properties of physical and chemical cellulose gels via 1-butyl-3-methylimidazolium chloride solvent, *J. Sol-Gel Sci. Technol.*, 2010, **56**, 19–26.

215 P. Li, Y. Zhang, W. Fa, Y. Zhang and B. Huang, Synthesis of a grafted cellulose gel electrolyte in an ionic liquid (BmimI) for dye-sensitized solar cells, *Carbohydr. Polym.*, 2011, **86**, 1216–1220.

216 A. Kimura, N. Nagasawa and M. Taguchi, Cellulose gels produced in room temperature ionic liquids by ionizing radiation, *Radiat. Phys. Chem.*, 2014, **103**, 216–221.

217 H. H. Rana, J. H. Park, G. S. Gund and H. S. Park, Highly conducting, extremely durable, phosphorylated cellulose-based ionogels for renewable flexible supercapacitors, *Energy Storage Mater.*, 2020, **25**, 70–75.

218 L. Li, Z. B. Lin, X. Yang, Z. Z. Wan and S. X. Cui, A novel cellulose hydrogel prepared from its ionic liquid solution, *Chin. Sci. Bull.*, 2009, **54**, 1622–1625.

219 H. Satani, M. Kuwata and A. Shimizu, Simple and environmentally friendly preparation of cellulose hydrogels using an ionic liquid, *Carbohydr. Res.*, 2020, **494**, 108054.

220 P. Berton, X. Shen, R. D. Rogers and J. L. Shamshina, 110th anniversary: high-molecular-weight chitin and cellulose hydrogels from biomass in ionic liquids without chemical crosslinking, *Ind. Eng. Chem. Res.*, 2019, **58**, 19862–19876.

221 H. Peng, S. Wang, H. Xu and G. Dai, Preparations, properties, and formation mechanism of novel cellulose hydrogel membrane based on ionic liquid, *J. Appl. Polym. Sci.*, 2018, **135**, 45488.

222 M. Kimura, Y. Shinohara, J. Takizawa, S. Ren, K. Sagisaka, Y. Lin, Y. Hattori and J. P. Hinestroza, Versatile molding process for tough cellulose hydrogel materials, *Sci. Rep.*, 2015, **5**, 16266.

223 Z. Liu and H. Huang, Preparation and characterization of cellulose composite hydrogels from tea residue and carbohydrate additives, *Carbohydr. Polym.*, 2016, **147**, 226–233.

224 C. Wu, D. J. McClements, M. He, Z. Fan, Y. Li and F. Teng, Preparation of okara cellulose hydrogels using ionic liquids: structure, properties, and performance, *J. Mol. Liq.*, 2021, **331**, 115744.

225 D. Santra and K. Sen, Ionic liquid-modified cellulosic hydrogels or loading and sustained release of selenourea: an ensuing inhibition of tyrosinase activity, *Mater. Today Chem.*, 2020, **18**, 100365.

226 R. Su, F. Wang, J. Ding, Q. Li, W. Zhou, Y. Liu, B. Gao and Q. Yue, Magnetic hydrogel derived from wheat straw cellulose/feather protein in ionic liquids as copper nanoparticles carrier for catalytic reduction, *Carbohydr. Polym.*, 2019, **220**, 202–210.

227 X. Li, F. Dong, L. Zhang, Q. Xu, X. Zhu, S. Liang, L. Hu and H. Xie, Cellulosic protic ionic liquids hydrogel: a green and efficient catalyst carrier for Pd nanoparticles in reduction of 4-nitrophenol in water, *Chem. Eng. J.*, 2019, **372**, 516–525.

228 X. Liang, B. Qu, J. Li, H. Xiao, B. He and L. Qian, Preparation of cellulose-based conductive hydrogels with ionic liquid, *React. Funct. Polym.*, 2015, **86**, 1–6.

229 M. Xu, Q. Huang, X. Wang and R. Sun, Highly tough cellulose/graphene composite hydrogels prepared from ionic liquids, *Ind. Crops Prod.*, 2015, **70**, 56–63.

230 C. Tsioptsias, A. Stefopoulos, I. Kokkinomalis, L. Papadopoulou and C. Panayiotou, Development of micro- and nano-porous composite materials by processing cellulose with ionic liquids and supercritical CO2, *Green Chem.*, 2008, **10**, 965–971.

231 M. Deng, Q. Zhou, A. Du, J. van Kasteren and Y. Wang, Preparation of nanoporous cellulose foams from cell-

ulose-ionic liquid solutions, *Mater. Lett.*, 2009, **63**, 1851–1854.
232 M. Xu, W. Bao, S. Xu, X. Wang and R. Sun, Porous cellulose aerogels with high mechanical performance and their absorption behaviours, *BioResources*, 2016, **11**, 8–20.
233 L.-Y. Long, Y.-X. Weng and Y.-Z. Wang, Cellulose aerogels: synthesis, applications, and prospects, *Polymers*, 2018, **10**, 623.
234 U. G. K. Wegst, H. Bai, E. Saiz, A. P. Tomsia and R. O. Ritchie, Bioinspired structural materials, *Nat. Mater.*, 2015, **14**, 23–36.
235 S. F. Plappert, J.-M. Nedelec, H. Rennhofer, H. C. Lichtenegger, S. Bernstorff and F. W. Liebner, Self-assembly of cellulose in super-cooled ionic liquid under the impact of decelerated antisolvent diffusion: an approach towards anisotropic gels and aerogels, *Biomacromolecules*, 2018, **19**, 4411–4422.
236 H. Rennhofer, S. F. Plappert, H. C. Lichtenegger, S. Bernstorff, M. Fitzka, J.-M. Nedelec and F. W. Liebner, Insight into the nanostructure of anisotropic cellulose aerogels upon compression, *Soft Matter*, 2019, **15**, 8372–8380.
237 X. An, X. Zhang, M. Li, D. Pei, X. Ma and C. Li, Bubble-templated design of superelastic cellulose foam as a durable ionotropic sensor, *ACS Sustainable Chem. Eng.*, 2022, **10**, 1714–1721.
238 O. Aaltonen and O. Jauhiainen, The preparation of lignocellulosic aerogels from ionic liquid solutions, *Carbohydr. Polym.*, 2009, **75**, 125–129.
239 J. Li, Y. Lu, D. Yang, Q. Sun, Y. Liu and H. Zhao, Lignocellulose aerogel from wood-ionic liquid solution (1-allyl-3-methylimidazolium chloride) under freezing and thawing conditions, *Biomacromolecules*, 2011, **12**, 1860–1867.
240 Y. Lu, Q. Sun, D. Yang, X. She, X. Yao, G. Zhu, Y. liu, H. Zhao and J. Li, Fabrication of mesoporous lignocellulose aerogels from wood via cyclic liquid nitrogen freezing-thawing in ionic liquid solution, *J. Mater. Chem.*, 2012, **22**, 13548–13557.
241 H. Zhang, Y. Li, Y. Xu, Z. Lu, L. Chen, L. Huang and M. Fan, Versatile fabrication of a superhydrophobic and ultralight cellulose-based aerogel for oil spillage clean-up, *Phys. Chem. Chem. Phys.*, 2016, **18**, 28297–28306.
242 A. Demilecamps, C. Beauger, C. Hildebrand, A. Rigacci and T. Budtova, Cellulose-silica aerogels, *Carbohydr. Polym.*, 2015, **122**, 293–300.
243 H. Wang, Z. Shao, M. Bacher, F. Liebner and T. Rosenau, Fluorescent cellulose aerogels containing covalently immobilized (ZnS)x(CuInS2)1_x/ZnS (core/shell) quantum dots, *Cellulose*, 2013, **20**, 3007–3024.
244 J.-H. Lee and S.-J. Park, Recent advances in preparations and applications of carbon aerogels: a review, *Carbon*, 2020, **163**, 1–18.
245 J. W. S. Hearle, Textile fibers: a comparative overview, in *Encyclopedia of Materials: Science and Technology*, ed. K. H. J. Buschow, R. W. Cahn, M. C. Flemings, B. Ilschner, E. J. Kramer, S. Mahajan and P. Veyssière, Elsevier, Oxford, UK, 2001, pp. 9100–9116, ISBN 978-0-08-043152-9.
246 A. Libanori, G. Chen, X. Zhao, Y. Zhou and J. Chen, Smart textiles for personalized healthcare, *Nat. Electron.*, 2022, **5**, 142–156.
247 X. Shi, Y. Zou, P. Zai, J. Shen, Y. Yang, Z. Gao, M. Liao, J. Wu, J. Wang, X. Xu, Q. Tong, B. Zhang, B. Wang, X. Sun, L. Zhang, Q. Pei, D. Jin, P. Chen and H. Peng, Large-area display textiles integrated with functional systems, *Nature*, 2021, **591**, 240–245.
248 F. M. Häemmerle, The cellulose gap (the future of cellulose fibres), *Lenzinger Ber.*, 2011, **89**, 12–21.
249 C. Felgueiras, N. G. Azoia, C. Gonçalves, M. Gama and F. Dourado, Trends on the cellulose-based textiles: raw materials and technologies, *Front. Bioeng. Biotechnol.*, 2021, **9**, 608826.
250 M. Hummel, A. Michud, M. Tanttu, S. Asaadi, Y. Ma, L. K. J. Hauru, A. Parviainen, A. W. T. King, I. Kilpeläinen and H. Sixta, Ionic liquids for the production of man-made cellulosic fibers: opportunities and challenges, *Adv. Polym. Sci.*, 2016, **271**, 133–168.
251 F. Hermanutz, M. P. Vocht, N. Panzier and M. R. Buchmeiser, Processing of cellulose using ionic liquids, *Macromol. Mater. Eng.*, 2019, **304**, 1800450.
252 G. Laus, G. Bentivoglio, H. Schottenberger, V. Kahlenberg, H. Kopacka, T. Röder and H. Sixta, Ionic liquids: current developments, potential and drawbacks for industrial applications, *Lenzinger Ber.*, 2005, **84**, 71–85.
253 G. Bentivoglio, T. Röder, M. Fasching, M. Buchberger, H. Schottenberger and H. Sixta, Cellulose processing with chloride-based ionic liquids, *Lenzinger Ber.*, 2006, **86**, 154–161.
254 B. Kosan, C. Michels and F. Meister, Dissolution and forming of cellulose with ionic liquids, *Cellulose*, 2008, **15**, 59–66.
255 D. Ingildeev, F. Effenberger, K. Bredereck and F. Hermanutz, Comparison of direct solvents for regenerated cellulosic fibers via the Lyocell process and by means of ionic liquids, *J. Appl. Polym. Sci.*, 2013, **128**, 4141–4150.
256 C. Zhu, R. M. Richardson, K. D. Potter, A. F. Koutsomitopoulou, J. S. van Duijneveldt, S. R. Vincent, N. D. Wanasekara, S. J. Eichhorn and S. S. Rahatekar, High modulus regenerated cellulose fibers spun from a low molecular weight microcrystalline cellulose solution, *ACS Sustainable Chem. Eng.*, 2016, **4**, 4545–4553.
257 L. Zhou, Z. Kang, Y. Nie and L. Li, Fabrication of regenerated cellulose fibers with good strength and biocompatibility from green spinning process of ionic liquid, *Macromol. Mater. Eng.*, 2021, **306**, 2000741.
258 J. Zhang, K. Tominaga, N. Yamagishi and Y. Gotoh, Comparison of regenerated cellulose fibers spun from ionic liquid solutions with Lyocell fiber, *J. Fiber Sci. Technol.*, 2020, **76**, 257–266.
259 A. Michud, A. King, A. Parviainen, H. Sixta, L. Hauru, M. Hummel and I. Kilpeläinen, Process for the pro-

duction of shaped cellulose articles, *International Patent*, 2014/162062A1, 2014.

260 L. K. J. Hauru, M. Hummel, A. Michud and H. Sixta, Dry jet-wet spinning of strong cellulose filaments from ionic liquid solution, *Cellulose*, 2014, **21**, 4471–4481.

261 H. Sixta, A. Michud, L. Hauru, S. Asaadi, Y. Ma, A. W. T. King, I. Kilpeläinen and M. Hummel, Ioncell-F: a high-strength regenerated cellulose fibre, *Nord. Pulp Pap. Res. J.*, 2015, **30**, 43–57.

262 A. Michud, M. Hummel and H. Sixta, Influence of process parameters on the structure formation of man-made cellulosic fibers from ionic liquid solution, *J. Appl. Polym. Sci.*, 2016, **133**, 43718.

263 A. Michud, M. Hummel and H. Sixta, Influence of molar mass distribution on the final properties of fibers regenerated from cellulose dissolved in ionic liquid by dry-jet wet spinning, *Polymer*, 2015, **75**, 1–9.

264 Y. Ma, H. Hummel, M. Määttänen, A. Särkilahti, A. Harlin and H. Sixtaa, Upcycling of waste paper and cardboard to textiles, *Green Chem.*, 2016, **18**, 858–866.

265 Y. Ma, M. Hummel, I. Kontro and H. Sixta, High-performance man-made cellulosic fibres from recycled newsprint, *Green Chem.*, 2018, **20**, 160–169.

266 S. Haslinger, Y. Wang, M. Rissanen, M. B. Lossa, M. Tanttu, E. Ilen, M. Määttänen, A. Harlin, M. Hummel and H. Sixta, Recycling of vat and reactive dyed textile waste to new colored man-made cellulose fibers, *Green Chem.*, 2019, **21**, 5598–5610.

267 S. Elsayed, B. Viard, C. Guizani, S. Hellsten, J. Witos and H. Sixta, Limitations of cellulose dissolution and fiber spinning in the Lyocell process using mTBDHOAc and DBNHOAc solvents, *Ind. Eng. Chem. Res.*, 2020, **59**, 20211–20220.

268 C. Guizani, S. Larkiala, K. Moriam, D. Sawada, S. Elsayed, S. Rantasalo, M. Hummel and H. Sixta, Air gap spinning of a cellulose solution in DBNHOAc ionic liquid with a novel vertically arranged spinning bath to simulate a closed loop operation in the Ioncell® process, *J. Appl. Polym. Sci.*, 2021, **138**, e49787.

269 N. Sun, W. Li, B. Stoner, X. Jiang, X. Lu and R. D. Rogers, Composite fibers spun directly from solutions of raw lignocellulosic biomass, *Green Chem.*, 2011, **13**, 1158–1161.

270 T. Nypelö, S. Asaadi, G. Kneidinger, H. Sixta and J. Konnerth, Conversion of wood-biopolymers into macrofibers with tunable surface anergy via dry-jet wet spinning, *Cellulose*, 2018, **25**, 5297–5307.

271 H. Zahra, D. Sawada, C. Guizani, Y. Ma, S. Kumagai, T. Yoshioka, H. Sixta and M. Hummel, Close packing of cellulose and chitosan in regenerated cellulose fibers improves carbon yield and structural properties of respective carbon fibers, *Biomacromolecules*, 2020, **21**, 4326–4335.

272 A. Ota, R. Beyer, U. Hageroth, A. Müller, P. Tomasic, F. Hermanutz and M. R. Buchmeiser, Chitin/cellulose blend fibers prepared by wet and dry-wet spinning, *Polym. Adv. Technol.*, 2021, **32**, 335–342.

273 Y. Ma, S. Asaadi, L.-S. Johansson, P. Ahvenainen, M. Reza, M. Alekhina, L. Rautkari, A. Michud, L. Hauru, M. Hummel and H. Sixta, High-strength composite fibers from cellulose-lignin blends regenerated from ionic liquid solution, *ChemSusChem*, 2015, **8**, 4030–4039.

274 C. Olsson, B. Hangström, E. Sjöholm and A. Reimann, in *18th International Symposium on Wood, Fibre, Pulp Chemistry (ISWFPC)*, Vienna, Austria, 2015, Proceeding vol. II, pp. 126–129.

275 E. Frank, L. M. Steudle, D. Ingildeev, J. M. Spörl and M. R. Buchmeiser, Carbon fibers: precursor systems, processing, structure and properties, *Angew. Chem., Int. Ed.*, 2014, **53**, 5262–5298.

276 N. Byrne, R. D. Silva, Y. Ma, H. Sixta and M. Hummel, Enhanced stabilization of cellulose-lignin hybrid filaments for carbon fiber production, *Cellulose*, 2018, **25**, 723–733.

277 N.-D. Le, M. Trogen, Y. Ma, R. J. Varley, M. Hummel and N. Byrne, Cellulose-lignin composite fibers as precursors for carbon fibers: Part 2 - The impact of precursor properties on carbon fibers, *Carbohydr. Polym.*, 2020, **250**, 116918.

278 M. Trogen, N.-D. Le, D. Sawada, C. Guizani, T. V. Lourençon, L. Pitkänen, H. Sixta, R. Shah, H. O'Neill, M. Balakshin, N. Byrne and M. Hummel, Cellulose-lignin composite fibres as precursors for carbon fibres. Part 1 - Manufacturing and properties of precursor fibres, *Carbohydr. Polym.*, 2021, **252**, 117133.

279 N.-D. Le, M. Trogen, R. J. Varley, M. Hummel and N. Byrne, Effect of boric acid on the stabilisation of cellulose-lignin filaments as precursors for carbon fibres, *Cellulose*, 2021, **28**, 729–739.

280 N.-D. Le, M. Trogen, Y. Ma, R. J. Varley, M. Hummel and N. Byrne, Understanding the influence of key parameters on the stabilisation of cellulose-lignin composite fibres, *Cellulose*, 2021, **28**, 911–919.

281 N.-D. Le, M. Trogen, R. J. Varley, M. Hummel and N. Byrne, Chemically accelerated stabilization of a cellulose-lignin precursor as a route to high yield carbon fiber production, *Biomacromolecules*, 2022, **23**, 839–846.

282 C. Olsson, E. Sjöholm and A. Reimann, Carbon fibres from precursors produced by dry-jet wet-spinning of kraft lignin blended with kraft pulps, *Holzforschung*, 2017, **71**, 275–283.

283 A. Bengtsson, J. Bengtsson, C. Olsson, M. Sedin, K. Jedvert, H. Theliander and E. Sjöholm, Improved yield of carbon fibres from cellulose and kraft lignin, *Holzforschung*, 2018, **72**, 1007–1016.

284 A. Bengtsson, J. Bengtsson, M. Sedin and E. Sjöholm, Carbon fibers from lignin-cellulose precursors: effect of stabilization conditions, *ACS Sustainable Chem. Eng.*, 2019, **7**, 8440–8448.

285 A. Bengtsson, P. Hecht, J. Sommertune, M. Ek, M. Sedin and E. Sjöholm, Carbon fibers from lignin-cellulose precursors: effect of carbonization conditions, *ACS Sustainable Chem. Eng.*, 2020, **8**, 6826–6833.

286 A. Bengtsson, J. Bengtsson, K. Jedvert, M. Kakkonen, O. Tanhuanpää, E. Brännvall and M. Sedin, Continuous stabilization and carbonization of a lignin-cellulose precursor to carbon fiber, *ACS Omega*, 2022, **7**, 16793–16802.

287 H. Zahra, D. Sawada, S. Kumagai, Y. Ogawa, L.-S. Johansson, Y. Ge, C. Guizani, T. Yoshioka and M. Hummel, Evolution of carbon nanostructure during pyrolysis of homogeneous chitosan-cellulose composite fibers, *Carbon*, 2021, **185**, 27–38.

288 N. Sun, R. P. Swatloski, M. L. Maxim, M. Rahman, A. G. Harland, A. Haque, S. K. Spear, D. T. Daly and R. D. Rogers, Magnetite-embedded cellulose fibers prepared from ionic liquid, *J. Mater. Chem.*, 2008, **18**, 283–290.

289 M. L. Maxim, N. Sun, R. P. Swatloski, M. Rahman, A. G. Harland, A. Haque, S. K. Spear, D. T. Daly and R. D. Rogers, Properties of cellulose/TiO2 fibers processed from ionic liquids, *ACS Symp. Ser.*, 2010, **1033**, 261–274.

290 H.-Z. Song, Z.-Q. Luo, C.-Z. Wang, X.-F. Hao and J.-G. Gao, Preparation and characterization of bionanocomposite fiber based on cellulose and nano-SiO_2 using ionic liquid, *Carbohydr. Polym.*, 2013, **98**, 161–167.

291 H. Zhang, Z. Wang, Z. Zhang, J. Wu, J. Zhang and J. He, Regenerated-cellulose/multiwalled-carbon-nanotube composite fibers with enhanced mechanical properties prepared with the ionic liquid 1-allyl-3-methylimidazolium chloride, *Adv. Mater.*, 2007, **19**, 698–704.

292 S. S. Rahatekar, A. Rasheed, R. Jain, M. Zammarano, K. K. Koziol, A. H. Windle, J. W. Gilman and S. Kumar, Solution spinning of cellulose carbon nanotube composites using room temperature ionic liquids, *Polymer*, 2009, **50**, 4577–4583.

293 S. Haslinger, Y. Ye, M. Rissanen, M. Hummel and H. Sixta, Cellulose fibers for high-performance textiles functionalized with incorporated gold and silver nanoparticles, *ACS Sustainable Chem. Eng.*, 2020, **8**, 649–658.

294 K. Moriam, M. Rissanen, D. Sawada, M. Altgen, L.-S. Johansson, D. V. Evtyugin, C. Guizani, M. Hummel and H. Sixta, Hydrophobization of the man-made cellulosic fibers by incorporating plant-derived hydrophobic compounds, *ACS Sustainable Chem. Eng.*, 2021, **9**, 4915–4925.

295 M. J. Lundahl, D. Sawada, M. Merilä and M. Hummel, Effect of graphitic additives on the rheology of cellulose solutions for the preparation of templated carbon fiber precursors, *J. Appl. Polym. Sci.*, 2022, e52670.

296 B. A. da Silva, R. D. S. Cunha, A. Valério, A. D. N. Junior, D. Hotza and S. Y. G. González, Electrospinning of cellulose using ionic liquids: an overview on processing and applications, *Eur. Polym. J.*, 2021, **147**, 110283.

297 A. Kramar and F. J. González-Benito, Cellulose-based nanofibers processing techniques and methods based on bottom-up approach – a review, *Polymers*, 2022, **14**, 1–35.

298 S. Xu, J. Zhang, A. He, J. Li, H. Zhang and C. C. Han, Electropinning of native cellulose from nonvolatile solvent system, *Polymer*, 2008, **49**, 2911–2917.

299 S.-L. Quan, S.-G. Kang and I.-J. Chin, Characterization of cellulose fibers electrospun using ionic liquid, *Cellulose*, 2010, **17**, 223–230.

300 T. P. T. Pham, C.-W. Cho and Y.-S. Yun, Environmental fate and toxicity of ionic liquids: a review, *Water Res.*, 2010, **44**, 352–372.

301 M. Petkovic, K. R. Seddon, L. P. Rebelo and C. S. Pereira, Ionic liquids: a pathway to environmental acceptability, *Chem. Soc. Rev.*, 2011, **40**, 1383–1403.

302 K. S. Egorova and V. P. Ananikov, Toxicity of ionic liquids: eco(cyto)activity as complicated, but unavoidable parameter for task-specific optimization, *ChemSusChem*, 2014, **7**, 336–360.

303 J. Flieger and M. Flieger, Ionic liquids toxicity – benefits and threats, *Int. J. Mol. Sci.*, 2020, **21**, 6267.

304 C.-W. Cho, T. P. T. Pham, Y. Zhao, S. Stolte and Y.-S. Yun, Review of the toxic effects of ionic liquids, *Sci. Total Environ.*, 2021, **786**, 147309.

305 A. Mehrkesh and A. T. Karunanithi, Life-cycle perspectives on aquatic ecotoxicity of common ionic liquids, *Environ. Sci. Technol.*, 2016, **50**, 6814–6821.

306 S. Koutsoukos, F. Philippi, F. Malaret and T. Welton, A review on machine learning algorithms for the ionic liquid chemical space, *Chem. Sci.*, 2021, **12**, 6820–6843.

307 E. R. D. Seiler, Y. Takeoka, M. Rikukawa and M. Yoshizawa-Fujita, Development of a novel cellulose solvent based on pyrrolidinium hydroxide and reliable solubility analysis, *RSC Adv.*, 2020, **10**, 11475–11480.

308 J. B. Guinée, R. Heijungs, G. Huppes, A. Zamagni, P. Masoni, R. Buonamici, T. Ekvall and T. Rydberg, Life cycle assessment: past, present, and future, *Environ. Sci. Technol.*, 2011, **45**, 90–96.

309 H. Baaqel, I. Díaz, V. Tulus, B. Chachuat, G. Guillén-Gosálbez and J. P. Hallett, Role of life-cycle externalities in the valuation of protic ionic liquids – a case study in biomass pretreatment solvents, *Green Chem.*, 2020, **22**, 3132–3140.

310 L. Liang, J. Yan, Q. He, T. Luong, T. R. Pray, B. A. Simmons and N. Sun, Scale-up of biomass conversion using 1-ethyl-3-methylimidazolium acetate as the solvent, *Green Energy Environ.*, 2019, **4**, 432–438.

311 X. Liang and H. Liu, High-efficiency recovery of 1-ethyl-3-methylimidazolium acetate for sugarcane bagasse pretreatment with industrialized technology, *Sep. Purif. Technol.*, 2020, **238**, 116437.

312 W. Lan, C.-F. Liu, F.-X. Yue, R.-C. Sun and J. F. Kennedy, Ultrasound-assisted dissolution of cellulose in ionic liquid, *Carbohydr. Polym.*, 2011, **86**, 672–677.

313 J.-P. Mikkola, A. Kirilin, J.-C. Tuuf, A. Pranovich, B. Holmbom, L. M. Kustov, D. Y. Murzin and T. Salmi, Ultrasound enhancement of cellulose processing in ionic liquids: from dissolution towards functionalization, *Green Chem.*, 2007, **9**, 1229–1237.

314 M. E. Gibril, L. Huan, L. X. Da, Z. Yue, K. Han and Y. Muhuo, Reactive extrusion process for the preparation of a high concentration solution of cellulose in ionic

liquid for in situ chemical modification, *RSC Adv.*, 2013, **3**, 1021–1024.

315 R. Milotskyi, L. Szabó, T. Fujie, K. Sakata, N. Wada and K. Takahashi, Low waste process of rapid cellulose transesterification using ionic liquid/DMSO mixed solvent: towards more sustainable reaction systems, *Carbohydr. Polym.*, 2021, **256**, 117560.

316 S. C. Hernandez, R. Milotskyi, S. Takagi, E. R. D. Ito, S. Suzuki, N. Wada and K. Takahashi, Continuous production of cellulose mixed esters via homogeneous reactive twin-screw extrusion catalyzed by ionic liquid, *Cellulose*, 2023, **30**, 2873–2882.

317 R. Milotskyi, G. Sharma, T. Fujie, D. Hirose, N. Wada and K. Takahashi, Continuous process of cellulose dissolution and transesterification reaction catalysed by ionic liquid in twin screw extruder, *React. Chem. Eng.*, 2023, 1–8.

318 G. Chen, Z. Shen, A. Iyer, U. F. Ghumman, S. Tang, J. Bi, W. Chen and Y. Li, Machine-learning-assisted de novo design of organic molecules and polymers: opportunities and challenges, *Polymers*, 2020, **12**, 163.

319 A. Bendaoud and Y. Chalamet, Plasticizing effect of ionic liquid on cellulose acetate obtained by melt processing, *Carbohydr. Polym.*, 2014, **108**, 75–82.

320 L. Li, Y. Zhang, Y. Sun, S. Sun, G. Shen, P. Zhao, J. Cui, H. Qiao, Y. Wang and H. Zhou, Manufacturing pure cellulose films by recycling ionic liquids as plasticizers, *Green Chem.*, 2020, **22**, 3835–3841.

321 S. Livi, J. Duchet-Rumeau, J.-F. Gérard and T. N. Pham, Polymers and ionic liquids: a successful wedding, *Macromol. Chem. Phys.*, 2015, **216**, 359–368.

322 C. G. Otoni, H. M. C. Azeredo, B. D. Mattos, M. Beaumont, D. S. Correa and O. J. Rojas, The food-materials nexus: next generation bioplastics and advanced materials from agri-food residues, *Adv. Mater.*, 2021, **33**, 2102520.

323 **https://www.japan.go.jp/tomodachi/2020/summer2020/innovating_paper.html** (last accessed on 28/09/2022).

324 **https://www.japantimes.co.jp/life/2022/09/05/people/banana-stem-one-planet-cafe-grows-change** (last accessed on 28/09/2022).